THESIS APPROVAL

GRADUATE SCHOOL, KASETSART UNIVERSITY

Master of Science (Biochemistry)

DEGREE

Biochemistry — **FIELD**

Biochemistry — **DEPARTMENT**

TITLE: Development of an Inhibiting Activity Assay of Tyrosine Kinase of EGFR for Screening the New EGFR Inhibitor

NAME: Miss Sirigade Ruekit

THIS THESIS HAS BEEN ACCEPTED BY

THESIS ADVISOR

(Assistant Professor Kiattawee Choowongkomon, Ph.D.)

THESIS CO-ADVISOR

(Miss Nattanan Panjaworayan, Ph.D.)

DEPARTMENT HEAD

(Assistant Professor Kiattawee Choowongkomon, Ph.D.)

APPROVED BY THE GRADUATE SCHOOL ON _____

DEAN

(Associate Professor Gunjana Theeragool, D.Agr.)

THESIS

DEVELOPMENT OF AN INHIBITING ACTIVITY ASSAY OF TYROSINE KINASE OF EGFR FOR SCREENING THE NEW EGFR INHIBITOR

SIRIGADE RUEKIT

A Thesis Submitted in Partial Fulfillment of
the Requirements for the Degree of
Master of Science (Biochemistry)
Graduate School, Kasetsart University
2009

Sirigade Ruekit 2009: Development of an Inhibiting Activity Assay of Tyrosine Kinase of EGFR for Screening the New EGFR Inhibitor. Master of Science (Biochemistry), Major Field: Biochemistry, Department of Biochemistry. Thesis Advisor: Assistant Professor Kiattawee Choowongkomon, Ph.D. 160 pages.

EGFR regulates a wide range of cellular processes. For these reasons, EGFR became a target protein for cancer therapy. Herbs have been considered valuable sources for anti-cancer drug discovery. In our studies, we tried to develop the method for activity assay of tyrosine kinase (TK) of EGFR in order to screening for new EGFR inhibitors from Thai herbs. These included the suitable host for TK expression and comparing the suitable activity assay for testing TK inhibitors. We compared the expression of TK protein in both bacterial and insect expression systems. From bacterial expression system, The non-fusion TK protein had no activity but GST-TK that expressed at 16°C had a weak activity (lower V_{max} and higher K_m values). The final yield of purified GST-TK was 7.7 mg per liter of culture. Due to the lower yield and weak activity of TK in bacterial cells, we turned to use the insect expression system. The final yield of purified TK and GST-TK in insect expression systems were 6.74 mg protein/15 ml culture medium and 6.06 mg protein/15 ml culture medium, respectively. The K_m and V_{max} of GST-TK was similar to the commercial full-length EGFR. Moreover, recombinant TK has a high degree of glycosylation while recombinant GST-TK has no glycosylation at all. Thus, the suitable system for expression of active recombinant TK is using the insect cells expression system by expressing as the fusion GST-TK. For developing activity assays of TK, we used three methods for comparing efficiencies; ABTK assay, ATP/NADH couple assay and PURETIME assay. The ABTK assay had sensitivity and specificity more than other methods. Then we used ABTK assay for screening inhibitor from Thai herbs. The crude ethanol extracts from 25 Thai herbal plants were used in this experiment. The results showed that the crude extraction of *S. indicum* and *M. acochinchinensis*, *T. chebula*, *C. loureiroi* and *Ruellia tuberose* had inhibition activity against TK of EGFR. This is the first report of the identification of Thai herbal extracts which can inhibit EGFR kinase activity by using molecular biology techniques combined with enzyme kinetic studies. These findings may lead to the further development of novel anti-cancer drugs.

/ /

Student's signature Thesis Advisor's signature

ACKNOWLEDGEMENTS

I would like to grateful thank and deeply indebted to Asst. Prof. Dr. Kiattawee Choowongkomon, my thesis advisor for advice, encouragement and valuable suggestion for completely writing of thesis.

I also would like to thank Dr. Nattanan Panjaworayan and Dr. Sasimanuss Unajak for their advices and helpful suggestion.

I would like to thank Thailand Research Fund and the Faculty of Science, Kasetsart University (TRF-MAG Window II: MRG-WII515S014) providing graduate scholarship to support this research. Additionally, special thank for all the members of Department of Biochemistry, Faculty of Science, Kasetsart University.

I would like to thank all members in KC's Lab, especially the acting for Ph.D., Napat Songtawee, Kun Silaprasit, Anussorn wisessing, Orathai Sawaddeechaikul, my kindly sister--Piyachat Meesawat and my best friend--Supaporn Seetaha for their comments, helps, friendships and encouragements.

I am especially appreciated my family, my mom, my dad and my pretty sister for their continuing encouragements. Without their love and support though my study, I would never have been finished my graduate.

Finally, I am deeply appreciated to Mr. Chawalit Sutjarit for encouragement, understanding and listen to me all the time.

P.S. I really thank Google.com for answer me when I must rely on myself.

Sirigade Ruekit

November 2009

TABLE OF CONTENTS

Page

LIST OF TABLES

LIST OF TABLES (Continued)

LIST OF FIGURES

LIST OF FIGURES (Continued)

LIST OF FIGURES (Continued)

LIST OF ABBREVIATIONS

ABTK	=	Antibody beacon tyrosine kinase assay
ATP	=	Adenosine triphosphate
bp	=	Base pair
°C	=	Degree Celsius
DTT	=	Dithiothreitol
DMSO	=	Dimethyl sulfoxide
E.coli	=	*Escherichia coli*
EDTA	=	Ethylenediaminetetra acetic acid diasodium salt
EGFR	=	Epidermal growth factor receptor
DNA	=	Deoxyribonucleic acid
dNTP	=	Deoxyribonucleotide triphosphate
FBS	=	Fetal bovine serum
FRET	=	Fluorescence resonance energy transfer
g	=	Gram
Glu	=	Glutamic acid
h	=	Hour
His	=	Histidine
IPTG	=	Isopropyl β-D-1-thiogalactopyranoside
Kb	=	Kilobase pair
KDa	=	Kilodalton
K_i	=	Inhibition constant
K_m	=	Michaelis-Menten constant
l	=	Liter
LB	=	Luria-Bertani
$MgCl_2$	=	Magnesium chloride
M	=	Molar
mg	=	Milligram
min	=	Minute
ml	=	Milliliter
MW	=	Molecular weight

LIST OF ABBREVIATIONS (Continued)

NaCl	=	Sodium Chloride
NADH	=	Nicotinamide adenine dinucleotide
OD	=	Optical density
PCR	=	Polymerase chain reaction
PEG	=	Polyethylene glycol
PEP	=	Phosphoenolpyruvate
Sf900II	=	Serum free medium 900 II
TK	=	Tyrosine kinase
Tyr	=	Tyrosine
TEMED	=	Tetramethylethylenediamine
pH	=	Logalithm of reciprocal of hydrogen ion concentration
PMSF	=	phenylmethylsulfonyl fluoride
s	=	Second
SDS	=	Sodium dodecyl sulfate
Sf9	=	*Spodoptera flugiperda* clone 9
Tris	=	Tris hydroxymethyl aminomethane
U	=	Unit
µg	=	Microgram
µM	=	Micromolar
V_{max}	=	Maximum velocity

DEVELOPMENT OF AN INHIBITING ACTIVITY ASSAY OF TYROSINE KINASE OF EGFR FOR SCREENING THE NEW EGFR INHIBITOR

INTRODUCTION

Cancer is the first leading cause of death in Thailand accounting for 80-85%. Several cancers cause the over-expression and mutation of many proteins in cell cycle, including epidermal growth factor receptor (EGFR). EGFR regulates a wide range of cellular processes including proliferation, differentiation, motility, survival, angiogenesis and invasion (Holbro and Hynes, 2004). In 40–80% of non-small cell lung cancers (NSCLCs) has been found to be EGFR over-expression, as well as in a number of other common solid tumors (Mendelsohn and Baselga, 2000). After binding to its ligands (EGF, transforming growth factor (TGF) α, and heregulin), EGFR forms asymmetric homo or hetero-dimer (Zhang *et al.*, 2006) and then causes an activation of the intrinsic kinase domain, resulting in phosphorylation of specific tyrosine kinase residues within the cytoplasmic tail and there targeting proteins. Receptor activation leads to recruitment and phosphorylation of several intracellular substrates which, in turn, engage mitogenic signaling and other tumor-promoting activities (Baselga and Cortes, 2005). For these reasons, EGFR has became a target protein for cancer therapy (Ciardiello and Tortora, 2008). A number of inhibiting strategies of this receptor has been evaluated including monoclonal antibodies, small molecule tyrosine kinase inhibitors (Kobayashi *et al.*, 2005), antisense oligonucleotides, and antibody-based immunoconjugates. Monoclonal antibodies bind to the extracellular domain of EGFR and competitively inhibit ligand binding. The EGFR-monoclonal antibody complex is subsequently internalized, causing a transient decrease in EGFR expression, which prevents EGFR heterodimerization in a phosphorylation status-independent manner. Unlike monoclonal antibodies, tyrosine kinase inhibitors (TKIs) do not affect internalization of the receptor and are often not specific for EGFR, affecting kinase activity of other ErbB family receptors. EGFR TKIs block the ATP pocket of EGFR, thereby inhibiting EGFR phosphorylation and

downstream signal transduction. Similar to cetuximab, EGFR TKIs such as gefitinib (ZD 1839, Iressa; AstraZeneca) and erlotinib (OSI-774; Tarceva, Genentech) block the cell cycle in the G1 phase (Wakeling *et al*., 2002) and induce apoptosis *in vitro*. However, all tyrosine kinase inhibitors (TKIs) are cancer drug patent.

In previous study, herbs have been considered valuable sources for anticancer drug discovery. Herbal medicine, recorded in many countries, e.g., Chinese pharmacopoeia, has been prescribed for many diseases over centuries and began to be matched by increasing scientific attention (Vickers, 2002). Based on recent scientific research on herbs, herbal therapies have been considered alternative treatments for malignancies (Risberg *et al.*, 1998). Several studies have demonstrated that extracts from several herbal medicines or mixtures have an anticancer potential and could inhibit cancer cell proliferation *in vitro* or *in vivo* (Harvey, 2008).

Therefore the researchers have been interested in an inhibiting activity assay for tyrosine kinase of EGFR in order to screen new EGFR inhibitors. However, the expression of TK in bacterial cells (Koland *et al.*, 1990) has been found in the inclusion bodies due to incorrect folding of TK protein. Some proteins need the eukaryotic folding machineries in order to get the correct folding of protein. Thus, in this study we tried to express the active tyrosine kinase protein of EGFR in insect cells system (Yun *et al.*, 2008) and measured the activity of tyrosine kinase namely Antibody Beacon tyrosine kinase (ABTK) (Seethala and Menzel**,** 1997) for screen new EGFR inhibitors from Thai herbs.

OBJECTIVES

1. To clone and express tyrosine kinase domain of EGFR in suitable host.

2. To develop an inhibiting activity assay of tyrosine kinase of EGFR for screening the new EGFR inhibitor.

LITERATURE REVIEW

1. EGFR

The processes of cell division, growth, differentiation, and death in response to external stimuli are highly regulated physiological phenomena in mammalian organisms. The principal components of this system include sensors for external signals, a transmission and communication machinery, and intracellular effectors elements. One of the critical elements in this cascade involved in the sensing of extracellular stimuli are the membrane receptors. There are several classes of transmembrane receptors that play a pivotal role in the regulation of diverse cellular functions (Bassing *et al.,* 1994; Friesel and Maciag, 1995; Goldstein, 1992; Jiang *et al.,*1996; Visser *et al.,*2001; van der Geer *et al.,*1994). One of the best characterized families of membrane receptors is the receptor tyrosine kinase (RTK), and within this category, the epidermal growth factor receptor (EGFR). The epidermal growth factor (EGF) was one of the first peptide growth factors discovered in the early 1950s. Two decades later, the 170-kDa transmembrane EGFR was discovered and characterized as a RTK family member of growth factor receptors and remains as one of the best characterized RTKs today. The EGFR family is composed of four members: EGFR (also known as ErbB1/HER1), ErbB2/HER2, ErbB3/HER3 and ErbB4/HER4 (Figure 1).

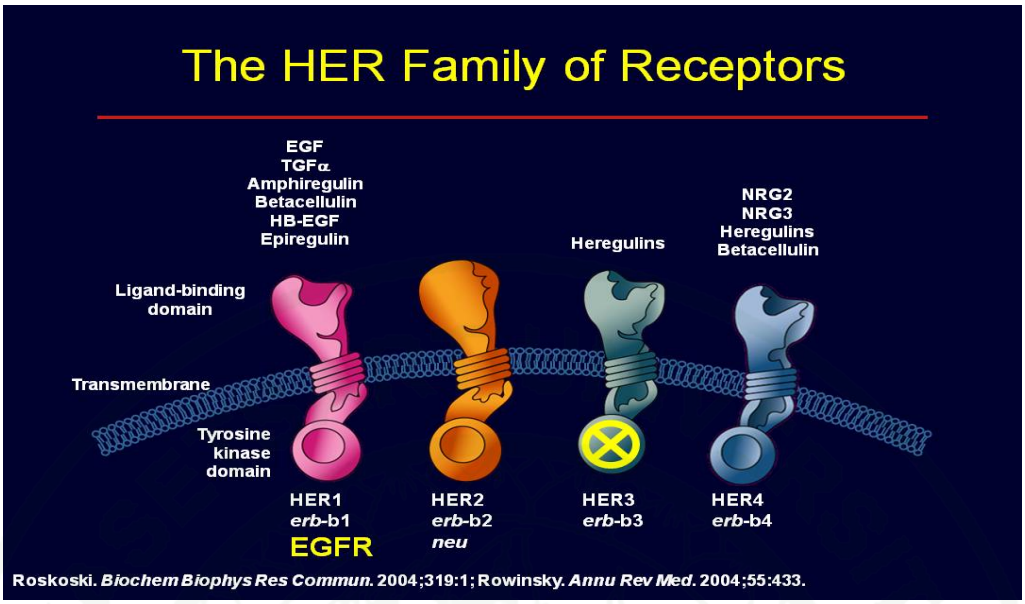

Figure 1 EGFR family scheme.

Source: Roskoski (2004); Rowinsky (2004)

All EGFR family members share the same modular structure composed of an extracellular domain, a single transmembrane region, and an intracellular protein tyrosine kinase domain (Ullrich and Schlessinger, 1990; Alroy and Yarden, 1997). Binding of activating ligands to the extracellular domain of the receptor results in activation of the receptor and, consequently, activation of a series of downstream signal transduction mediators that transmit signals to the cell nuclei (Alroy and Yarden, 1997; Yarden, 2001). The EGFR is involved in the regulation of several key cellular processes such as cell proliferation, survival, adhesion, migration, and differentiation and is involved in the morphogenesis of many organs (Olayioye *et al.,* 2000). Important insight in the function of the EGFR has been obtained from experiments with knockout mice. Mice lacking the EGFR have abnormal eyes and epidermal tissues and die because of altered formation of epithelial organs. (Miettimen *et al.,* 1995; Sibilia and Wagner, 1995; Threadgill *et al.,* 1995).

Several lines of evidence, including pre-clinical and clinical studies have clearly indicated that the aberrant expression and activation of the EGFR results in

transformation and tumor development (Olayioye *et al.,* 2000; Klapper *et al.,* 2000). In addition, the EGFR is anomalously expressed or activated in multiple human neoplasms and has been, in general, associated with a worse prognosis (Solomon *et al.,* 1995). Importantly, inhibition of the EGFR has been demonstrated to have antitumor properties in multiple preclinical models (Chen *et al.,* 1987; Carter *et al.,* 1992; Drebin *et al.,* 1985; Goldstein *et al.,* 1995)**.** On the basis of these data, the EGFR has become a target for anticancer drug development, and several inhibitors of the EGFR are currently in clinical development. This review article provides a summary of the principal biologic features of the EGFR, its role in cancer development, and the different strategies being used to inhibit the EGFR in clinical trials.

1.1 EGFR family of receptor tyrosine kinases

The EGFR family of RTKs comprises four members (collectively referred to as the ErbB or HER family): EGFR itself, ErbB2 (HER2/Neu), ErbB3 (HER3), and ErbB4 (HER4) (Figure 1). Like all RTKs, each ErbB receptor comprises a large extracellular region, a single spanning transmembrane (TM) domain, an intracellular juxtamembrane (JM) region, a tyrosine kinase domain, and a C-terminal regulatory region (Figure 2a). The ligands that regulate ErbB receptors can be separated into two main groups (Figure 3): the EGF agonists that activate EGFR, and the neuregulins (NRG) that bind ErbB3 and ErbB4 (Yarden and Sliwkowski, 2001). There are at least seven different EGF agonists: EGF, transforming growth factor α (TGFα), amphiregulin (AR), betacellulin (BTC), epigen (EPN), epiregulin (EPR), and heparin binding EGF-like growth factor (HBEGF) (Harris *et al.,* 2003). Of these, a subset can also activate ErbB4 and are known as the bi-specific ligands (BTC, EPR, and HB-EGF). ErbB3 and ErbB4 are regulated by multiple differently spliced variants of the four different NRG gene products (Falls, 2003). Each ErbB ligand contains an EGF-like core domain of about 60 amino acids (Figure 3) that is sufficient for its biological activity (Harris *et al.,* 2003). ErbB2 has no known soluble ligand and has been proposed to play a role in ErbB receptor activation by forming heterodimers with other liganded ErbB family members (Citri *et al.,* 2003; Yarden and Sliwkowski,

2001). ErbB2 is also distinguished from other members of this receptor family in that overexpression of ErbB2 causes ligand-independent cell transformation (Di Fiore *et al.*, 1987). As shown in figure 3, and discussed in detail below, ErbB2 also turns out to be an outlier structurally.

The extracellular regions of EGFR family members contain two homologous ligand binding domains (domains I and III) and two cystine-rich domains (domains II and IV; Figure 2). The only other RTKs with a similar extracellular domain arrangement are members of the insulin receptor (IR) family, which share the same domain I/II/III organization, but the membrane proximal cystine-rich domain IV of ErbB receptors is replaced by fibronectin type III domains in the IR family. By contrast with the EGFR and IR families most other RTKs have extracellular regions comprised of immunoglobulin or fibronectin type III domains (Hubbard and Till, 2000). Just as they are distinct in their domain composition, so do the IR and ErbB families differ from other RTKs in their mechanisms of ligand activation (Ward *et al.,* 2007).

Although high-resolution structural studies of intact RTKs pose technical challenges that have not yet been overcome, there is a wealth of structural data on both the extra- and intracellular regions of the EGFR family. X-ray crystal structures have been determined for the extracellular regions of all four ErbB receptors (sErbBs) in their unliganded state (Bouyain *et al.,* 2005; Cho and Leahy, 2002; Ferguson *et al.,* 2003; Franklin *et al.,* 2004) (Figure 3). The structure of the EGFR soluble extracellular region (sEGFR) has also been determined in a dimeric—presumably activated—state induced by binding of EGF or TGFα (Garrett *et al.,* 2002; Ogiso *et al.,* 2002) (Figure 4). Additional insight into the mechanisms of extracellular control has also been provided by three different structures of sErbB proteins in complex with the Fab fragments of inhibitory therapeutic antibodies (Cho *et al.,* 2003; Franklin *et al.,* 2004; Li *et al.,* 2005). The structure of the intracellular kinase domain of EGFR has also been extensively studied in different activation states (Stamos *et al.,* 2002; Wood *et al.,* 2004; Yun *et al.,* 2007; Zhang *et al.,* 2006). Structural details of the individual domains of EGFR and their homologues have been extensively reviewed

else-where (Adams *et al.,* 2000; Hubbard and Till, 2000; Leahy, 2004) and are summarized briefly in the legend to figure 2.

Despite this wealth of structural information, there are important regions of EGFR for which relatively little data are available. For example, little is known about the structure of the first ~30 amino acids of the intracellular JM region (Figure 2a), which may play an important regulatory role (Hubbard *et al.,* 2004; McLaughlin *et al.,* 2005). Moreover, the most C-terminal ~190 amino acid region of EGFR that contains multiple tyrosine phosphorylation sites is poorly characterized but is implicated in regulation of receptor activation (Linggia and Carpenter, 2006).

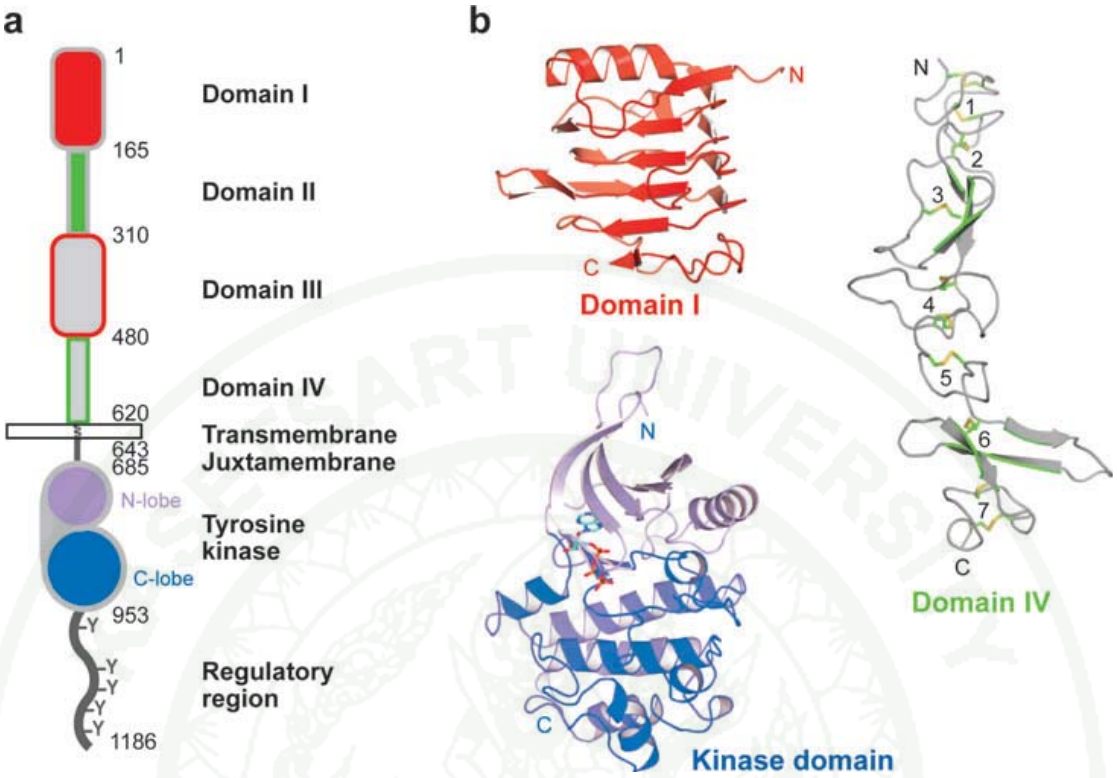

Figure 2 The domains of EGFR. (*a*) The extracellular region comprises four domains: I–IV, sometimes referred to as L1, CR1, L2, and CR2 or L1, S1, L2, and S2, respectively. Domains I (*red*) and III (*gray with red outline*) share about 37% sequence identity, while domains II (*green*) and IV (*gray with green outline*) are cystine-rich. The N-lobe of the kinase domain is in lavender and the C-lobe is in blue. (*b*) Representative ribbon diagrams of the domains of EGFR. Domains I and III adopt a β-helix fold; here domain I from PDB ID 1YY9 is shown. Domains II and IV adopt extended structures comprising a series of disulfide-bonded modules. Domain IV from PDB ID 1YY9 is shown with the disulfides in stick representation and the disulfide-bonded modules numbered. The inactive kinase is shown (PDB ID 2GS7) with the ATP analogue (AMP-PNP) in stick representation.

Source: Ferguson (2008)

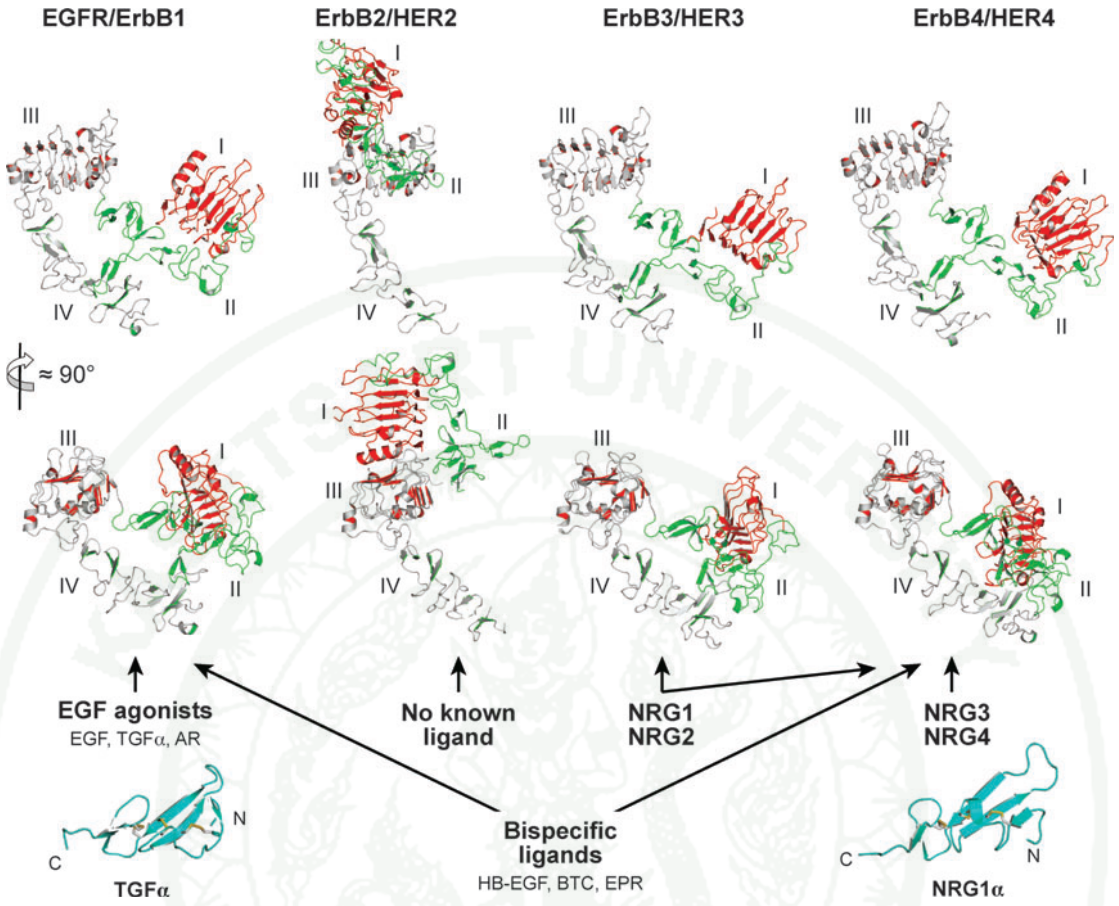

Figure 3 The extracellular regions of ErbB receptors and their activating ligands. Two orthogonal ribbon diagrams are shown for each unliganded ErbB receptor (PDB IDs 1NQL, 1N8Z, 1M6B, and 2AHX). The coordinates of domain III only were used to align the structures. ErbB2 is an outlier adopting an extended rather than tethered arrangement of domains. This extended arrangement of the domains of ErbB2 is similar to the domain arrangement observed in the ligand-induced dimer of sEGFR (Figure 4). Ligands are listed, grouped according to the receptors they activate. Ribbon diagrams of TGFα (*left*; PDB ID 1MOX) and NRG1α (*right*; PDB ID 1HRE) are shown in cyan as representative structures of the EGF-like domain of ErbB ligands. The scale for the ligands is twice that used for the receptor extracellular regions.

Source: Ferguson (2008)

1.2 The unexpected receptor-mediated dimer of the extracellular region of EGFR

In 2002, two papers published back-to-back in *Cell* radically changed the mechanistic view of ligand-induced EGFR dimerization. They described a dimer in which all contacts between the two molecules were receptor mediated (Garrett *et al.,* 2002; Ogiso *et al.,* 2002). This contrasts starkly with the direct contribution of the bound ligand to the dimer interface of other cytokine receptor and RTK dimers that have been studied (Boulanger and Garcia, 2004; Burgess *et al.,* 2003; Hubbard and Till, 2000; Schlessinger, 2000). For many RTKs, such as those of the platelet derived growth factor (PDGF)/Kit receptor family, the ligands themselves are dimeric and bivalent. In Kit, each protomer in the ligand contacts a different receptor molecule, so that the dimeric ligand effectively cross-links the receptor into a dimeric complex (Liu *et al.,* 2007; Yuzawa *et al.,* 2007). In other cases, such as the fibroblast growth factor (FGF) receptor, accessory molecules (heparan sulfate proteoglycans) link the two ligands to yield a bivalent complex that effectively cross-links two receptor molecules (Schlessinger, 2000).

In the dimeric complexes formed when EGF or TGFα bind to the first three domains of sEGFR, the growth factor binding sites are distant from the dimer interface and do not contribute directly to dimer contacts (Figure 4b). All contacts across the dimer interface are mediated by domain II of the receptor—making these dimers receptor mediated rather than ligand mediated (Schlessinger, 2002). A beta hairpin, referred to as the dimerization arm, in domain II makes extensive contacts with the domain II of its binding partner, reaching at its tip to interact with the opposite domain I (Figure 4b, c). EGF/TGFα is bivalent; each ligand binds simultaneously to domains I and III of the same receptor molecule.

Structures of unliganded sErbB receptors indicated that exposure of the dimerization arm is a key event in regulation of receptor dimerization. Indeed, in the inactive/unliganded form of sEGFR and sErbB3, the dimerization arm is buried by intramolecular interactions with domain IV (Cho and Leahy, 2002; Ferguson *et al.,*

2003; Li *et al.,* 2005). The intramolecular interactions in this so called tethered conformation of the receptor and the intermolecular interactions across the dimer interface are mutually exclusive. This led to the proposal that the tethered sEGFR and sErbB3 structures represent an autoinhibited conformation (Burgess *et al.,* 2003; Ferguson *et al.,* 2003), since also seen for sErbB4 (Bouyain *et al.,* 2005).

The tethered configuration of unliganded sEGFR, sErbB3, and sErbB4 also places the two ligand-binding sites on domains I and III relatively distant from one another. For a single EGF molecule to contact these two binding sites simultaneously, a large domain rearrangement is required in sEGFR (Figure 4c). This domain rearrangement allows domains I and III to dock onto the same EGF molecule, while simultaneously exposing the dimerization arm in an extended sEGFR conformation that closely resembles the structure observed in the dimeric complexes with bound EGF or TGFα (Figure 4c) (Ferguson *et al.,* 2003).

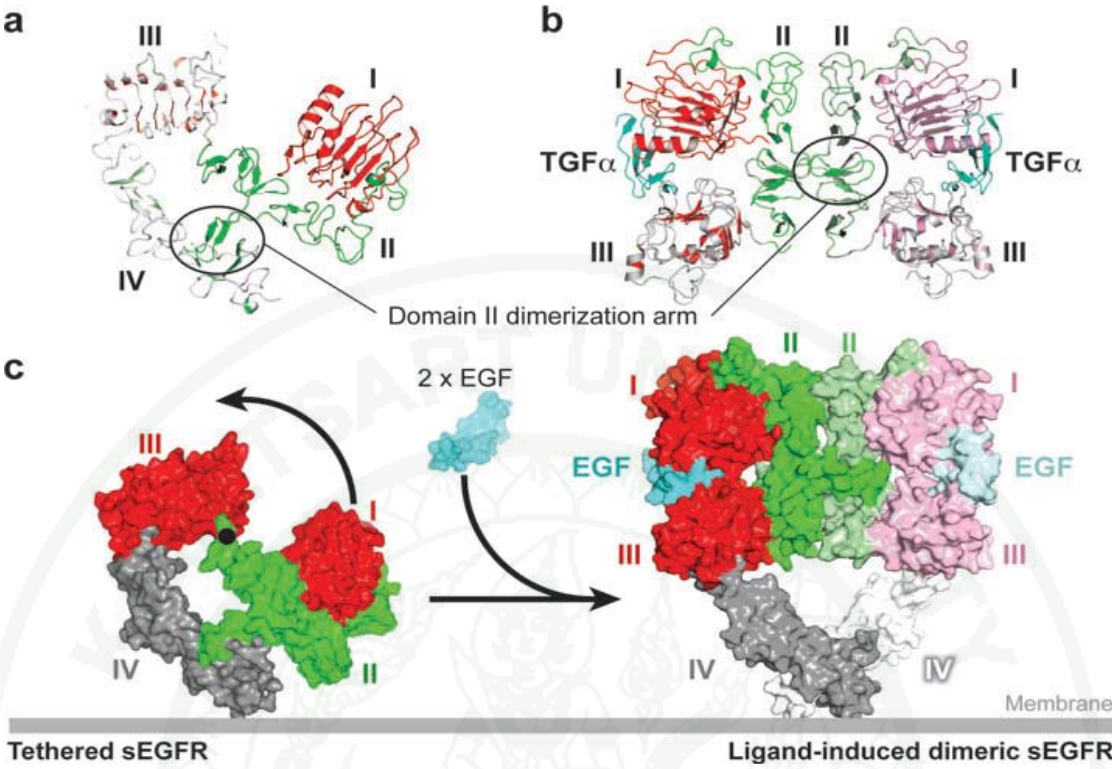

Figure 4 Ligand-induced dimerization of the extracellular region of EGFR. (*a*) Ribbon diagram of the tethered sEGFR (PDB ID 1YY9) oriented as in the upper panel of figure 3. (*b*) Ribbon diagram of the TGFα-induced dimer of sEGFR501 (PDB ID 1MOX). The orientation of domain III is as in the lower panels of sErbB ribbon diagrams in Figure 3. The colors of the left-hand molecule have been lightened for contrast. (*c*) A molecular surface representation of tethered sEGFR in the same orientation as in panel *a*, with domains I and III in red, II in green, and IV in gray. A ≈130° rotation about the indicated axis (*black dot*) plus 20 °A translation into the plane of the page is required to bring domain I from its position in the tethered structure (*left*) to its location in the dimer (*right*) (22). In this model of the sEGFR dimer, domain IV is included so as to maintain the same domain III/IV relationship as in the tethered structure. Domains I, II, and III in the dimer are from PDB ID 1IVO and are shown in the same orientation as in panel *b*.

Source: Ferguson (2008)

1.3 A structure-based model for ligand-induced EGFR dimerization

Exposure of the dimerization arm is the most obvious change induced upon binding of growth factor ligands to the EGFR extracellular region (Figure 5), but it remains unclear exactly how this is achieved. The ligand binding domains I and III are identical in structure whether bound to ligand or not (Ferguson, 2004; Li *et al.,* 2005), arguing against an allosteric mechanism for triggering exposure of the dimerization arm. EGF (or TGFα) binds to a truncated sEGFR (sEGFR501) that cannot form the intramolecular domain II/IV tether (with domain IV removed) only ~20–30-fold more strongly than it binds to intact sEGFR (Dawson *et al.,* 2005; Elleman *et al.,* 2001; Ferguson *et al.,* 2003). This observation suggests that the tether provides only a modest energy barrier to the close apposition of domains I and III—of the order of 2 kcal mol^{-1}. If the tether is this weak, it seems reasonable to suggest that the EGFR extracellular region could exist in a dynamic equilibrium, sampling multiple conformations including tethered and various untethered states. Binding of growth factor to domains I and III could then trap untethered receptors in a dimerization-competent extended configuration, driving the system toward the active dimeric form (Burgess *et al.,* 2003). There has been no direct analysis of the structural dynamics of sEGFR invoked by this model, and this remains an important knowledge gap in the field.

Although there is no doubt that exposing the domain II dimerization arm is necessary for EGFR dimerization, it is not sufficient. Indeed, sEGFR501 remains monomeric unless EGF/TGFα is added (Elleman *et al.,* 2001). Recent studies argue that much smaller adjustments in the conformation of domain II at the dimer interface are also critical (Dawson *et al.,* 2005). As can be appreciated in Figure 5, significant local conformational changes in domain II accompany the dramatic domain rearrangement. These changes result in a different trajectory of the dimerization arm in the extended compared to the tethered receptor, and significantly alter the overall curvature of the long axis of domain II (Figure 5a). Because domain II forms the dimer interface, this change in curvature upon ligand binding could have substantial implications for dimerization strength.

The domain II conformation remains similar in the tethered and extended receptors for the first three disulfide-bonded modules, which are stabilized by interaction with domain I. However, the structures begin to deviate significantly at disulfide-bonded module 4 (Figure 5a), so that domain II has a different overall curvature between disulfide bonded modules 5 and 8 in the tethered and extended forms. The consequences of the different domain II curvatures can be better appreciated if the two conformations are superimposed using the central disulfide bonded module 5 as a reference point (Figure 5d). In dimers constructed from these domain II conformations, disulfide bonded modules 2 and 6 projects further into the dimerization interface in the extended or activated structure than in the tethered or inactive structure. The relative projection of these two modules into the dimer interface allows them to form direct contacts across the dimer interface, as directly observed in the crystal structures of ligand-bound sEGFR (Garrett *et al.,* 2002; Ogiso *et al.,* 2002). Mutational analysis demonstrates that interfacial interactions from module 6 (involving D279 and H280) contribute substantially to dimer stability, while those from module 2 (involving Q194) contribute to a smaller extent (Dawson *et al.,* 2005). The conformation of domain II in the region of disulfide-bonded module 6 is stabilized in part by direct interactions with domain III (Figure 5b) (Dawson *et al.,* 2005; Ogiso *et al.,* 2002). Binding of EGF or TGFα to sEGFR drives a dramatic reorientation of domain III (compare Figure 4b with 3c) and promotes domain II/III interactions that stabilize the precise conformation of domain II in this region (around module 6) that is required for dimerization.

It has also been suggested that domain IV contributes directly to stabilization of the ligand-induced sEGFR dimer (Burgess *et al.,* 2003; Ferguson *et al.,* 2003), although it was not present in the published dimer structures. If the relationship between domains III and IV remains fixed in tethered (monomeric) and extended (dimeric) sEGFR, the two copies of domain IV are predicted to make contact across the dimer interface (Figure 4c). However, in studies of soluble sEGFR variants, deletion of a putative domain IV interaction loop or deletion of almost all of domain IV had only minimal effects on dimerization strength (Dawson *et al.,* 2005). It is possible that rather weak domain IV interactions aid in orientating the membrane

proximal parts of the EGFR extracellular region in an intact EGFR dimer at the cell surface (Berezov *et al.*, 2002). Indeed, such weak association between the membrane proximal domains of another RTK, Kit, has recently been crystallographically visualized in a ligand-induced dimer (Yuzawa *et al.*, 2007), and this could be an important theme for interactions in the extracellular region of many RTKs.

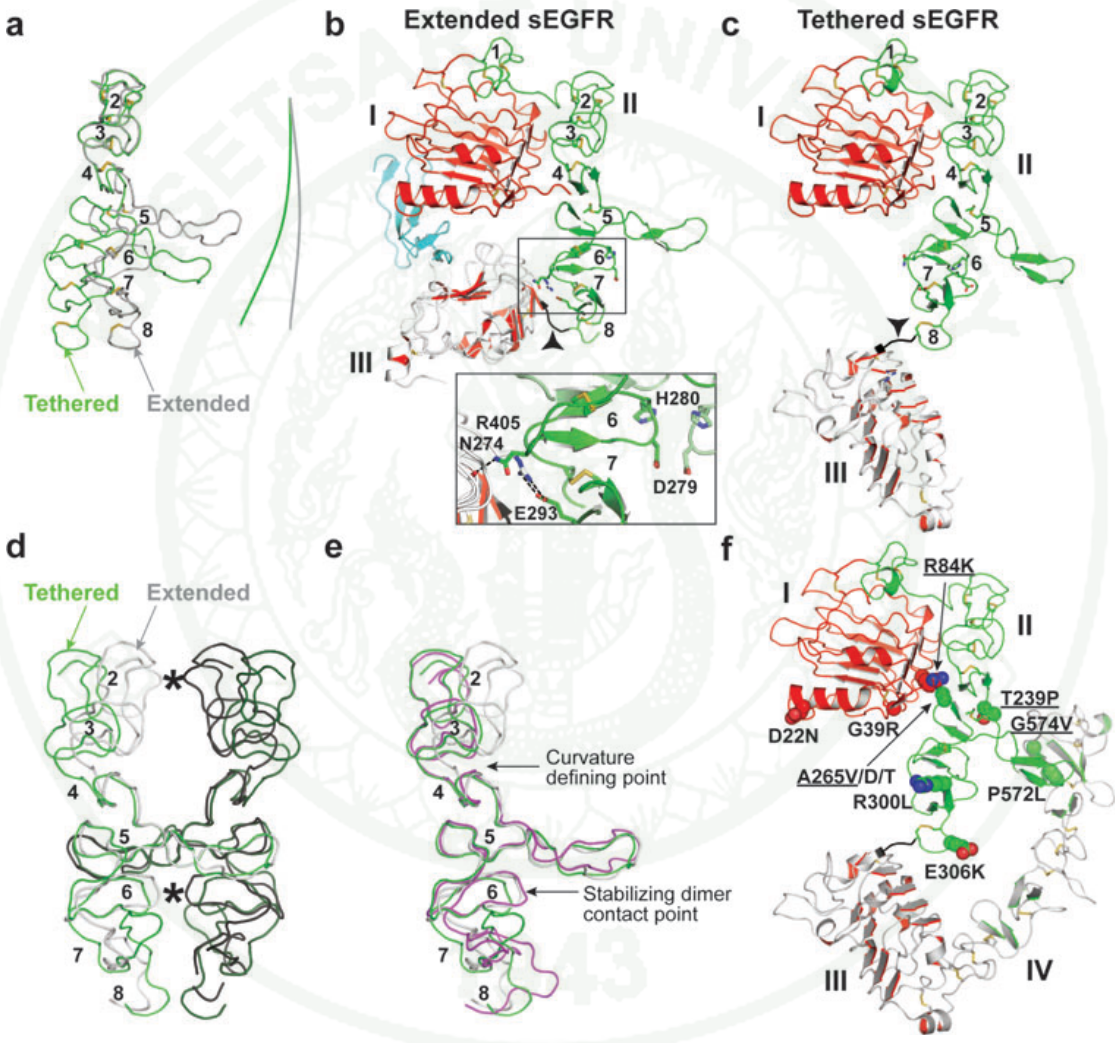

Figure 5 Conformational changes in domain II of sEGFR. (*a*) Smoothed backbone representations of domains II from extended (*gray*) and from tethered (*green*) sEGFR. The coordinates of domain I and of the first three disulfide-bonded modules of domain II (amino acids 1–225) were used to superimpose the two structures. The lines to the right indicate the curvature of the long axis of domain II. Disulfide bonds are shown (*a–c*, *f*)

Figure 5 (Continued)

and disulfide-bonded modules numbered (*a*–*e*, module 1 is not shown in *a*, *d,* or *e*). (*b*) Ribbon diagram of domains I, II, and III from extended sEGFR (PDB ID 1MOX) oriented as in panel *a*. The area of detail (*inset*) shows the domain II/III interactions that contribute to stabilizing module 6. Contacts between domains II and III buttress module 6 of domain II, positioning the D279/H280 loop for optimal interaction across the dimer interface. (*c*) Ribbon diagram of domains I, II, and III from tethered sEGFR (PDB ID 1YY9), oriented as in *a*. Note the distinctly different trajectory of the end of domain II (in *black* and marked with an *arrowhead*) compared to panel *b*. (*d*) Domain II from the sEGFR501/TGFα dimer is shown with the left-hand molecule in gray and the right-hand molecule in black. Contact points across the dimer are indicated with asterisks. Using coordinates from disulfide-bonded module 5 only, domain II from tethered sEGFR has been superimposed first on the right-hand extended domain II (*green*) and then on the left-hand extended domain II (*dark green*) to create a model for a dimer of two domain II molecules that are in the conformation adopted in the tethered structures. (*e*) Domain II from extended (*gray*) and from tethered (*green*) sEGFR and from sErbB2 (*magenta*) shown in same orientation as in panel *d*. Module 6 of sErbB2 overlays with that of extended sEGFR. However, the structure of sErbB2 domain II deviates from that of extended sEGFR in both the N- and C-terminal parts of domain II. (*f*) Ribbon diagram of tethered sEGFR in the same orientation as in panel *c* and with the positions of somatic mutations in glioblastoma shown in space filling representation. Those mutations that have been shown to cause activation of EGFR are underlined.

Source: Ferguson (2008)

1.4 Extracellular EGFR mutation in cancer

Somatic mutations were recently identified in glioblastomas that map to the extracellular region of EGFR, and a subset of these enhanced receptor activation (Figure 5f) (Lee *et al.,* 2006). Several of these mutations fall in the vicinity of the intramolecular tether (e.g. P572L and G574V) and could destabilize domain II/IV interactions—although these mutations are not likely sufficient for EGFR activation given the discussion presented above. Other mutations cluster in different parts of the extracellular region. One group falls close to disulfide-bonded module 8 of domain II and could affect the main chain rigidity in this region—although the effects of these mutations on EGFR activation was not reported. Another cluster of mutations at the domain I/II interface is interesting. In the tethered receptor, A265 from disulfide bonded module 5 of domain II packs against the aliphatic portion of R84 from domain I (Figure 5f). Mutations at either of these positions lead to EGFR activation (Lee *et al.,* 2006), which could possibly result from alterations in the conformation of domain II.

Further studies of the effects of these mutations (and their combinations) on the conformational properties of the EGFR extracellular region should provide important insight into the structural restraints that keep sEGFR in a tethered-like conformation, and into the energetic barriers to its extension and dimerization.

1.5 Activation of the intracellular tyrosine kinase domain of EGFR

The unique mechanism of ligand-induced dimerization is not the only feature that sets EGFR apart from other RTKs. Recent structural studies of the intracellular EGFR tyrosine kinase domain (EGFR-TK) also suggest that it is regulated through an unexpected set of interactions (Zhang *et al.,* 2006). The formation of an asymmetric kinase domain dimer is critical.

The first reported crystal structures of EGFR-TK revealed a conformation with characteristics of an activated kinase (Stamos *et al.,* 2002), based on the

structural features of its activation loop and the orientation of the C helix (in the N-terminal lobe). Although the apparently constitutive adoption of such an active conformation was surprising, it was consistent with the fact that EGFR is unusual in not requiring activation-loop phosphorylation to promote its activity (Gotoh *et al.,* 1992). These structures suggested a notable absence of autoinhibitory interactions in the EGFR kinase domain, by contrast with the well-defined interactions that maintain the kinase domains from the insulin receptor, FGF receptor, and other RTKs in their inactive states (Huse and Kuriyan, 2002). From among the possible interpretations of this structural view (Burgess *et al.,* 2003), elegant studies from the Kuriyan laboratory (Zhang *et al.,* 2006) argue that crystal packing mimics interactions found in an active receptor dimer, which lead to activation of EGFR-TK through an allosteric mechanism.

Structures of EGFR-TK bound to the therapeutic inhibitor lapatinib (Wood *et al.,* 2004) and of an EGFR kinase mutant bound to AMP-PNP (Zhang *et al.,* 2006) revealed that EGFR-TK can also adopt a characteristic inactive structure (Figure 6a) with clear intramolecular autoinhibitory interactions. The two inactive EGFR-TK structures are virtually identical to one another and resemble inactive forms of cyclin-dependent kinases (CDKs) and Src-family kinases (Huse and Kuriyan, 2002). In each case, a short helical region in the activation loop is packed against the catalytically critical C-helix, which contains a conserved glutamate that must form an ion pair with a lysine that coordinates ATP's α- and β- phosphates. The C-helix is displaced (and this ion pair is disrupted) by interaction with the activation loop in inactive EGFR-TK, Src-family, or CDK kinases.

Mutations that disrupt the interactions between the C-helix and activation loop (Figure 6) activate EGFR-TK (Choi *et al.,* 2007; Riese *et al.,* 2007; Zhang *et al.,* 2006) and are clinically important. The C-helix/activation loop interactions are also incompatible with the packing of EGFR-TK molecules in crystals of the active state. In numerous crystals of active EGFR-TK, an asymmetric dimer can be identified in which the helical C-lobe of one EGFR-TK molecule abuts the N-lobe of its neighbor in the crystal in an interaction that is highly reminiscent of the activating interaction

between helical cyclins and the CDKs (Jeffrey *et al.,* 1995; Zhang *et al.,* 2006). This asymmetric dimer occurs in the crystal lattice of all cases where the active conformation is observed for EGFR-TK, and interactions of the C-helix of one EGFR-TK molecule (in the N-lobe) with the C-lobe of its neighbor (Figure 6b) appear to disrupt the autoinhibitory interactions described above (and are stabilized by the inhibitor lapatinib). In fact, EGFR-TK could only be crystallized in its inactive conformation in the presence of lapatinib (Wood *et al.,* 2004) or with a mutation that disrupts the CDK/cyclin-like dimer (Zhang *et al.,* 2006). Moreover, mutations designed to disrupt the asymmetric dimer interface shown in figure 6b prevented EGF activation of the intact EGFR (Zhang *et al.,* 2006).

Thus, contrary to initial suggestions, EGFR-TK does adopt an autoinhibited conformation in the absence of ligand-induced dimerization, as observed for most other RTKs. However, the mechanism of EGFR-TK activation is unique whereas most RTKs reach full activity following *trans*-autophosphorylation of their kinase domains within a dimer, EGFR-TK forms an asymmetric dimer that allosterically activates the kinase domain.

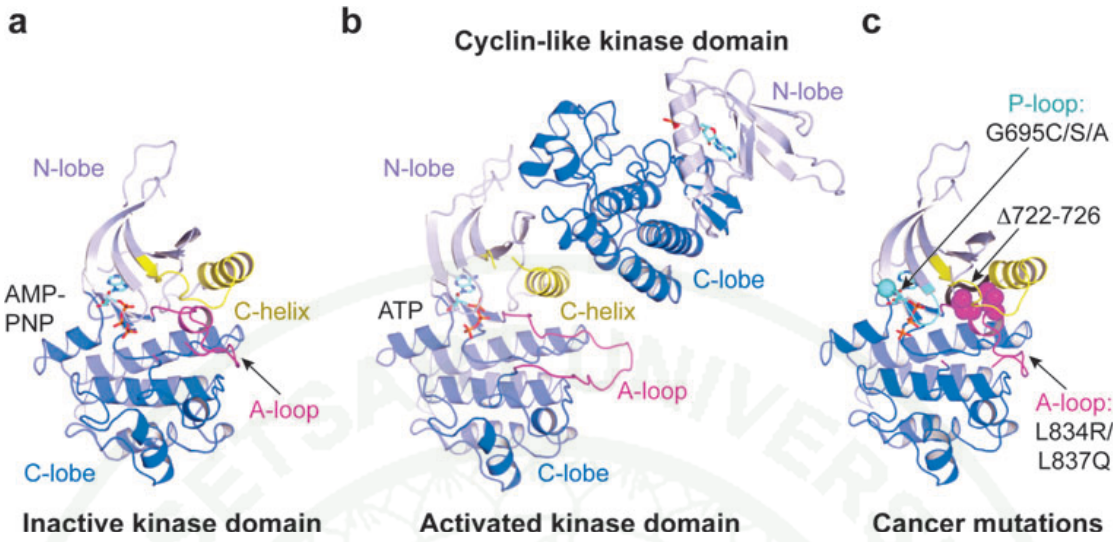

Figure 6 Activation of the EGFR kinase domain. (*a*) Ribbon diagram of the EGFR kinase domain in the inactive conformation with AMP-PNP in stick representation (PDB ID 2GS7). The activation loop (A-loop) is in magenta and the catalytically important C-helix is in yellow. (*b*) Ribbon diagram of the asymmetric EGFR kinase domain dimer (PDB ID 2GS6) with the ATP moiety of the bound ATP-peptide conjugate in stick representation. The conformation of the activation loop (*magenta*) and position of the C-helix (*yellow*) are consistent with an active kinase (Huse and Kuriyan, 2002). (*c*) Ribbon diagram of the inactive kinase domain in the same orientation and colors as in panel *a*. The locations of somatic mutations identified in nonsmall cell lung cancer are indicated.

Source: Ferguson (2008)

1.6 Mechanism of EGFR activation at the cell membrane

In figure 6, an overall model is presented that combines structural information for EGFR on the outside and on the inside of the membrane. In the resting state, EGFR is shown with its extracellular region in the tethered configuration and its kinase domain in the inactive form. Ligand binding to the extracellular region induces receptor-mediated dimerization that brings the intracellular domains into

close proximity, and promotes the association of the kinase domains in an asymmetric dimer. In the asymmetric EGFR-TK dimer, one molecule is activated through interaction of its N-lobe with the C-lobe of the cyclin-like activator (shown in the inactive conformation). It is thought that the activated kinase phosphorylates the C-terminal tail of the activator (cyclin-like) receptor. In a subsequent step (not shown) it is proposed that the roles of the two receptors switch, such that both intracellular domains can become *trans*-autophosphorylated.

There is structural information for all but the most C-terminal half dozen amino acids of the extracellular region, which link to the presumably helical TM domain. The TM helices of ErbB receptors self- and hetero-associate in membranes (Mendrola *et al.,* 2002). Although TM interactions of this sort may aid in stabilizing the dimer, or in orienting its components, mutations that disrupt TM domain association do not influence receptor signaling (Carpenter *et al.,* 1991; Kashles *et al.,* 1988). On the intracellular side of the membrane, several key pieces of information remain missing—as implied in Figure 6. There is no reliable structural information for the first ~30 amino acids of the intracellular JM region. By analogy with other RTKs, this region may play a regulatory role—possibly contributing to autoinhibition (Hubbard, 2004). A basic stretch at the beginning of this JM region has been reported to associate with acidic lipids in the inner leaflet of the membrane and this could promote association of the kinase domain itself with the membrane through electrostatic interactions (McLaughlin *et al.,* 2005). Membrane tethering of this type is proposed to have an autoinhibitory influence on EGFR, which is reversed when calcium/calmodulin (Ca/CaM) binds to the JM region and dissociates it from the membrane. Once released from the membrane the intracellular domains are proposed to come together to form the asymmetric dimer outlined above. If the asymmetric dimer depicted in figure 6 forms with its TM domains in contact, the JM region will have to adopt an extended structure in order to link the N termini of the two kinase domains, which are separated in this model by ~50 A°.

The C-terminal ~190 amino acids of EGFR have not yet been resolved in any crystal structures. Circular dichroism studies indicate a significant amount of

secondary structure in this region (Lee *et al.,* 2006). Hydrodynamic studies show that the relationship between the large C-terminal regulatory region and the TK domain is altered upon autophosphorylation (Cadena *et al.,* 1994). FRET studies indicate that the C-terminal and TK domains become separated—to give a more extended molecule—following activation and phosphorylation (Lee and Koland, 2005), possibly reflecting loss of intramolecular interactions. It is intriguing that the side chains of Y974 and Y992 in the C-terminal domain, two of the EGFR autophosphorylation sites (Schulze *et al.,* 2005), make well-defined interactions with theTKdomain (Wood *et al.,* 2004; Zhang *et al.,* 2006). Disruption of interactions like this could be responsible for the changes in overall intracellular region structure upon EGFR autophosphorylation and could in turn influence enzymatic activity of the TK domain. The C-terminal region of EGFR may thus play an autoinhibitory role (Walton *et al.,* 1990), and autophosphorylation could reverse this through the types of conformational changes seen in hydrodynamic and FRET studies. A structural view of this region remains one of the key challenges in this field.

1.7 EGFR Signaling cascade

The process of receptor dimerization activates the tyrosine kinase domain of the receptor resulting in autophosphorylation of several tyrosine residues in the intracellular domain of the receptor which, in turn, creates docking sites for cytoplasmatic signal molecules, containing Src homology 2 (SH2) or phosphotyrosine-binding (PTB) sites. Included in this category are adaptor proteins (such as Shc, Crk, Grb2, Grb7, Gab1), kinases (such as Src, Chk, PI3K), and protein tyrosine phosphatases (such as SHP1, SHP2). The EGF family of receptors activates a variety of signal transduction pathways such as the PLC-γ1, Ras/Raf/MEK/MAPKs, phosphatidylinositol-3 kinase (PI3K)/Akt, tyrosine kinase Src, stress-activated protein kinases (SAPKs), PAK/JNKK/JNK, and signal transducers and activators of transcription (Yarden, 2001). Although there is significant overlap with regard to the specific signaling pathways activated by the EGF family of receptors, the MAP kinase pathway is commonly activated by all members of the family (Prenzel *et al.,* 2001). Each HER RTK displays a different pattern of C-terminal tyrosine residues and,

hence, has some selectivity with regard to the specific signaling pathways that are activated on receptor phosphorylation. For example, the HER3, because of its multiple binding sites for p85, the regulatory unit of PI3K, preferentially activates the PI3K pathway (Carraway *et al.,* 1994).

The multitude of ligands, the formations of different homodimers and heterodimers among the EGFR family members and the diversity of signaling pathways activated by the EGF family of receptors tremendously increases the complexity and diversity of this network. Among the multitude of signaling pathways, the MAP kinase and the PI3K/Akt pathways are the best characterized and are discussed in more detail below (Figure 7). As mentioned above, the phosphorylated tyrosine residues in the intracellular domain of the receptor serve as binding sites for the SH2-containing adaptors Shc and Grb2. These events are followed by activation of the small G protein Ras through the guanine nucleotide exchange factor Sos, which stimulates the exchange of GTP for GDP on Ras (Schlessinger and Bar-Sagi, 1997; Bar-Sagi and Hall, 2000; Margolis *et al.,* 1999; Pawson, 1995). The activated Ras protein is able to activate other effector molecules such as Raf and the dual specific kinase MEK1, finally activating Erk 1/2, which ultimately regulates transcription factors such as Elk-1 and c-fos (Schlessinger, 2000; Garrington and Johnson, 1999). The MAP kinase pathway regulates a variety of different substrates located in the cytosol, membrane, and nucleus, thus regulating important cellular processes, including cell survival and gene transcription (Figure 7) (Ballif and Blenis, 2001; Davis, 2000; Hunter, 2000). The second-best characterized EGFR-regulated signaling pathway is the PI3K/Akt signaling pathway. The PI3K is composed of two subunits, the p85 regulatory subunit and the p110 catalytic subunit. The p85 subunit contains two SH2 and one SH3 domains and forms a complex with phosphotyrosine sites on receptor or the adaptor protein Gab1. The p110 catalytic subunit phosphorylates PIP2 and generates the second messenger PIP3 (Garrington and Johnson, 1999; Bjorge *et al.,* 1990). Because the EGFR has no binding site for the SH2-domain of PI3K, EGF-induced activation of PI3K is relatively weak compared with other members of the family such as HER3, which contains six putative binding sites and potently activates the enzyme (Carraway *et al.,* 1997). PIP3 acts as an important mediator for membrane

translocation of multiple signaling proteins. An important downstream target of PI3K is Akt, which is phosphorylated after membrane recruitment and activation by the threonine kinase PDK1 (Kapeller *et al.,* 2000; Czech, 2000; Rameh and Cantley, 1999), Akt has three different isoforms, which are activated in a distinct but overlapping manner, hence, contributing to the diversification of the EGFR signaling (Walker *et al.,* 1994; Okano *et al.,* 2000). Activation of the PI3K/Akt pathway affects numerous targets either directly or indirectly, which can be basically classified in targets that either regulates survival and death factors or protein translation (Alessi and Cohen, 1998; Datta *et al.,* 1999; Downward, 1998). Cellular survival is dependent on a number of factors, including the pro-apoptotic proteins BAD81 and caspase (Cardone *et al.,* 1998) the growth inhibitory proteins glycogen synthase kinase-3β, (Cross *et al.,* 1995) and the forkhead transcription factors (FKHR, FKGR-L1, AFX), which are all down-regulated by activated Akt (Romashkova and Makarov, 1999; Kane *et al.,* 1999; Mayo and Donner, 2001). Furthermore, the activation of Akt leads to up-regulation of NF-κB via its regulatory kinase IKK-α, which results in transcription of anti-apoptotic genes, and phosphorylation of the p53 inhibitor Mdm2, leading to cytoplasmic accumulation and degradation of the tumor suppressor p53 (Romashkova and Makarov, 1999; Kane *et al.,* 1999; Mayo and Donner, 2001).Stimulation of Akt mediates phosphorylation of BAD, which leads to the inhibition of BAD's ability to bind and block the anti-apoptotic proteins Bcl-2 and Bcl-xl. The second group of Akt-associated targets can regulate protein translation and consists of the mammalian target of rapamycin (mTOR, also known as *FRAP, RAFT*) and its downstream targets p70s6 kinase (p70s6k) and eukaryotic initiation factor binding protein 1 (4E-BP1, also called *PHAS-1*) (Sonenberg and Gingras, 1998; Gingras *et al.,* 1998; Raught *et al.,* 2001). The activity of Akt is negatively regulated by PTEN, a lipid phosphatase. PTEN cleaves the D3 phosphate of PIP3 and prevents activation of Akt (Maehama *et al.,* 1998). Mutations of the PTEN gene lead to aberrant activation of the PI3K/Akt pathway and appear frequently in advanced cancer, which are often associated with advanced clinical stage and poor prognosis (Teng *et al.,* 1997; McMenamin *et al.,* 1999). Besides its crucial role in signal transduction of the PI3K pathway, Akt negatively interferes with the Ras-MAPK pathway by phosphorylating and inactivating Raf (Figure 7) (Zimmermann *et al.,*

1999), making the complete picture of the vast and diverse EGFR signaling network even more complex.

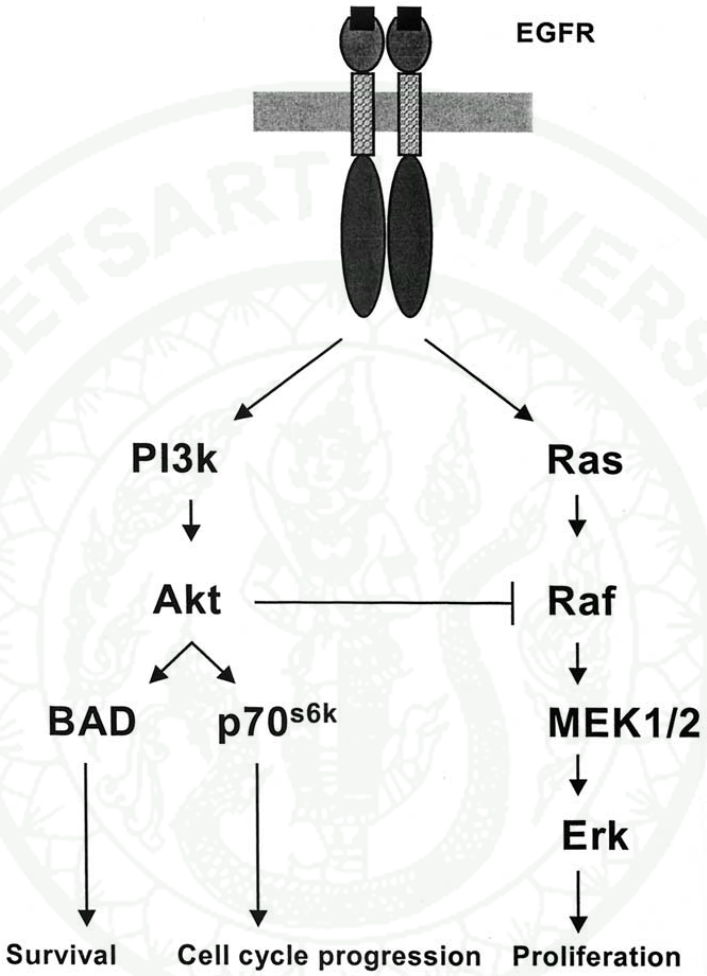

Figure 7 Ligand binding initiates HER dimerization and autophosphorylation, mediating further activation of downstream signaling pathways. The ligands' ability to induce receptor dimerization differs among the 4 classes of ligands, and receptor dimers recruit different downstream signaling proteins. For simplification, only the PI3k/Akt and the MAPK pathways are outlined in the figure, which promote cellular functions such as survival, cell cycle progression, and proliferation.

Source: Grünwald and Hidalgo (2002)

2. Implications of the EGFR in cancer development and progression: mechanisms of tumorigenesis

A substantial amount of pre-clinical and clinical data indicates that the aberrant functioning of the EGF family of receptors is involved in the process of tumor genesis and progression. One of the first pieces of evidence implicating the EGF family of receptor in cancer comes from the study of oncogenic viruses. The EGFR was discovered to be the cellular homolog of the avian erythroblastosis virus *v-erbB* oncogene. This gene encodes a C-terminus truncated form of erbB1 lacking the extracellular domain of the receptor capable of ligand independent activation (Downward *et al.,* 1984). The EGFR signaling pathway is also implicated in the pathogenesis of multiple oncogenic viruses. For example, both the hepatitis and Epstein-Barr viruses, associated with liver cancer and nasopharyngeal carcinoma, have up-regulated transcription of the EGFR promoter (Menzo *et al.,* 1993; Miller *et al.,* 1987). Furthermore, the papillomavirus E5 protein increases EGFR signaling by blocking the degradation of the activated EGFR at the endosomal level (Straight *et al.,* 1993). Additional support from the role of the EGFR signaling in tumor development is provided by studies in which the transfection of the receptor or its ligand results in transformation. For example, overexpression of the EGFR ligand TGF-α under the control of the mouse mammary tumor virus (MMTV) results in epithelial hyperplasia in mammary carcinomas (Matsui *et al.,* 1990; Muller *et al.,* 1996; Halter *et al.,* 1992; Guy *et al.,* 1992; Bouchard *et al.,*1989). In these studies, coexpressing of *neu*, the mouse homolog of the HER2 receptor, greatly accelerates the development of tumors and the early generation of metastases. The cooperation of different EGFR family members was reported to be important to initiate oncogenic transformation. In NIH3T3 cells, coexpression of EGFR and HER2106 and the coexpression of HER3 and HER2, (Alimandi *et al.,* 1995) were reported to mediate increased malignant transformation. Furthermore, NRG-induced malignant transformation was seen in NIH3T3 cells coexpressing EGFR or HER2 with HER3 or HER4 only, (Zhang *et al.,* 1996) indicating the important role of HER heterodimers as highly potent and diverse signaling activators. Disregulation of this tight signaling network has presumably a high impact on essential cellular functions. In table 1,

members of the EGF family and their ligands are frequently overexpressed in epithelial tumors, and their expression has been associated with a more aggressive behavior and worse prognosis.

The EGFR can result in tumor development by different mechanisms acting either separately or in combination. As detailed in Table 1, most epithelial tumors overexpress the EGFR. In most cases, and differently for HER2 overexpression that is most commonly the result of gene amplification, overexpression of the EGFR is not associated with gene amplification. Frequently, the expression of the EGFR coexists with activating ligands such as TGF-α, and this has been associated with a more aggressive phenotype and worse prognosis (D'Errico *et al.,* 2000; Yacoub *et al.,* 1987; Issing *et al.,* 1996).

Table 1 EGFR expression in different cancers

Tumor type	Expression (average)	Range
Head-and-Neck	75%	(53%-83%)
Colorectal carcinoma	46%	(16%-70%)
Lung carcinoma	41%	(27%-46%)
Esophageal carcinoma	39%	(19%-82%)
Gastric carcinoma	37%	(28%-81%)
Breast carcinoma	31%	(14%-65%)

Source: Grünwald and Hidalgo (2002)

Recently, the discovery of constitutive active mutations of the EGFR has been described, providing another mechanism for EGFR-induced tumorigenesis. Deletions and mutations of the EGFR are frequently found in a number of different cancers, including breast cancer, non-small-cell lung carcinoma, glioblastomas, ovarian carcinomas, and prostate cancer. Among the different genetic alterations reported thus far, deletions in the extracellular domain of the receptor are the most commonly encountered. At least 3 types of mutated receptors have been described namely

variant (v) I, II, and III (Bigner *et al.,* 1990; Humphrey *et al.,* 1991; Humphrey *et al.,* 1990; Moscatello *et al.,* 1996). The vIII is the best characterized and most frequently found in human tumors. As mentioned above, the vIII EGFR lacks 801 bp in the extracellular domain from amino acids 6-273 and arises from intragene rearrangements or from alternative mRNA splicing resulting in the insertion of a glycine residue at the deletion point. This deletion was initially discovered in malignant glioblastoma and has been subsequently reported in other tumor types such as breast, non-small-cell lung carcinoma, ovarian, and prostate cancer (Sugawa *et al.,* 1990; Schwechheimer *et al.,* 1995; Ekstrand *et al.,* 1992; Moscatello *et al.,* 1995; Garcia *et al.,* 1993). The mutated vIII receptor has a constitutive-active, ligand independent TK that stimulates cell proliferation in the absence of activating ligands (Moscatello *et al.,* 1998; Chu *et al.,* 1987). These features may explain, at least partially, increased tumorigenicity and malignancy observed in EGFR vIII expressing cells, when compared with non-mutated EGFR–containing cells (Tang *et al.,* 2000). In addition, in patients with glioblastoma, the expression of EGFR vIII correlated with poorer prognosis, (Feldkamp *et al.,* 1999) outlining the important role of EGFR vIII with regard to tumorigenicity. Importantly, the EGFR vIII has not been described in normal tissues, making it an attractive target for specific antitumor therapeutics (Olapade-Olaopa *et al.,* 2000).

Finally, the overexpression of activating ligands and autocrine stimulation of the EGFR also contributes to tumor development (Rusch *et al.,* 1996). In this regard, TGF-α, which is the most prominent EGFR ligand, is frequently co-overexpressed with the EGFR in a number of malignancies, including non-small-cell lung cancer, prostate cancer, and gastrointestinal stromal tumor (GIST), and has been associated with a worse prognosis (Hsieh *et al.,* 1999; Seth *et al.,* 1999; Cai *et al.,* 1999).

In summary, compelling laboratory and clinical data implicate the EGFR in the process of tumor development and progression. As described above, the EGFR can result or contribute to the oncologic process by different mechanisms (Figure 8). It is important to note that overexpression of the receptor is only one of the multiple mechanisms by which disarrangements of the EGFR can result in tumor formation.

As discussed in the clinical section of this article, this factor may explain why tumors that do not have abundant EGFR can still be EGFR-driven and therefore by appropriate targets for the development of these agents.

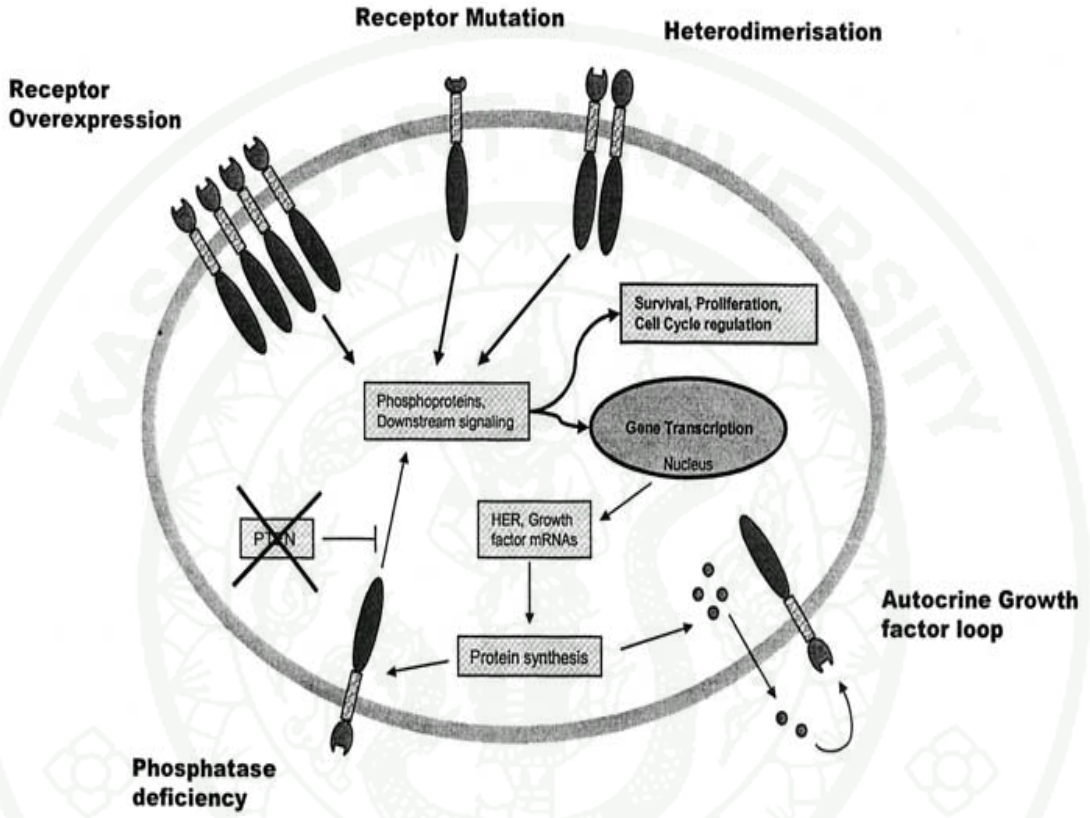

Figure 8 HER RTKs are important mediators in oncogenic transformation in cells. Different underlying mechanisms have been identified to induce the malignant phenotype, including receptor overexpression, receptor mutation, receptor heterodimerization, autocrine receptor activation, and phosphatase (PTEN) deficiency. A common pattern for all mechanisms mentioned above is the activation of downstream signaling pathways, which eventually mediate cell survival, proliferation, and cell cycle progression.

Source: Grünwald and Hidalgo (2002)

3. Rationale and strategies to target the EGFR for anticancer therapy

On the basis of the pre-clinical data indicating that altered function of the EGFR results in transformation in multiple experimental models and the frequent observation of abnormal EGFR expression and activation in common human tumors, the EGFR has become a strategic target for drug development. Figure 9 graphically displays the different strategies that, at least theoretically, can be used to inhibit the EGFR cascade. Currently, several therapeutically strategies are under investigation, which target distinct steps of receptor and signaling network activation including the following: (1) monoclonal antibodies (mAb), (2) immunotoxins and ligand-toxin conjugates, (3) small molecule tyrosine kinase inhibitors, (4) antisense oligonucleotides, and (5) downstream inhibitors of the EGFR signaling pathway. As discussed in some detail below, some of these strategies have been extensively explored in clinical trials. Although no EGFR inhibitor has been approved yet for the treatment of cancer patients, some compounds have completed pivotal trials and are in the process of being reviewed by regulatory agencies.

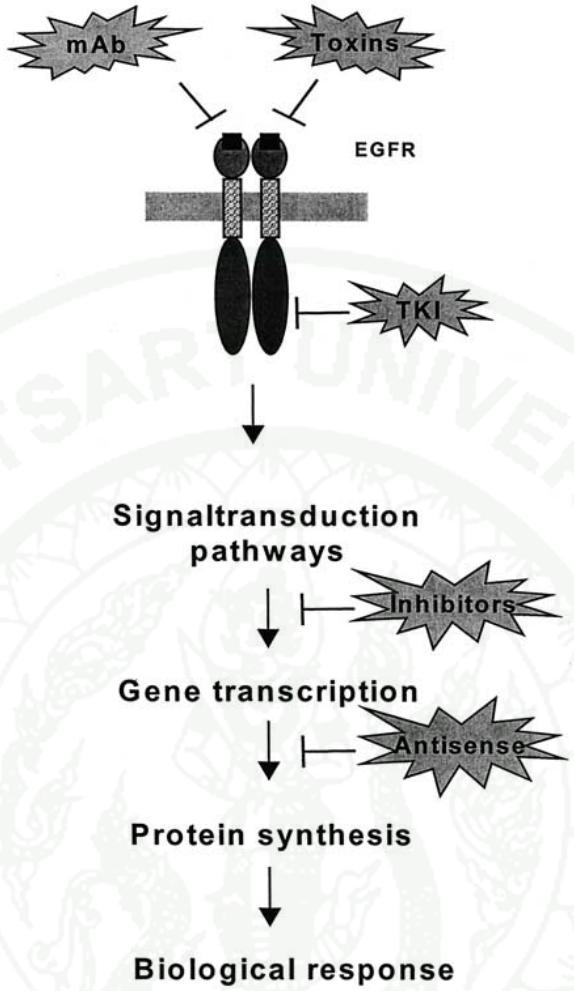

Figure 9 Different therapeutic strategies to disrupt EGFR signaling network are currently under investigation, including use of monoclonal antibodies (mAb), immunotoxins, and ligand-toxin conjugates, small molecule tyrosine kinase inhibitors (TKI), antisense oligonucleotides, and downstream inhibitors of the EGFR signaling pathway. The therapeutic interactions with components of the EGFR signaling pathways are outlined in this figure.

Source: Grünwald and Hidalgo (2002)

The first therapeutic strategy used to inhibit the EGFR consists of monoclonal antibodies used against the extracellular domain of the receptor. Although the mechanism of action of these agents is not fully elucidated, it appears that blockage of

ligand binding to the receptor and, hence, receptor activation is the principal pharmacologic effect. Small molecule inhibitors target the intracellular kinase domain of the EGFR and inhibit the activation of downstream signaling pathways, such as PI3K or MAPK. Recombinant ligand-toxin fusion proteins contain EGF or TGF-α fused to toxins or natural tyrosine kinase inhibitor molecules and represent another class of EGFR inhibitors. Moreover, antisense strategies and signal transduction inhibitors of selected pathways, such as CCI-779, an inhibitor of the downstream target of the PI3K pathway mTOR, have been developed to target EGFR biologic activity.

3.1 Monoclonal antibodies against the EGFR

The development of therapeutic antibodies against the extracellular domain of the EGFR was the first approach to target aberrant signaling through the EGFR to be explored in clinical trials. Initial laboratory studies with the murine mAbs MAb 528 and MAb 225 demonstrated that these molecules bind with high affinity to the extracellular domain of the EGFR, compete with the binding of natural ligands, and therefore block EGF and TGF-α–induced activation of the EGFR. Subsequent studies showed that these agents induced tumor growth inhibition in a variety of relevant *in vivo* preclinical models and acted synergistically with conventional cytotoxic agents and radiation therapy. To avoid the potential problems associated with the generation of human anti-murine antibody (HAMA) after repeated administration, a chimeric human-mouse antibody that contains the human immunoglobulin G1 constant region, IMC-225, was developed for clinical use. This agent has already completed phase III clinical trials and is in the process of being reviewed by regulatory agencies for approval. Recently, a fully humanized EGFR mAb (ABX-EGF) with high affinity to the EGFR was generated and showed promising activity in pre-clinical models (Yang *et al.,* 1999).

3.2 Small molecule inhibitors of the EGFR

The second strategy to inhibit the EGFR, which is currently in clinical development, is the small molecules inhibitors of the EGFR TK activity. These agents are ATP mimetic molecules, which bind to the ATP binding site of the TK moiety of the receptor, inhibiting its kinase activity and, hence, inhibit the activating phosphorylation of the receptor. Although these molecules share a common mechanism of action, they differ in the specificity, potency and nature of the chemical interaction with the ATP binding site of the EGFR-TK.

There are three small-molecule EGFR tyrosine kinase inhibitors that are in clinical use: gefitinib (Iressa) (Barker *et al.* 2001), erlotinib (Tarceva) (Moyer *et al*. 1997) and lapatinib (Tykerb) (Rusnak *et al.* 2001) (Table 2). All are based on a 4-anilinoquinazoline scaffold and target at the ATP site. Typically, these compounds have IC_{50} values of a few nM against the kinase *in vitro* and of ~20–30 nM in cells.

Table 2 Clinically approved protein kinase targeted inhibitors

Generic Name	Brand Name	Number	Year Approved	Known Targets
Fasudil	-	HA-1077	1999	ROCK
Imatinib	Glivec	STI-571	2001	ABL, ARG, PDGFR, KIT
Nilotinib	Tasigna	AMN107	2007	ABL, ARG, KIT, PDGFR
Dasatinib	Sprycel	BMS-354825	2007	ABL, ARG, KIT, PDGFR SRC
Gefitinib	Iressa	ZD-1839	2004	EGFR
Erlotinib	Tarceva	OSI-774	2004	EGFR
Lapatinib	Tykerb	GW572016	2007	EGFR (ErbB1, ErbB2)
Sorafenib	Nexavar	BA 43-9006	2006	B-Raf, VEGFR, PDGFR, FLT3,c-KIT
Sunitinib	Sutent	SU11248	2006	VEGFR, PDGFR,FLT3, c-Kit
Temsirolimus	Torisel	CCI-779	2007	mTOR

Source: Johnson (2009)

Gefitinib and erlotinib have been approved for NSCLC. Treatment of the general, non selected NSCLC population with these inhibitors resulted in a modest response rate of 10–18% and a 2-month median survival advantage over placebo, and there were even some doubts over survival benefits (Thatcher *et al.* 2005). However, the discovery in a subset of patients with somatic mutations in the EGFR kinase domain, which resulted in an activated kinase (Lynch *et al.* 2004; Paez *et al.* 2004; Pao *et al.* 2004) and which was highly sensitive to the inhibitors, has transformed understanding and the development of patient-specific treatment strategies. In trials with a small number of these patients, response rates were higher than 65% and median survival was 20–30 months (reviewed by Sequist and Lynch, 2008; Sequist *et al.* 2008). Erlotinib has also been approved for metastatic pancreatic cancer where EGFR is commonly over-expressed. Although the benefits are modest (a 6% increase in survival rates), there is expectation that a better understanding of the defect and combination therapy should improve treatment (Laurent-Puig and Taieb, 2008).

Structural results have shed light on the mechanisms of binding of the drugs to the kinase, on the mechanisms of activating mutation, and on the significance of resistance mutations. In contrast to many protein kinases, EGFR does not require phosphorylation on the activation segment for activity. Activation in response to EGF requires ligand-induced receptor dimerisation (Schlessinger, 2000). A detailed analysis of active and inactive EGFR kinase crystal structures, together with biochemical and mutational studies, led to the discovery that the association of the N-terminal lobe of one kinase and the C-terminal lobe of another kinase in an asymmetric heterodimer was responsible for the dimerisation-promoted activation (Zhang *et al.* 2006). In the active kinase structure, the asymmetric association of the two kinases through the interaction of the C-terminal lobe of one kinase with the N-terminal lobe of the other kinase mimics an association that is observed for the cyclin subunit activating the cyclin-dependent protein kinase CDK2. Association results in the correct orientation of the C-helix and the adoption of the activation segment in the active conformation for the kinase molecule in which the N-terminal lobe is used in the association.

To date, there are more than 20 structures of the EGFR tyrosine kinase domain (reviewed by Kumar *et al*. 2008). Figure 10 illustrates the essential features of the structures of the wild-type EGFR kinase with gefitinib (Yun *et al.* 2007), with erlotinib (Stamos *et al.* 2002; Wood *et al.* 2004) (both drug complexes have the kinase in the active conformation) and with lapatinib (Wood *et al.* 2004) where the kinase is in the inactive state. In the active conformation (Figure 10a and b), which is generated by a lattice kinase/kinase contact (Stamos *et al*. 2002), EGFR exhibits the common kinase fold in which the C-helix is in the right conformation to promote the interaction between the conserved glutamate and lysine (Glu762 and Lys745, using the sequence numbering that includes the 24-amino-acid signal sequence). This interaction locates the triphosphate moiety of ATP. The activation segment adopts a conformation similar to that seen in phosphorylated receptors such as the insulin receptor but with the position of the segment stabilised not by a phosphotyrosine but by many favourable van der Waals and hydrogen bond interactions. The carboxylate group of Glu848 assumes a position similar to the position of the phosphoryl group in those kinases (such as CDK2) that are activated by phosphorylation. The DFG motif (comprising Asp855, Phe856 and Gly857) has the active conformation, as shown in figure 10a and b.

Gefitinib binds to the active conformation of the EGFR kinase at the ATP binding site in a conformation similar to that observed for quinazolines binding to CDK2 and p38 MAP kinases (Yun *et al.* 2007) (Figure 10a). The N1 of the quinazoline accepts a hydrogen bond from the main chain NH of Met793 (hinge region), whereas the N3 atom contacts the gatekeeper Thr790 side chain through a water molecule. The 3-chloro-4-fluoro aniline substituent binds in the gatekeeper hydrophobic pocket forming a 42° angle with the quinazoline. The 6-propylmorpholino group extends into solvent consistent with structure activity data that this group provides only a modest enhancement of binding affinity. The group was added to improve pharmacokinetic properties. Gefitinib was not the most potent inhibitor discovered in the series, but it was chosen because it achieves high and sustained blood levels in vivo over a 24-h period.

The structure of wild-type EGFR kinase with erlotinib (Figure 10b), the first EGFR kinase structure to be published (Stamos *et al.* 2002), is similar to that of the kinase with gefitinib. The quinazoline and anilino groups make similar interactions, whereas the acetylene moiety is located in the pocket behind the ATP site, which is only accessible if the gatekeeper (Thr790) residue is small. The other groups attached to the quinazoline are directed to solvent but make some non-polar contacts with residues Leu844, Phe795 and Gly796.

In contrast to the above structures with erlotinib and gefitinib, the complex of EGFR kinase with lapatinib showed the kinase in an inactive conformation with a significantly different structure that resembles the structures observed for inactive SRC or inactive CDK2 (Wood *et al.* 2004) (Figure 10c). In comparison with the erlotinib complex, the N-terminal and C-terminal lobes of the kinase are rotated by about 12° and the kinase is in the closed conformation. The ATP pocket is enlarged in the inactive conformation by rotation and translation of the C-helix, which is necessary to accommodate the 3-fluorobenzyloxy group and explains why lapatinib can only bind to an inactive conformation. In the crystal structure, the quinazoline moiety makes similar contacts to those observed for gefitinib and erlotinib, whereas the large 3'-chloro-4'-[(3-fluorobenzyl) oxy] aniline group goes into the gatekeeper pocket making mostly hydrophobic contacts. The glycine-rich loop is folded over the inhibitor. The methyl-sulfonyl-ethyl-aminomethyl-furyl group points into solvent and does not make significant contacts with the protein. The activation segment (residues 855–884) has an inactive conformation with a short helical segment from residues 858 to 862.

The inhibitors exhibit different specificities for EGFR and ErbB2. Erlotinib and gefitinib have inhibition constants K_i for the EGFR kinase of 0.4 and 0.7 nM, respectively, but are nearly 2000-fold less potent against ErbB2. In contrast, lapatinib has K_i of 3.0 nM for EGFR and K_i of 13 nM for ErbB2, i.e. it is an effective inhibitor against both EGFR and ErbB2 (Wood *et al.* 2004). There are dramatic differences in the off-rates for inhibitor dissociation: for gefitinib and erlotinib the off-rate is 30 min, whereas for lapatinib, it is very slow (half-life 300 min). The

substantial differences between the active and inactive EGFR kinase conformation and the notion that to release the inhibitor would require conformational changes provide a possible explanation for the slow off-rate of lapatinib. ErbB2 kinase domain has 88% sequence identity with EGFR kinase. Sequence differences around the inhibitor binding sites do not explain why erlotinib and gefitinib inhibit EGFR but not ErbB2 while lapatinib inhibits both enzymes with similar potency. Wood *et al.* (2004) suggest that the differences between active and inactive structures of EGFR allow inhibitors to target different forms of the enzyme, active or inactive. The lack of inhibition of ErbB2 by erlotinib may reflect the inability of ErbB2 to adopt the precise active conformation as observed for the apo and EGFR/erlotinib structures.

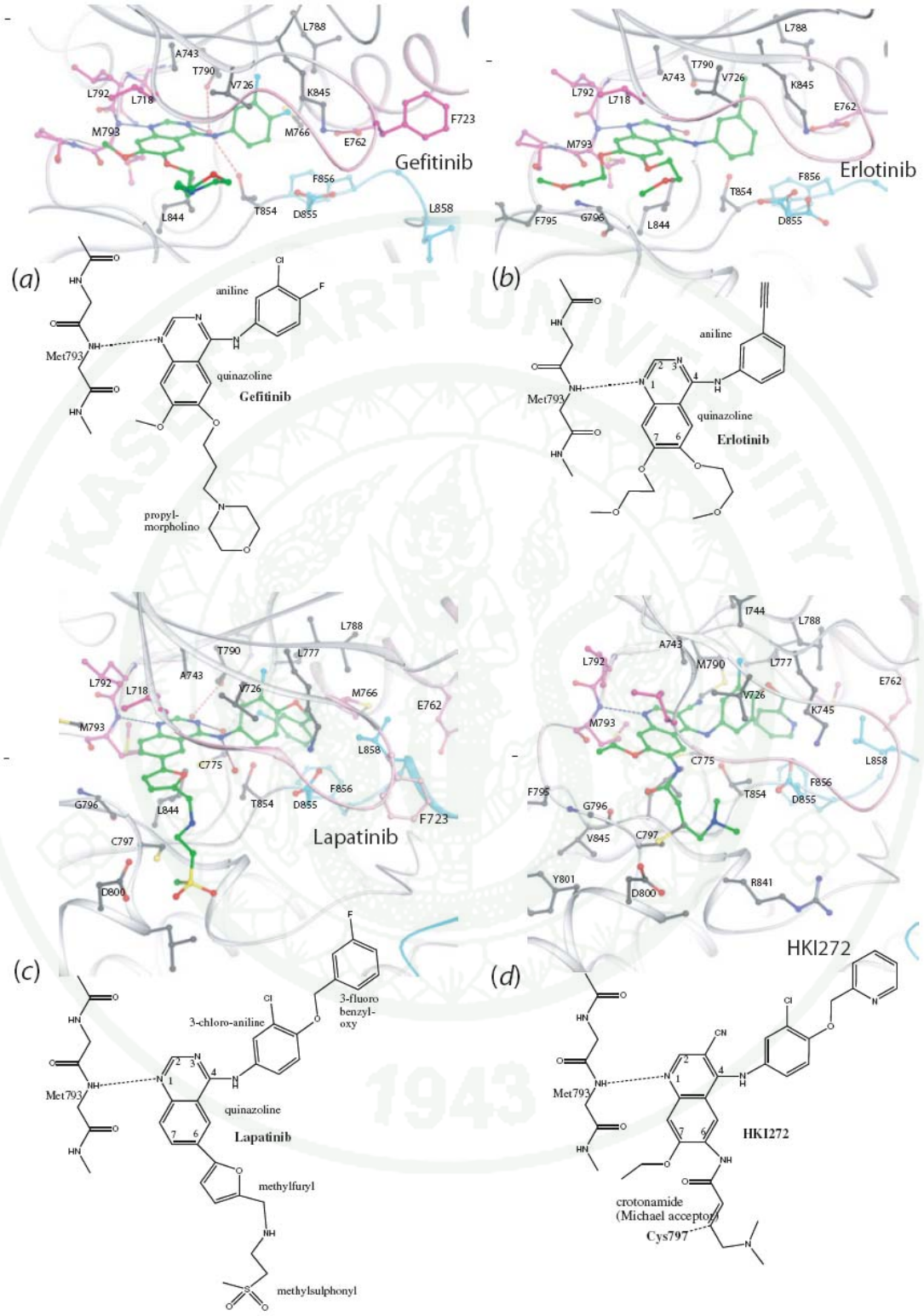

Figure 10 Details of the EGFR kinase in complex with gefitinib (Iressa), erlotinib (Tarceva), lapatinib (Tykerb) and HKI272. The 3D structures are shown

Figure 10 (Continued)

above the chemical structures. The colour code is glycine-rich loop (residues 719–724), C-helix (residues 756–767) and hinge (residues 791–794) in magenta, activation segment (residues 855–884) in cyan and the remainder of the kinase in grey. (a) EGFR in complex with gefitinib. The kinase is in the active conformation with the C-helix rotated in so that a hydrogen bond is made between Glu762 and Lys745. Phe723 and Leu858 are shown for reference (see text) From PDB ID 2ITY. (b) EGFR in complex with erlotinib. As with gefitinib the kinase is in the active conformation. From PDB ID 1M17. (c) EGFR in complex with lapatinib. The kinase is in the inactive conformation in which the glycine loop covers the inhibitor, the C-helix swung out, the DFG motif has Phe856 directed in to the ATP site and the activation adopts a helical conformation at Leu858. Residue Leu858 contacts a number of nonpolar groups including Phe723. In the activated mutant L858R, the larger and positively charged arginine would destabilise the inactive conformation and favour the active conformation. From PDB ID 1XKK. (d) EGFR T790M mutant in complex with HKI272. The kinase is in the inactive conformation. There is a covalent bond between Cys797 and the inhibitor. From PDB ID 2JIV.

Source: Johnson (2009)

3.2.1 Activating mutations

How do activating mutations in EGFR lead to greater drug sensitivity? A number of mutations have been identified that affect the catalytic site (Chan *et al.* 2006; Shigematsu and Gazdar, 2006). These include an in-frame deletion of exon 19, residues 747–749 (sequence LRE), at the region before the C-helix that accounts for ~44% of the activating mutations; a single nucleotide substitution in which Leu858 in the activation segment is substituted by arginine that accounts for ~41% of activating mutations (achieved by just a single base change); a Gly719 to

serine, alanine or cysteine substitution in the glycine-rich loop that accounts for a further 4% of activating mutations. Any one of these mutations leads to an active kinase that is transforming when present in cells. The L858R mutant is 50-fold more active, 10-100 fold more sensitive to gefitinib and erlotinib, and binds gefitinib 20 times more tightly than the wild-type kinase. In a comprehensive analysis with gefitinib, Yun *et al.* (2007) showed that the L858R and G719S EGFR mutants adopt very similar active conformations to that observed for the wild-type kinase. In the L858R mutant, the arginine points into the solvent. The structural results show that this mutation destabilises the inactive conformation of EGFR kinase. In the inactive conformation, the C-helix is shifted and rotated outward, allowing the start of the activation segment to take a helical turn. Leu858 is in this helical turn and makes non-polar contacts with nearby residues including Phe723 from the glycine-rich loop (Figure 10c) as recognised by Zhang *et al*. (2006). Substitution with the large and positively charged arginine is not compatible with the inactive conformation but is with the active conformation. The lower affinity for ATP and the higher affinity for gefitinib and erlotinib in the L858R mutant combine to block growth of tumours that are ‘addicted ’ to the activated EGFR for survival and explain the greater efficacy of the inhibitors in treatment of NSCLC patients carrying this mutation.

Lapatinib, which binds preferentially to the inactive state, would be less effective against the activating mutant EGFR kinases that occur in NSCLC patients. Instead lapatinib, with its ability to inhibit both EGFR and ErbB2 (Her2), has had success in treatment of Her2-positive breast cancer for patients with trastuzumab resistance. It has been approved for use in combination with capecitabine (trade name Xeloda; a prodrug that is converted to 5-fluorouracil in the tumour and inhibits DNA synthesis). In a phase III study, favourable tumour responses were seen in ~25% of patients (Geyer *et al.* 2006). It has been suggested that treatment could be improved and made more cost effective with different dose administration regimens (Gomez *et al.* 2008). The pre-clinical background for anti-EGFR drugs in combination with cytotoxic agents has been reviewed (Milano *et al.* 2008) in an attempt to understand why in some cases there are synergistic effects while in others there are not. Currently, a large randomised phase III trial is in progress to assess the dual benefits

of lapatinib (Tykerb) and trastuzumab (Herceptin) separately, sequentially or together for treatment of Her2-positive breast cancer patients.

3.2.2 Resistances

Development of resistance to the EGFR kinase inhibitors has become a major clinical problem. Patients initially responsive to gefitinib and erlotinib become resistant through second site mutations; most notable are mutations in the gatekeeper residue Thr790 for ~50% of patients. In ABL, the equivalent T315L mutation sterically blocks the binding of imatinib and hence confers resistance to the drug. In EGFR kinase, structural and biochemical studies have shown the mechanism is more complex (Yun *et al.* 2008). Binding studies showed that the T790M mutant bound gefitinib with a K_d = 2.4 nM, almost as tightly as the most sensitive L858R mutant. Crystal structures of the T790M mutant alone and in complex with two inhibitors showed that the gatekeeper mutation did not block binding of inhibitors in either the active or the inactive states. The two inhibitors were AEE788 (a compound that is similar to gefitinib and erlotinib, which binds to the active conformation and which is also in phase II clinical trials for glioblastoma) and HKI-272 (neratinib) (an irreversible inhibitor, which reacts with a cysteine Cys797 at the ATP site, binds to the inactive conformation and for which the T790M EGFR mutant is not resistant). The inhibitor AEE788 bound to the mutant T790M in a similar fashion as to active wild-type EGFR with a small change in the Met790 side chain, which adopts a different rotamer conformation to allow access of the phenylethylamine group to the gatekeeper pocket. The irreversible inhibitor HKI-272 bound to the inactive conformation in which the C-helix was swung out to accommodate the bulky aniline group, similar to the change needed for lapatinib binding (Fig. 4d). HKI-272 forms a covalent bond with Cys797, rendering the binding irreversible (Yun *et al.* 2008).

The explanation for resistance lies in the relative values of ATP affinity (as measured by K_m) and gefitinib affinity (as measured by K_d) (Yun *et al.* 2008). Kinetic studies showed that although the L858R mutant has a lowered affinity for ATP (K_m 148 mM), allowing the drug (K_d 2.4 nM) to compete successfully for the

ATP site, the T790M mutant and the double-mutant L858R/T790M have almost the same ATP affinity as the wild type (K_m 5.9 and 8.4 mM) with K_d of 4.6 and 10.9 nM, respectively, for gefitinib. Analysis of abilities of the drug to compete with cellular concentrations of ATP showed that whereas the lowered affinity of L858R mutant for ATP allows gefitinib to compete successfully, the wild-type-like affinity of the T790M or T790M/L858R mutants for ATP leads to a decrease in efficacy of the drug. (The structural explanation for the change in ATP affinity for the double L858/T790M mutant is not readily apparent.) The balance between drug and ATP affinities is crucial in determining a favourable outcome for ATP site-directed inhibitors when in competition with cellular concentrations of ATP. Thus, a ratio K_d (drug)/K_m (ATP) of $1.6x10^{-5}$ appears favourable, but a ratio of $78x10^{-5}$ is not. In contrast, the irreversible inhibitor HKI-272 is able to overcome the T790M resistance because once covalently bound it is no longer in competition with ATP. HKI-272 is progressing in clinical trials as one of second-generation EGFR inhibitors (reviewed by Wissner and Mansour, 2008).

4. Natural Product in drug discovery

Natural products have been the source of most of the active ingredients of medicines. This is widely accepted to be true when applied to drug discovery in 'olden times' before the advent of high-throughput screening and the post-genomic era: more than 80% of drug substances were natural products or inspired by a natural compound (Sneader, 1996). It is, however, arguably still true: comparisons of the information presented on sources of new drugs from 1981 to 2007 (Newman and Crag; Butler, 2008) indicate that almost half of the drugs approved since 1994 are based on natural products. Thirteen natural-product- related drugs were approved from 2005 to 2007 (Butler, 2008), and, as pointed out by Butler (Butler, 2008), five of these represented the first members of new classes of drugs: the peptides exenatide and ziconotide, and the small molecules ixabepilone, retapamulin and trabectedin.

These recently approved natural-product-based drugs have been described extensively in earlier reviews (Chin, 2006; Lam, 2007). They include compounds

from plants (including elliptinium, galantamine and huperzine), microbes (daptomycin) and animals (exenatide and ziconotide), as well as synthetic or semi-synthetic compounds based on natural products (e.g. tigecycline, everolimus, telithromycin, micafungin and caspofungin). They cover a range of therapeutic indications: anti-cancer, anti-infective, anti-diabetic, among others, and they show a great diversity of chemical structures. The chemical properties of the small-molecule natural products that have recently been developed into drugs have been analysed (Ganesan, 2008). Half of them were found to be closely compliant with Lipinski's Rule of Five for orally available compounds, but the remainder had higher molecular weights, more rotable bonds and more stereogenic centres, although they retained relatively low log P values. It is clear that, on average, natural products are more readily absorbed than synthetic drugs.

Despite these advantages and the past successes, many large pharmaceutical companies have decreased the use of natural products in drug discovery screening. This has been because of the perceived disadvantages of natural products (difficulties in access and supply, complexities of natural product chemistry and inherent slowness of working with natural products, and concerns about intellectual property rights), and the hopes associated with the use of collections of compounds prepared by combinatorial chemistry methods (Singh and Barrett, 2006; Baker, 2007; McChesney, 2007; Rishton, 2008).

Over a 100 natural-product-derived compounds are currently undergoing clinical trials and at least a 100 similar projects are in preclinical development (Table 3). Most are derived from leads from plants and microbial sources (Butler, 2008). The projects based on natural products are predominantly being studied for use in cancer or as anti-infectives, but many other therapeutic areas are represented (Table 4). Seven years ago, a similar analysis of the same database (Harvey, 2001) identified 312 projects, indicating a drop of about 30% in natural-product-based development projects between 2001 and 2008. There is, however, also a growing interest in the possibility of developing products that contain mixtures of natural compounds from traditionally used medicines (Charlish, 2008) and a defined mixture of components

extracted from green tea (Veregen TM) has been approved by the FDA and has recently come on the market.

Table 3 Drugs based on natural products at different stages of development

Development stage	Plant	Bacterial	Fungal	Animal	Semi-synthetic	Total
Preclinical	46	12	7	7	27	99
Phase I	14	5	0	3	8	30
Phase II	41	4	0	10	11	66
Phase III	5	4	0	4	13	26
Pre-registration	2	0	0	0	2	4
Total	108	25	7	24	61	225

Source: Harvey (2008)

Table 4 Therapeutic categories of natural product-derived drugs at different stages of development

Therapeutic area	Preclincal	Phase I	Phase II	Phase III	Pre-registration	Total
Cancer	34	15	26	9	2	86
Anti-infective	25	4	7	2	2	40
Neuropharmacological	6	3	9	4	0	22
Cardiovascular	9	0	5	6	0	20
Inflammation	6	2	9	1	0	18
Metabolic	7	3	6	1	0	17
Skin	7	1	2	0	0	10
Hormonal	3	0	2	1	0	6
Immunosuppressant	2	2	0	2	0	6
Total	99	30	66	26	4	225

Source: Harvey (2008)

5. Kinase assay in drug discovery

A wide variety of technologies have been developed to measure kinase activity and therefore to screen for novel inhibitors. Several excellent reviews have been published on these technologies in the past, from both a biochemical as well as a cell-based assay perspective (Whitney, 2004; Klumpp *et al.,* 2006; Jia *et al.,* 2008). These assays also provide for identification of kinase inhibitors not easily identified by rational design based on crystal structure analysis. Compounds that inhibit kinase activity by binding to regions in the catalytic domain other than the ATP binding sites can be identified using screening technologies allowing for detection of compounds that stabilize the kinase in an inactive state. Furthermore, screening assays can reveal allosteric regulators of protein kinases as well as those that block kinase translocation. Finally, for the RTKs, assays measuring ligand binding or dimerization of the receptors can identify compounds that inhibit activation of the kinase. Such inhibitors can confer very high degrees of specificity for particular kinases.

5.1 Cell-free protein kinase assays

5.1.1 Radiometric assays

An early, and widely used, approach to measure kinase activity measured the enzymatic incorporation of ^{32}P into peptide or protein substrates (Ishida *et al.,* 2007; Hardie, 1999; Bischoff *et al.,* 1998). A modification of this standard basic research approach that has been utilized in screening against protein kinase employs the scintillation proximity assay (SPA) from GE Healthcare (Pollards Wood, U.K.). In this assay, a biotinylated ^{33}P-labeled substrate generated by kinase action is captured on a streptavidin-coated SPA bead. Light is then emitted from the beads via ^{33}P-labeled substrate and detected by either scintillation spectrometry or using a charge-coupled device imager (Beveridge *et al.,* 2000; Cook *et al.,* 2002). An alternative approach is the use of FlashPlate® (PerkinElmer, Waltham, MA) technology in which the radiolabeled substrate is captured on a microtiter plate surface either using streptavidin (to capture biotinylated substrate) or with nickel chelate (to capture His-

tagged substrate). Incorporation of ^{33}P substrate into the solid-phase substrate on the FlashPlate then comes in close proximity to a scintillant coating on the plate. The resulting signal is then measured following a washing step by scintillation spectrometry.

The main advantages of both of these technologies are that they are simple to employ and do not require the generation of specific antibodies against phosphorylated substrate, which can be costly. In addition, a wide diversity of kinases, in either crude preparations or purified recombinant form, can be studied kinetically by this approach. Consequently, the technique has been widely adopted in lead profiling activities or mechanism of action studies, in which Michaelis-Menten kinetics can be used in a wide range of assay conditions and substrate concentrations (Diks *et al.,* 2004). Nonetheless, there are major disadvantages of employing this approach in HTS because of the use of radioactivity and the inherent high costs of waste disposal associated with the technique.

5.1.2 Non-radiometric assays

The development of selective antibodies that can distinguish phosphorylated from nonphosphorylated forms of the kinase substrates has accelerated the development of a range of nonradiometric assays for HTS (Sachsenmaier and Schachtele, 2002; Wesche *et al.,* 2005). Presently, polyclonal and monoclonal antibodies against phosphorylated tyrosine, serine, or threonine residues in phosphoprotein or phosphopeptide or substrates have been used in many kinase assays. Originally developed as radioimmunoassays, the technology has been adopted to nonradiometric protocols that do not require wash and separation steps, *i.e*., they are homogeneous in nature and highly amenable to the kind of automated fluid dispensing instruments used in HTS. In addition, the difficulty of obtaining high-affinity, selective antibodies, notably to phosphoserine/threonine residues found in STK substrates, has led to the adoption of Lewis metal ions, rather than antibodies, to coordinate the phosphorylated substrates. In general, the methods discussed above assess kinase activity by measurement of phosphorylated product accumulation. Other

methods have also been developed that have been suggested to be more generic across kinases. These include assessment of the depletion of ATP during the kinase reaction, as well as measurement of ADP accumulation. In the sections below, each of these approaches will be discussed in turn.

Table 5 Cell-Free Protein Kinase Assays

Readout	Substrate Phosphorylation		ATP/ADP Modulation	Substrate Binding
	Radioactive	Non-radioactive		
Assay	FlashPlate SPA	DELFIA (TR-fluorescence) LANCE (TR-FRET) AlphaScreen (TR-FRET) LanthaScreen (TR-FRET) IMAP (TR-FRET) (FP) Far-Red PolarScreen (FP) KinEASE (FP) Z'LYTE (FRET) IQ kinase Antibody Beacon TruLight	EasyLite Kinase-Glo ADP Quest ADP-FP	AlphaScreen EFC
Advantages	Simple to use, Detects most protein Kinases, No antibody needed, No modification of substrate	Simple, Sensitive, Most homogeneous, HTS, Any substrate, For some no antibody needed and Most can be used in lysate	No antibody or substrate modification, Homogeneous Cost-effective	Competitive binding assay, EFC assay for all kinases, No antibody or ATP needed HTS
Disadvantages	Radioactive waste, Limited HTS	Most require labeling of substrate and require antibody, limiting number of kinases studied, Optical interference of compounds Expensive	Weak kinase results in low response for ATP depletion assay, High background, Not a problem for ADP formation	Identifies inhibitors at ATP binding site

Source: Eglen and Reisine (2009)

A classical fluorometric assay to measure kinase activity using anti-tyrosine or anti-serine/threonine phosphoantibodies is the dissociation-enhanced lanthanide fluoroimmunoassay (DELFIA®, PerkinElmer), (Olive, 2004) which employs a lanthanide-labeled antibody for detection. The lanthanide labels have the advantage of a long decay time, as well as a wide Stokes' shift, collectively resulting in robust signal to noise ratio in the assay. The assay protocol comprises the use of biotinylated substrate, and following the kinase reaction the phosphorylated substrate is then transferred to streptavidin-coated microplates. The phosphorylated substrate binds to the plate, which then reacts to the europium-labeled antibody against phosphorylated substrate. Time-resolved (TR) fluorometry of the enhanced fluorescence of the lanthanide, which is dissociated by a proprietary enhancement solution, is then carried out to increase sensitivity. This assay protocol, while sensitive, involves the use of a wash and separation step and has limited utility in HTS protocols. An alternative method that can be conducted in a homogeneous fashion is the use of fluorescence resonance energy transfer (FRET)- and TRFRET- based assays.

Kinase assays using FRET or TR-FRET techniques are widely available to detect kinase activity (Han *et al.,* 2005; Schröter *et al.,* 2008; Braunwalder *et al.,* 1996; Morgan *et al.,* 2004). Here, a kinase substrate with an acceptor moiety is incubated with enzyme (Zhang *et al.,* 2006). In the LANCE® *Ultra* formats (PerkinElmer), the phosphorylated substrate is detected with a specific anti-phosphopeptide antibody labeled with europium chelate molecules (Eu), which serve as donors (Diks *et al.,* 2004; Zhang *et al.,* 2006). The binding of the Eu labeled-antibody to the phosphorylated peptide substrate with an acceptor moiety (U*Light*™ in the case of the LANCE *Ultra* assay) causes the donor and acceptor dyes to come in close proximity and upon excitation results in energy transfer and light emission, which is detected as the assay response. Analogous FRET-based assays to measure kinase activity are the Z'-LYTE™ kinase assay and LanthaScreen™ TR-FRET (Invitrogen, Carlsbad, CA) and HTRF TR-FRET (CisBio, Bagnols-sur-Cȯze, France) (Rodems *et al.,* 2002; Mathis, 1999).

The homogeneous kinase AlphaScreen® technology (PerkinElmer) employs a bead-based proximity assay approach rather than a FRET approach to detect the phosphorylated substrate (Diks *et al.,* 2004; Warner *et al.,* 2004). Thus, biotinylated or glutathione *S*-transferase-tagged substrates are phosphorylated by the kinase under study, and the phosphorylated substrate then binds to the donor beads via either streptavidin or glutathione. Anti-tyrosine or anti-serine/threonine antibodies are conjugated to the acceptor beads. Donor and acceptor beads are brought into close proximity as a result, and transfer of singlet oxygen, from the donor to acceptor bead, occurs upon laser excitation. This results in a signal generated by the acceptor bead, which is then detection in a plate reader (Mathis, 1999; Guenat *et al.,* 2006).

Since the distance relies upon an oxygen channeling technique, as opposed to FRET/TR-FRET approaches, large analytes, such as phosphoproteins, can be detected. Indeed, the distance between the two beads may be as much as 200 nm, which is very much larger than the distance than can be accommodated by a FRET pair (Guenat *et al.,* 2006). Practically, this means that the AlphaScreen format can be used in kinase assays where the kinase substrate is a protein, as opposed to a peptide.

As mentioned above, in recent years the use of Lewis metals, rather than antibodies, has been suggested as a means to detect phosphorylated substrates. These metals are known to bind phosphate groups and have been used in assays involving AlphaScreen, immobilized metal assay for phosphopeptides (IMAP) and TR-FRET (MDS Analytical Technologies, Toronto, Canada) (Corthals *et al.,* 2005; 1999; Moser and White, 2006). Advantages of the approach are that it is sensitive and homogeneous and does not require phosphor-specific antibodies. However, there are limits to the use of the assay, notably in terms of the concentrations of ATP than can be used in the assay. High concentrations of ATP will also bind to the Lewis metals and thus raise assay background. Moreover, that several kinases have moderate activity and require high ATP concentrations to attain maximal velocity suggests limits on the use of the technique.

Fluorescence polarization (FP) assays have also been developed to measure kinase activity (Seethala and Menzel, 1998; Sportsman *et al.,* 2004). These assays are simple to use, homogeneous, and relatively simple to automate. Commercially available FP assays include the Far-Red PolarScreen™ FP assay (Invitrogen), KinEASE™ (Millipore, Billerica, MA), and the IMAPFP assay (MDS Analytical Technologies). However, use of FP by itself as a technique has declined in recent years, principally because of the levels of interference from compounds in the screening library that either autofluorescence or quench the fluorescent signal. In many laboratories the use of FP techniques in kinase screening has declined in favor of TR-FRET-based approaches where the assay background is inherently lower. As discussed above, several formats of TR-FRET assays are available, including those using HTRF technology (CisBio) and LANCE *Ultra* (PerkinElmer).

Finally, other assay technologies available to measure accumulation of phosphopeptides include the Antibody Beacon TK fluorescence quenching assay (Invitrogen), the IQ™ kinase assay (Thermo Fisher, Waltham, MA), (Morgan *et al.,* 2004) the TruLight™ kinase assay (Merck Biosciences, Darmstadt, Germany), and the enzyme fragment complementation (EFC) assay using β-galactosidase (DiscoveRx, Fremont, CA) (Eglen, 2002; Eglen and Singh, 2003). All of these assays utilize a competitive immunoassay format via an anti-phosphopeptide antibody.

5.1.3 ATP depletion assays

Kinase activity converts ATP into ADP via incorporation of a phosphate group into a substrate. Therefore, measurement of either ATP depletion or ADP accumulation serves as a measure of kinase turnover (Charter *et al.*, 2006; Singh *et al.*, 2004; Koresawa and Okabe, 2004). The Kinase-Glo® luminescent kinase assay (Promega, Madison, WI) and the easyLite-Kinase™ assay (PerkinElmer) determine the depletion of ATP in a kinase assay via firefly luciferase readout. These assays are homogeneous, do not require specific substrates or antibodies, and can be read on simple luminescent readers. Although the format is such that almost any kinase can be screened (since all kinases convert ATP to ADP), the technique has several

drawbacks. One of these involves the use of purified kinases, since it does not distinguish ATP depletion induced by a kinase from induced by contamination levels of enzymes such as ATPases.

In parallel to the ATP depletion assays, the ADP Quest™ assay from DiscoveRx measures the formation of ADP as a consequence of kinase activity (Charter *et al.,* 2006). The newly formed ADP reacts with the fluorescence emitter, and the change in light emitted is the readout. In letion assay, Similarly, Bellbrook Labs (Madison, W I) has developed TR-FRET and FP assays to measure ADP generation as a result of protein kinase activity. These assays comprise a terbium-conjugated monoclonal antibody that selectively recognizes ADP. When bound, ADP couples with the fluorscein trace, and a TR-FRET signal is detected because of the close proximity of the fluorscein and terbium. ADP generated from the action of protein kinases displaces the trace reducing the TR-FRET signal in a concentration-dependent manner.

5.1.4 Substrate-kinase binding assays

An alternative, less widely used, screening approach to identify selective inhibitors of kinases is to employ a competitive binding assay in order to assess either binding of substrates to a purified kinase or the binding of small molecules known to bind to the catalytic domain. Consequently, inhibitors of the kinase could be detected by their ability to compete with either the substrate or small molecule ligand from the catalytic domain. AlphaScreen (PerkinElmer) has been used to measure binding of substrate to protein kinase (Warner *et al.,* 2004). Here, a glutathione *S*-transferasetagged substrate was bound to a donor bead, and a His-tagged target protein kinase bound to an acceptor bead. When substrate and kinase bind, the donor and acceptor beads come into close proximity to allow for a luminescent response.

A small molecule ligand binding assay using the EFC technology of DiscoveRx is based on the use of small molecules like staurosporine that bind to the

ATP binding site of most protein kinases (Vainshtein *et al.,* 2002). This complementation assay consists of two components: EA, which is a truncated β-galactosidase that is inactive, and Prolabel™, a peptide that spontaneously recombines with EA to form an active β-galactosidase that can be detected in a chemiluminescent or fluorescent assay. For the protein kinase assay, Prolabel is covalently coupled to staurosporine to generate the signaling molecule Prolabel-staurosporine. This molecule is generated in such a way that Prolabel-staurosporine can recombine with EA to induce β-galactosidase activity and that Prolabel-staurosporine can bind to most any protein kinase with high affinity. When Prolabel-staurosporine binds to a protein kinase it is no longer accessible to EA, so no β-galactosidase activity is measurable. In the presence of competitive inhibitors of protein kinase (staurosporine, ATP, or active site inhibitors), Prolabel-staurosporine is released from the kinase and is able to recombine with EA to restore b-galactosidase activity.

5.2 Cell-based protein kinase assays

5.2.1 *In vivo* protein phosphorylation assay

While molecular assays have been the standard for primary screening efforts to identify protein kinase inhibitors, cell-based assays are essential in establishing the biological effectiveness of any kinase-targeted drug. The physiological actions of protein kinases are dependent on a number of cellular factors, including location, adaptor proteins, and a host of regulatory proteins. These factors cannot be easily simulated in cell-free assays. Thus, while it is possible to identify a compound that can inhibit the activity of the purified kinase, it may be another matter whether that same compound works in cells. Importantly, the cell-based assays can determine whether a compound identified in initial screening efforts is cell permeable and whether it is toxic to cells, and therefore likely to cause side effects.

The initial approaches to cell-based assays to measure protein kinase activity involved loading cells with [^{32}P]ATP and measuring activation of particular

kinases by their ability to incorporate ^{32}P into cellular substrates. This approach provided information on the gamut of potential targets for a kinase. A non-radiometric modification of this approach is still used today as a proteomic approach to identify kinase targets. Instead of labeling ATP pools with [^{32}P]ATP, phosphorylation is accessed by matrix-assisted laser desorption ionization-time of flight mass spectroscopy, which is able to distinguish whether particular proteins are phosphorylated. These approaches are primarily used for research purposes and are not easily employed for drug screening.

Table 6 Cell-Based Protein Kinase Assays

Readout	Substrate Phosphorylation		ATP/ADP Modulation	Substrate Binding
	Radioactive	Non-radioactive		
Assay	32P labeling	AlphaScreen Surefire BRET, FRET	EFC, PCA Confocal microscopy	BRET, PCA EFC
Advantages	Detects all cell substrates	Targets selective substrates, Sensitive, Homogeneous, AlphaScreen amenable for HTS	Measures movement of activated kinase, Can distinguish different functions of kinase, Totally cell based, Amenable for HTS, Can detect allosteric inhibitors of kinases	Detects allosteric inhibitors of receptor kinases
Disadvantages	Disadvantages Waste removal Insensitive Not easy to quantify Not amenable for HTS	Requires labeling of kinase and substrate, Cannot be used for orphan kinases	Kinase labeling, Requires extensive knowledge about kinase cell biology	

Source: Eglen and Reisine (2009)

Phosphorylation of proteins in response to protein kinase activation in cells can also be measured using simple enzyme-linked immunosorbent assays

against target substrates that can distinguish phosphorylated from nonphosphorylated proteins. Using a similar idea, the AlphaScreen Surefire™ technology is a luminescent assay for phosphoproteins (TGR Biosciences, Adelaide, Australia/PerkinElmer). This homogeneous approach involves an antibody against a substrate that is coupled to biotin so that it can be captured by a streptavidin-coated donor bead and a second antibody directed against the phosphorylated form of the substrate that is coupled to an acceptor bead by protein A. Luminescence is detected when both antibodies bind to the same phosphorylated substrate bringing donor and acceptor in close proximity.

As a second approach to measure kinase-induced phosphorylation to monitor protein kinase activity in cells, Violin *et al*., 2003 and Gallegos *et al*., 2006, developed a cell-based assay to measure PKC-induced phosphorylation using FRET. They generated a reporter (C-kinase activity reporter) of PKC consisting of a peptide substrate of the kinase fused to cyan fluorescent protein and yellow fluorescent protein and an FHA2 phosphopeptide-binding module and expressed the fusion protein in target cells. When the substrate is not phosphorylated, a robust FRET signal is detected, and when PKC phosphorylates C-kinase activity reporter, the FRET response is lost. They showed that the reporter responded in a predictable manner to known stimulators and inhibitors of PKC. Interestingly, Gallegos *et al*., 2006, further modified the assay so that C-kinase activity reporter could be targeted to different cellular locations such as the plasma membrane, cytosol, mitochondria, Golgi apparatus, and nucleus using subcellular targeting sequences. This allowed them to assess PKC activity at different cellular compartments and to determine effect of different drugs on PKC activity in those different locations. They found drugs affected activity differently in different compartments. This may provide an important technology to identify drugs that can discriminate distinct functions of PKC. Similar approaches should be possible with other protein kinases in which substrates have been identified.

5.2.2 Cellular imaging to measure protein kinase activity: protein–protein interactions

Besides measuring protein phosphorylation, activity of kinases can be measured using other parameters. As described above, the interaction of protein kinases with other cellular proteins is critical for their activity and also provides the subtlety of the complex nature by which they regulate multiple cellular functions in the cell. Thus, interaction of IkB kinase with NEMO is essential for full catalytic activity, and association of cyclins with CDKs is necessary for activation of this family of kinases. Cell-based assays that can measure these protein–protein interactions provide a way to detect the activation of different protein kinases and also yield assay formats that can be used to identify drugs that modulate activity without necessarily directly interacting with the catalytic domain of the kinases. That is, if a drug can block the interaction of NEMO with IkB kinase, it will prevent the activation of the kinase but not the basal activity. Such allosteric regulators may provide a number of therapeutic advantages over more classical drugs that directly affect the catalytic domain of kinases.

An example of such protein–protein interaction assay in one focused on PKA. PKA is known to be activated when the catalytic subunit dissociates from the regulatory subunit. Measuring the dissociation of these two proteins reveals the activation of this kinase. Using bioluminescence resonance energy transfer (BRET), Prinz *et al*., 2006 and Moll *et al*., 2006 tagged the regulatory and catalytic subunits of PKA with the donor *Renilla* luciferase or green fluorescent protein. When the subunits are associated, the catalytic activity is inhibited, and a BRET signal is detected. Stimulation by cAMP causes the subunits to dissociate to increase kinase activity. This reduces the BRET signal. This assay can be used to identify activators of PKA as well as compounds that stabilize the complex to inhibit PKA activity.

Similarly, Stefan *et al*. (2007) have developed a *Renilla* luciferase complementation assay in which fragments of the luciferase are attached to the regulatory and catalytic subunits of PKA. When the kinase is inactive, the fragments are in close proximity, and full luciferase activity is detected. When PKA is stimulated by cAMP, the subunits and the fragments dissociate, and no luciferase activity is detected. These authors suggested that the sensitivity of this assay is far

greater than BRET- or FRET-type assay formats and can be employed for drug screening against GPCRs because of the high sensitivity of the cell-based readout.

Numerous technologies employing either FRET or BRET as an assay readout have been developed to measure protein–protein interactions to provide other measures of protein kinase activity. For example, Hundsrucker *et al*. (2006) were able to study interactions of PKA with its AKAP anchor proteins. As described in Protein Kinase Translocation and Compartmentalization, this association is important for the activation of PKA in discrete locations in cells. Hundsrucker *et al*. (2006) used BRET technology to measure AKAP association with the regulatory subunit of PKA. BRET probes were inserted into AKAP and the regulatory subunit of PKA. When the proteins were associated, a BRET signal was detected, and when they dissociated, the signal was lost.

Employing FRET to study protein kinase dynamics, Fujioka *et al*. (2006), studied interactions of the MAPKs ERK2 and MAPK/ERK kinase (MEK) in intact cells. First, they developed an assay to study intramolecular changes in ERK2 conformation by placing FRET probes (yellow and cyano fluorescence proteins) at the ends of ERK2. When in an open conformation, the FRET signal is minimal, but when ERK2 binds to MEK, an interaction needed for the activation of ERK2, a conformational change is induced causing an increase in FRET signal. Thus, this simple assay can be employed as a cell-based assay to identify inhibitors of the activation of ERK2 by MEK.

Technologies measuring protein–protein interactions have now been adapted for HTS of compound libraries for protein kinase drug discovery. Odyssey Thera (San Ramon, CA) has developed and employs a protein fragment-complementation assay (PCA) to measure protein–protein interactions in cells in a HTS format (Remy and Michnick, 1999). The technology employs fragments of reporters such as dihyrofolate reductase (DHFR) attached to interacting proteins (Remy and Michnick, 1999). The fragments themselves are inactive, but when the target proteins to which they are linked associate, the fragments combine to form an

active reporter that can be measured with a luminescent readout. For example, Remy and Michnick, 1999 generated two fragments of DHFR and linked the fragments to either the FK506 binding protein (FKBP) or the FKBP– rapamycin binding protein, which are known from a number of studies to associate in cells. When FKAP and FKBP–rapamycin binding protein associate, DHFR is formed. Methotrexate is known to bind with high affinity to DHFR in cells but does not interact with the fragments of DHFR. Thus, they could detect formation of DHFR in cells by using the binding of fluorescein-methotrexate and fluorescent microscopy as a measure of FKAP and FKBP–rapamycin binding protein interaction. This technology has been adapted by Odyssey Thera to use other reporters such as β-lactamase, *Renilla* luciferase, green fluorescent protein, and yellow fluorescent protein to detect intracellular protein–protein interactions, and the green fluorescent protein and yellow fluorescent protein tags have now been employed in an HTS format that can be used for drug discovery. While their approach can be used to measure many different biomolecular interactions, it is most suited for detecting weak associations of allosteric regulators of protein kinase activity. Furthermore, Remy and Michnick, 1999 also adapted the technology to measure binding of growth factors to their cell surface receptors, and thus the approach can be used to discover allosteric inhibitors of RTKs.

In this regard, several technologies focused on measuring protein–protein interactions have now become available to measure the interaction of growth factors with their RTKs. These technologies use BRET, FRET, or DiscoveRx's EFC technology and can be adapted for HTS to identifying small molecule inhibitors of the receptor subunit interactions or growth factor binding. BRET has been used to measure dimerization of cell surface receptors. Boute *et al*. (2001) used BRET to study insulin receptor activation. They showed that they could measure insulin dimer formation and that BRET signal increased upon activation of the receptor complex with insulin and other growth factors. They suggested that the BRET signal was due to conformational changes in the receptor complex and suggested that the assay could be employed for HTS of small molecule stimulators or inhibitors of the complex. Couturier and Jockers (2003) have used BRET to measure in intact cells dimerization of the leptin receptor, a member of the cytokine receptor family. Similarly, BRET has

been used to measuring subunit interactions of the growth hormone receptor (Brown *et al*., 2005) and IL-2 receptor (Damjanovich *et al*., 1997). Using a version of DiscoveRx's EFC technology, Wehrman *et al*. (2007) developed an assay to measure interaction of the EGFR and Erb2 subunits. In follow-up studies, Wehrman *et al*. (2007) reported that EFC could be employed to study the dynamic interactions of TrkA and p75, suggesting that it could be employed to study subunit interactions of a host of growth factor receptors. Since the assay is adapted to an HTS format, much like the PCA technology of Odyssey Thera, it could be used as a primary screen to identify either small molecule antagonists or growth factor receptor ligands.

5.2.3 Cellular imaging to measure protein kinase activity: protein kinase translocation assays

Protein kinases translocate between different cellular compartments when they are activated. This process is necessary because for many kinases their substrates are in different cellular locations than the sites at which they are activated. Monitoring the movement of kinases provides a means to detect the different functions of kinases and also provides approaches to discover drugs capable of blocking their selective functions.

Imaging technologies have been available for a number of years to measure movement of proteins in cells, especially those employing confocal microscopy (Warner *et al.,* 2004). Confocal microscopy has been employed to study the activation and translocation of one specialized family of protein kinases, the G protein receptor kinases (GRKs). The activation of most GPCRs induces the translocation of GRKs from the cytosol to the cell membrane, where they catalyze the phosphorylation of cytoplasmic domains of the receptors. This results in the recruitment of β-arrestins to the receptor. Because the activation of most if not all GPCRs is believed to involve the recruitment and translocation of GRKs and β-arrestins to the cell membrane (Barak *et al.,* 1997), Norak Biosciences (Research Triangle Park, NC) developed both GRK and β-arrestin translocation assay as a drug discovery technology to identify agonists at any GPCR. The technology employs

confocal microscopy to measure movement of either GRK or β-arrestin from the cytosol to the cell membrane as readout of GPCR activation.

Translocation of other protein kinases in cells can also be measured by confocal microscopy. While this approach is widely employed for research purposes, only until lately have technologies been developed to allow for use of confocal microscopy for drug screening. Specifically, Evotec (now PerkinElmer) developed instrumentation and technology referred to as Opera™ that can be used to detect movement of proteins in individual cells. Employing a family of fluorescent microscopic techniques run in parallel (Palo *et al.,* 2002), the confocal microscopy can be used in a microplate image reader system that allows for HTS of compound libraries. In essence, they can use protein kinase translocation as readout for drug screening.

While the use of confocal microscopy provides a very sensitive and spatially precise measurement of protein kinase movement, the technology is expensive, especially the use of the Opera instrumentation. Thus, in addition to confocal microscopy, less costly alternative approaches for HTS of protein translocation involve the use of complementation assays such as Odyssey Thera's PCA technology and EFC technology (Fung *et al.,* 2006) can be used to detect protein kinase translocation as a drug screening end point.

Knowledge gained on the biology of protein kinases has provided new insights on how to discover kinase regulators that are more specific and potentially more subtle in their action. Technologies are becoming available to target allosteric regulatory sites of kinases. These sites should confer a high degree of specificity of targeted drug since the structures of the allosteric sites are unique for each kinase. They may also provide ways to subtly affect some functions of the kinases but not necessarily all that may be of therapeutic value. This could also occur through the use of approaches to discover drugs that selectively alter the translocation of kinases to some but not all compartments of cells.

While growth factor and cytokine receptors are important for normal physiological control of cells and are critical in certain diseases, the discovery of small molecule regulators of these protein kinases has been limited. Antibodies directed at the protein growth factor have been developed basically to sequester circulating growth factors. Furthermore, antibodies that block growth factor binding to the receptors have been developed. In general, there are many drawbacks to the use of protein therapeutics, including cost, immune reactivity, and other toxicity issues. With the development of technologies to measure protein–protein interactions, it should now be possible to identify small molecules that block oligomerization of growth factor receptors, an essential step in the activation of the transmembrane receptors.

The kinase has been one of the most important targets for drug discovery and development in the pharmaceutical industry. Based on the new discoveries in the field, one would predict that this popularity should continue in the future.

MATERIALS AND METHODS

Materials

1. Chemicals

1.1 Antibody Beacon™ Tyrosine Kinase Assay Kit (A-35725): Invitrogen, USA

1.1.1 Oregon Green 488 ligand, Antibody Beacon reagent for phosphotyrosine detection (Component A), 200 µL of a 2.5 µM solution in 1X reaction buffer

1.1.2 Anti-phosphotyrosine antibody, P-Tyr-100 (Component B), 200 µL of a 5 µM (0.75 mg/ml) solution in pH 7.4 buffer containing 5 mM sodium azide

1.1.3 2X Tyrosine kinase reaction buffer (Component C), 25 mL of 100 mM Tris-HCl, 20 mM $MgCl_2$, 2 mM EGTA, 0.02% Brij 35, pH 7.5 (at 22°C)

1.1.4 Tyrosine kinase substrate # 1 (Component D), 400 µL of a 10 mg/ml poly (Glu:Tyr) solution, 4:1 ratio, in dH_2O

1.1.5 Dithiothreitol (DTT) (Component F), 31 mg

1.1.6 Adenosine triphosphate (ATP) (Component G), 200 µL of a 100 mM solution in buffer

1.1.7 Reference phosphotyrosine-containing peptide (Component H), 50 µl of a 500 µM solution of phospho-pp60 c-src (521.533) in dH_2O; sequence = TSTEPQpYQPGENL; MW = 1543.7

1.2 2–mercaptoethanol: Merck, Germany

1.3 3-(N-morpholino)propanesulfonic acid (MOPS): Sigma-Adrich, USA

1.4 Acetic acid: J. T. Baker, Thailand

1.5 Acrylamide: Bio Basic, Canada

1.6 Adenosine triphosphate (ATP): Fermentus, USA

1.7 Agar bacteriologico americano: Pronadisa, Spain

1.8 Ammonium persulfate: Ajax Finechem, Australia

1.9 Ammonium sulfate: Bio Basic, Canada

1.10 Antibiotics (ampicillin, gentamycin and tetacycline)

1.11 Bis-acrylamide: Bio Basic, Canada

1.12 Bovine serum albumin (BSA): Fluka Biochemika, USA

1.13 Bradford Reagent: Bio Rad, USA.

1.14 Bromo-chloro-indolyl-galactopyranoside (X-gal): Fermentus, USA

1.15 Bromophemol blue: Fisher Scientific, UK

1.16 Cellfectin® reagent: Invitrogent, USA

1.17 Coomassic brilliant blue R-250: Bio Basic, Canada

1.18 Crystal violet: Bio Basic, USA

1.19 Dimethyl sulfoxide (DMSO): Labscan, Thailand

1.20 Epidermal Growth Factor Receptor (EGFR) human:Sigma-Adrich, USA.

1.21 Ethylenediaminetetraacetic acid disodium salt (EDTA): Univar, Australia

1.22 Ethylene Dinitro Tetraaectic Acid (EDTA): Mallinckrodt Chemical, UK

1.23 Fast-Link™ DNA Ligation kit: Fermentus, USA

1.24 Fetal bovine serum (FBS): JRH Bioscience, USA

1.25 Gefitinib (IRESSA™): AstraZenneca, UK

1.26 GeneJet™ Gel extraction kit: Fermentus, USA

1.27 Glutathione-sepharose: GE Healthcare, Sweden

1.28 Glycerol: Ajax Finechem, Australia

1.29 Glycine: Ajax Finechem, Australia

1.30 Guanidine Hydrochloride: Bio Basic, USA

1.31 Imidazole: Bio Basic, Canada

1.32 Isopropyl β-D-1-thiogalactopyranoside (IPTG): Fermentus, USA

1.33 L-Arginine Hydrochloride: Bio Basic, USA

1.34 Liquid N_2: Thai Industrail Gas (TIG), Thailand

1.35 Magnesium chloride ($MgCl_2$): Ajax Finechem, Australia

1.36 Methanol: Ajax Finechem, Australia

1.37 Nicotinamide adenine dinucleotide (NADH): Sigma-Adrich, USA

1.38 Ni-NTA agarose : QIAGEN, USA

1.39 Phenyl methyl sufonyl fluoride (PMSF): SERVA, Geramany

1.40 Phosphoenolpyruvate (PEP): Sigma-Adrich, USA

1.41 Plasmids (pET-15b, pGex-4T1 and pFastBac-1): Novagen, Germany

1.42 Polyethylene glycol (PEG): Research Organic, USA

1.43 Poly (Glu:Tyr) agarose: Sigma-Adrich, USA.

1.44 PURETIME-17 EGF receptor tyrosine kinase substrate peptide: AssayMetrics, UK

1.45 Puruvate kinase: Lactate dehydrogenase (1:50): Sigma-Adrich, USA

1.46 Restriction enzyme (N*co*I, X*ho*I and B*ssH*II): Fermentus, USA

1.47 Serum free medium 900 II (Sf900II): Invitrogen, USA

1.48 Sodium chloride: J. T. Baker, Malaysia

1.49 Sodium dodecyl sulfate (SDS): Bio Basic, USA

1.50 Tetramethylethylenediamine (TEMED): Bio Basic, USA

1.51 Tris (hydroxymethyl) aminomethane: Research Organic, USA

1.52 Triton® X-100: USB, USA

1.53 Tryptone type-I: Himedia, India

1.54 Tween® 20: USB, USA

1.55 Urea: Research Organic, USA

1.56 Yeast extract powder: Himedia, India

2. Instruments

2.1 Autopipette: Gilson, Germany

2.2 Balance (4 digits): Denver balance

2.3 Biosafety Cabinet Class II: Microtech, USA

2.4 Centrifuge: Hermle refrigerate centrifuge model Z383K, Hermle Labortechnik GmbH, Germany

2.5 Fast protein liquid chromatography (FPLC): AKTAprime plus, GE Healthcare, Sweden.

2.6 Fluorescence spectroscopy: LS-50B Luminascence Spectrosopy, Perkin Elmer, USA

2.7 Freeze-dryer

2.8 Freezer -20 °C

2.9 Heat Box: D1100, Labnet, USA

2.10 Incubator 26°C: Model i250, Accuplus, Thailand

2.11 Liquid N_2 tank: Shangko-Yuxin, Japan

2.12 Microplate reader: TECAN, Austria

2.13 Microscope : Olympus, Japan

2.14 Nano drop UV/Visible spectrophotometer ND-1000: Nanodrop technologies, USA

2.15 Oven: Fisher Scientific, USA

2.16 PCR Thermal cycler TC-28/4 : Lio-Labinter, USA

2.17 Peristaltic pump: ECONO pump, Bio-Rad, USA

2.18 pH meter: Seven Easy pH meter, Mettler toledo, USA

2.19 Plastic ware for insect cells culture: corning, USA

2.20 Power supply: AE 8750, ATTO, Japan

2.21 Recorder: PowerChrom 280 system

2.22 Refrigerator 4°C

2.23 SDS-PAGE electrophoresis: AE 6530 ATTO, Japan

2.24 Shaker VS-8480SFN : Meditop, England

2.25 Slab gel electrophoresis: AE 6530, ATTO, Japan

2.26 Sonicator

2.27 UV detector: ECONO UV monitor, Bio-Rad, USA

2.28 UV Spectrophotometer: Cary 50 Conc, Varian, Australia

2.29 UV Transilluminator

2.30 Water bath: Memmert, Germany

Methods

1. Cloning and expression of recombinant TK in bacterial cells

Coding sequence of TK of human EGFR gene was kindly provided by Dr. Cathleen Carlin, department of Physiology and Biophysics, School of medicine, Case Western Reserve University, Ohio, USA, (Accession number NM_005228 from GenBank). The gene was amplified by a polymerase chain reaction (PCR) using primers TK/*NcoI*_F and TK/*XhoI*_R (Table 7) by using PCR condition as followed:

1.1 For each sample, set up the following 20 µl PCR reaction in a 0.5 ml microcentrifuge tube:

10 pg – 1 ng DNA	1	µl
10X PCR Buffer tag/$MgCl_2$	2	µl
25 mM dNTP Mix	2	µl
5 pmol/ µl Primers forward	2	µl
5 pmol/ µl Primers reverse	2	µl
Sterile Water	10.8	µl
Taq polymerase (5 units/µl)	0.2	µl
Total Volume	20	µl

1.2 Amplifying by using the following cycling parameters:

Step	Time	Temperature	Cycles
Initial denaturation	4:30 min	94°C	1X
Denaturation	30 s	94°C	
Annealing	30 s	51°C	25-35X
Extension	1 min	72°C	
Final extension	1 min	72°C	1X

The *NcoI* cleavage site was added into a forward primer while, *XhoI* clevage site was added into a reverse primer with 6-His-tag (CAC codon) and a termination TGA codon for cloning GST-TK (Figure 11) and TK (Figure 13). The PCR products, GST-TK and TK gene fragment were purified by GeneJET Plasmid Miniprep kit and cut for ligation into expression vector pGEX-4T-1 and pET-15b, respectively. The recombinant plastmids with TK gene were called pGEX-GST-TK (Figure 12) and pET-TK (Figure 14), which were under control of *tac*/T7 promoter and carried an ampicillin selection, were individually transformed into *E.coli* DH5α for amplifying plasmid DNA. The cells containing plasmid pGEX-GST-TK or pET-TK were cultured in 3 ml LB containing 50 µg/ml ampicilin with shaking 220 rpm at 37 °C overnight. Then plasmid pGEX-GST-TK or pET-TK were purified by GeneJET Plasmid Miniprep kit and transformed into *E.coli* BL21(DE3) for expression protein. The cells containing plasmid pGEX-GST-TK or pET-TK were cultured in 3 ml LB containing 50 µg/ml ampicillin with shaking 220 rpm at 37 °C overnight. Then, 1 % inoculation by transferring 3 ml cells cultures into a flask containing 500 ml LB with 50 µg/ml ampicillin and cultured with shaking at room temperature until $O.D._{600}$ reached 0.4. The culture was placed at 37 °C or 16 °C and the gene expression was induced by adding IPTG into the cultures with a final concentration of 1 mM. The induced cells were harvested after 4 h (for 37 °C) or overnight (for 16 °C) by centrifugation at 5,000xg for 15 min and the expressed protein was detected by using 12% SDS-PAGE.

Figure 11 Map of TK gene with a GST gene in N-terminus and His-Tag in C-terminus for construction of pGEX-4T-1 vector.

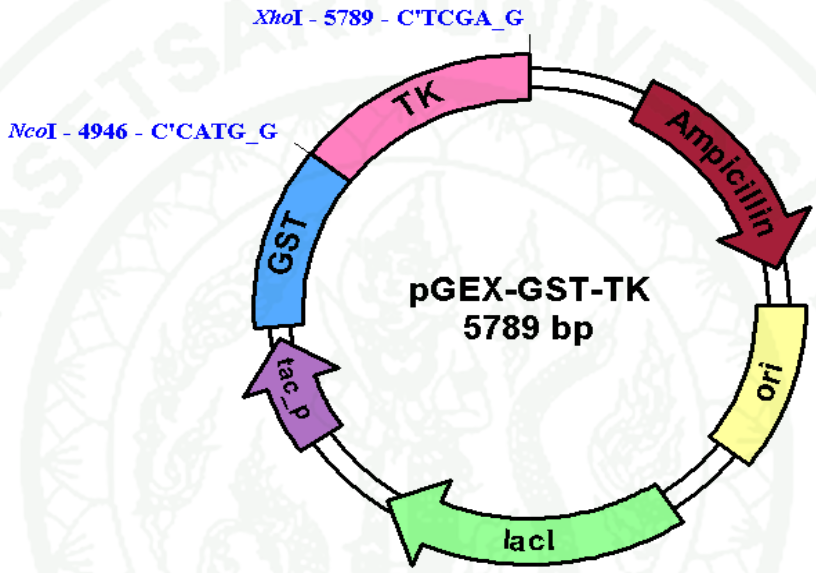

Figure 12 pGEX-GST-TK vector map, an *E.coli* expression vector, contains *tac* promoter and enable fusion of glutathione-s-transferase to the N-terminus of the TK gene.

Figure 13 Map of TK gene with a GST gene in N-terminal and His-Tag in C-terminal for construction of pET-15b vector.

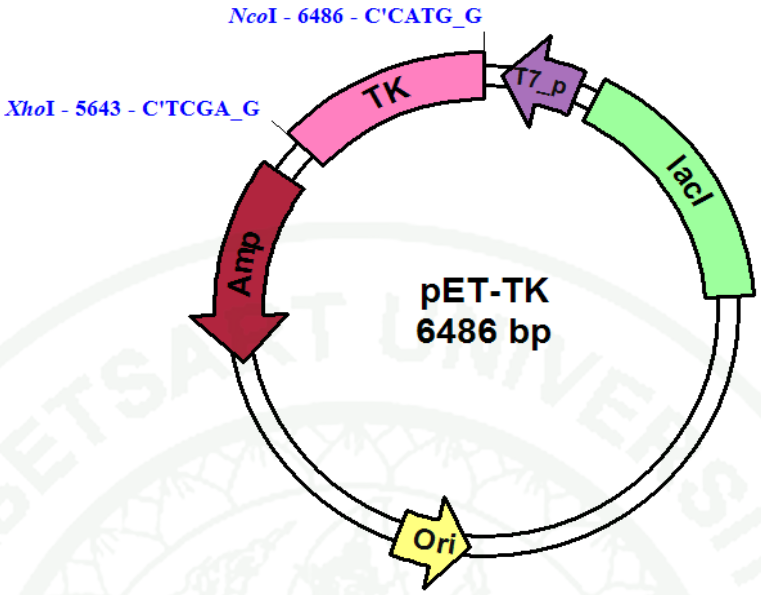

Figure 14 pET-TK vector map**,** a T7 promotor based *E. coli* expression vector.

Table 7 Primers used in plasmid construction in bacterial cells

Primer name	Sequence
TK/*NcoI*_F	5′ GCGA*CCATGG*AATTCAAAAAGATCAAA 3′
TK/*XhoI*_R	5′ TAT*CTCGAG*TCAGTGGTGGTGGTGGTGGTGTCTTTCATCCCCCTGAAT 3′

2. Cloning and expression of recombinant TK plasmid in insect cells

Coding sequence of tyrosine kinase (TK) of human EGFR gene in pGEX-GST-TK plasmids were amplified by a polymerase chain reaction (PCR) using primers TK/*BssH*II_F and TK/*XhoI*_R (Table 8) for expression of only TK protein with His-tag at C-terminal, then using primer GST/*BssH*II_F and TK/*XhoI*_R (Table 8) for expression of GST-TK fusion protein with GST at N-terminus and His-tag at C-terminus by using PCR condition as followed:

2.1 For each sample, set up the following 20 µl PCR reaction in a 0.5 ml microcentrifuge tube:

10 pg – 1 ng DNA	1	µl
10X PCR Buffer tag/$MgCl_2$	2	µl
25 mM dNTP Mix	2	µl
5 pmol/ µl Primers forward	2	µl
5 pmol/ µl Primers reverse	2	µl
Sterile Water	10.8	µl
Taq polymerase (5 units/µl)	0.2	µl
Total Volume	20	µl

2.2 Amplifying by using the following cycling parameters:

Step	Time	Temperature	Cycles
Initial denaturation	4:30 min	94°C	1X
Denaturation	30 s	94°C	
Annealing	30 s	55°C	25-35X
Extension	1 min	72°C	
Final extension	1 min	72°C	1X

Table 8 Primers used in plasmid construction in insect cells

Primer name	Sequence
TK/*BssH*II_F	5′ AT*GCGCGC*ATGAAGGAAACTGAATTCAAAAAG 3′
GST/*BssH*II_F	5′ AT*GCGCGC*ATGTCCCCTATACTAGGTTATTGGAA 3′
TK/*XhoI*_R	5′ TAT*CTCGAG*TCAGTGGTGGTGGTGGTGGTGTCTTTCATCCCCCTGAAT 3′

The PCR products, GST-TK and TK genes were purified by GeneJET Plasmid Miniprep kit and cut with *BssH*II and *Xho*I for ligation into expression vector pFastBac-1. The recombinant plastmids with TK genes were called pFastBac-GST-TK (Figure 15) and pFastBac-TK (Figure 16). Then both were individually transformed into *E.coli* DH10Bac (Invitrogen) to generate recombinant bacmids called bacmid-GST-TK and bacmid-TK. The cells containing bacmid-GST-TK and bacmid-TK were cultured in SOC medium at 37 °C for 4 h and the white colonies

were selected in LB agar plate containing 50 µg/ml kanamycin, 7 µg/ml gentamicin, 10 µg/ml tetracycline, 100 µg/ml X-gal, and 40 µg/ml IPTG at 37 °C for 48 h. The white colonies were checked for recombinant bacmids by PCR using M13 primer (Table 9) by using PCR condition as followed:

2.3. For each sample, set up the following 20 µl PCR reaction in a 0.5 ml microcentrifuge tube:

100 ng Recombinant bacmid DNA	1	µl
10X PCR Buffer (appropriate for enzyme)	5	µl
10 mM dNTP Mix	1	µl
50 mM $MgCl_2$	1.5	µl
PCR Primers (1.25 µl each 10 µM stock)	2.5	µl
Sterile Water	38.5	µl
Taq polymerase (5 units/µl)	0.5	µl
Total Volume	20	µl

2.4 Amplifying by using the following cycling parameters:

Step	Time	Temperature	Cycles
Initial denaturation	3 min	93°C	1X
Denaturation	45 s	94°C	
Annealing	45 s	55°C	25-35X
Extension	5 min	72°C	
Final extension	7 min	72°C	1X

Table 9 M13 Primers used in bacmid construction

Primer name	Sequence
M13 Forward	5′ GTTTTCCCAGTCACGAC 3′
M13 Reverse	5′ CAGGAAACAGCTATGAC 3′

The PCR products should have size of 2300 bp plus size of insert gene because Tn7L and Tn7R (Mini Tn7 elements) that permit site-specific transposition of the gene of interest into the baculovirus genome. The recombinant bacmids were transfected into Sf9 cell line using Cellfectin Reagent as followed:

1. Plate 9 x 10^5 Sf9 cells in 2 ml of Sf-900 II SFM containing antimicrobial 0.5X final concentration. Allow cells to attach for at least 1 h.

2. For each transfection sample, prepare complexes as followed:

2.1 Dilute 1-2 μg of baculovirus DNA in 100 μl of Sf-900 II SFM without antibiotics.

2.2 Mix Cellfectin before use, then dilutes 5 μl in 100 μl of Sf-900 II SFM without antibiotics.

2.3 Combine the diluted DNA with diluted Cellfectin (total volume = 200 μl). Mix gently and incubate for 30 min at room temperature (solution may appear cloudy).

3. Remove the growth medium from the cells and wash once with Sf-900 II SFM without antibiotics. Remove the wash medium.

4. Add 0.8 ml of Sf-900 II SFM to the complexes (Step 2c), mix gently and add to the cells. Incubate cells at 27°C for 5 h.

5. Remove the transfection mixture and replace with 2 ml of Sf-900 II SFM containing antibiotics.

The transfected cells were incubated at 26 °C for 72 h and were harvested by centrifugation at 5,000xg for 15 min. The medium (P1 viral baculovirus) was collected for large scale expression. The P1 viral baculovirus was determined multiplicity of infection (MOI) by plaque assay. MOI is defined as the number of virus particles per cell should be ranging from 0.5 to 1.0. In the large scale expression, Sf9 cells were sub-cultured to TC-flask size 75 cm^2 , 5 flasks and were incubated at 26 °C for 72 h or until appear monolayer cell. Then, P1 viral baculovirus was added to each flask, incubated at 26 °C until granular appearance and cell lysis. Finally, the transfected cells were harvested by centrifugation at 500xg for 15 min and collected

cells to TK activity assay. The expressed protein was detected by using 12% SDS-PAGE.

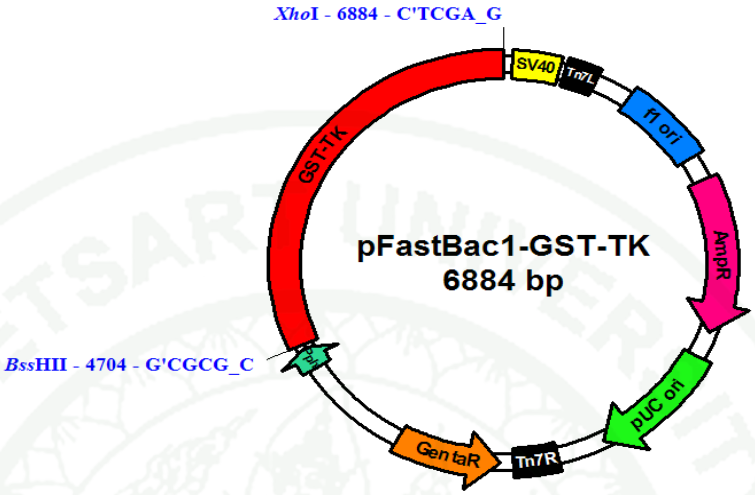

Figure 15 pFastBac-GST-TK, an insect cells expression vector, contains Polyhedrin promoter (PPH) that high-level expression of your recombinant protein in insect cells and Tn7L and Tn7R (Mini Tn7 elements) that permit site-specific transposition of the GST-TK gene into the baculovirus genome.

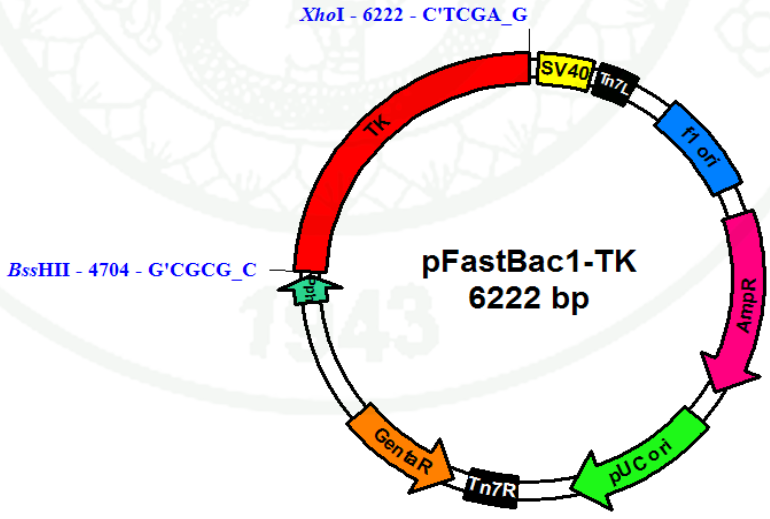

Figure 16 pFastBac-TK, an insect cells expression vector, contains Polyhedrin promoter (PPH) that high-level expression of your recombinant protein in insect cells and Tn7L and Tn7R (Mini Tn7 elements) that permit site-specific transposition of the TK gene into the baculovirus genome.

3. Purification of Tyrosine kinase

3.1 Glutathione-sepharose column

The collected cells that expressed in bacterial cells were lysed by lysis buffer A (50 mM Tris-HCl pH 8.0, 2mM DTT, 1mM PMSF and 1mM EDTA). Then, the lysated cells were centrifuged at 12000xg, 15 min, 4°C for separating supernatant and pellet. The supernatant of TK and GST-TK were purified by GST-column using washing buffer (50 mM Tris-HCl pH 8.0 and 2mM DTT) and elution buffer (50 mM Tris-HCl pH 8.0, 2mM DTT + 10 mM glutathione) and the expressed protein was detected by using 12% SDS-PAGE. The protein concentration was determined with Lowry assay. All proteins were stored at -20°C until used.

3.2 Ni-agarose column

The collected cells that expressed in bacterial cells were lysed by lysis buffer B (50 mM Tris-HCl pH 8.0, 300 mM NaCl, 2mM DTT, 1mM PMSF and 1mM EDTA). Then, the lysated cells were centrifuged at 12000xg, 15 min, 4°C for separate supernatant and pellet. The supernatant of TK and GST-TK were purified by Ni-cloumn using washing buffer (50 mM Tris-HCl pH 8.0, 300 mM NaCl, 2mM DTT), equilibrate buffer (50 mM Tris-HCl pH 8.0, 300 mM NaCl, 2mM DTT, 50 mM imidazole) and elution buffer (50 mM Tris-HCl pH 8.0, 300 mM NaCl, 2mM DTT, 250 mM imidazole) and the expressed protein was detected by using 12% SDS-PAGE. The protein concentration was determined with Lowry assay. All proteins were stored at -20°C until used.

3.3 Poly (Glu:Tyr) column

The transfected cells that expressed in insect cells were lysed by lysis buffer C (10 mM Tris-HCl pH 7.2, 0.1% triton X-100, 2mM DTT, 1mM PMSF and 1mM EDTA). Then, the lysated cells were centrifuged at 12000xg, 15 min, 4°C for separate supernatant and pellet. The supernatant of TK and GST-TK were purified by

Poly (Glu:Tyr) column using washing buffer (10 mM Tris-HCl pH 7.2, 0.1% triton X-100 and 2mM DTT) and elution buffer (10 mM Tris-HCl pH 7.2, 0.1% triton X-100, 2mM DTT and 0.1-0.5 M NaCl) and the expressed protein was detected by using 12% SDS-PAGE. The protein concentration was determined with Lowry assay. All proteins were stored at -20°C until used.

4. Refolding of Tyrosine kinase

The recombinant TK pellets of *E.coli* cells that expressed in inclusion body form were dissolved in buffer D (50 mM Tris buffer pH 7.0 and 150 mM NaCl). Then the solution was sonicated by sonicator for 15 min, 4 times and centrifuged at 10000xg, 15 min. And then collected the pellet dissolved in denaturing buffer (50 mM Tris buffer pH 7.0, 150 mM NaCl and 8 M urea). The denatured solution was detected by 12 % SDS-PAGE for ready to use to TK refolding.

4.1 Refolding conditions

For the large scale of TK refolding, we screened refolding conditions in small scale refolding conditions that adapted from Vincentelli *et al.,* 2004. The small scale refolding conditions were prepared in 96-well plate (Table 10) from stock solutions as follows: 500 mM NaOAc pH4, 5, 6 , 500 mM Tris pH 7, 8, 8.2 , 1M NaCl, 1M KCl, 2M Glucose, 2M arginine hydrochioride, 0.5% PEG4000, 50% glycerol, 20 mM KCl, 5 mM EDTA, 4M guanidine hydrochloride and 500 mM DTT

In each condition, we used GST-TK and TK protein 5 µl and measured turbidity of the solution at 540 nm, then incubated at 4 °C, 24 h and then measured the solution again. Compare the absorbance at 540 nm of before incubation and after incubation. If the absorbance of after incubation of any conditions lower before incubation, imply that the recombinant TK can refold in the conditions, was called refolding condition. Therefore, we used the refolding condition refolded recombinant TK protein in large scale.

4.2 Refolding methods

From screening condition in small scale, we used the refolding buffer in the large scale in two methods. First, the dialysis method, pipette pure TK protein into dialysis bag (cut off = 10 kDa) and dialyzed in 200 ml refolding buffer at 4 °C for overnight by replacing old refolding buffer with new refolding buffer every 1 h in first four hours. Second, the drop-wise method, gentle drop pure TK protein in 100 ml refolding buffer at 4°C until appear aggregation. Then, the solutions in two methods were concentrated by freeze-dry and stored at -20°C for measure activity.

Table 10 Refolding conditions in 96-well plate adapted from Vincentelli *et al.*, 2004

Well No.	1	2	3	4	5	6
A	50 mM NaOAc pH4 2 mM DTT 100 mM NaCl 20% Glycerol 500 mM Glucose	50 mM NaOAc pH4 2 mM DTT 100 mM KCl 0.05% PEG4000 1 mM EDTA	50 mM NaOAc pH5 2 mM DTT 100 mM NaCl 20% Glycerol 500 mM Glucose	50 mM NaOAc pH5 2 mM DTT 100 mM KCl 0.05% PEG4000 1 mM EDTA	50 mM NaOAc pH6 2 mM DTT 100 mM NaCl 20% Glycerol 500 mM Glucose	50 mM NaOAc pH6 2 mM DTT 100 mM KCl 0.05% PEG4000 1 mM EDTA
B	50 mM NaOAc pH4 2 mM DTT 100 mM NaCl 0.05% PEG4000 800 mM Arg-HCl	50 mM NaOAc pH4 2 mM DTT 0.05% PEG4000 800 mM Arg-HCl	50 mM NaOAc pH5 2 mM DTT 100 mM NaCl 0.05% PEG4000 800 mM Arg-HCl	50 mM NaOAc pH5 2 mM DTT 0.05% PEG4000 800 mM Arg-HCl	50 mM NaOAc pH6 2 mM DTT 100 mM NaCl 0.05% PEG4000 800 mM Arg-HCl	50 mM NaOAc pH6 2 mM DTT 0.05% PEG4000 800 mM Arg-HCl
C	50 mM NaOAc pH4 2 mM DTT 100 mM NaCl 0.05% PEG4000 500 mM Glucose	50 mM NaOAc pH4 2 mM DTT 0.05% PEG4000 500 mM Glucose	50 mM NaOAc pH5 2 mM DTT 100 mM NaCl 0.05% PEG4000 500 mM Glucose	50 mM NaOAc pH5 2 mM DTT 0.05% PEG4000 500 mM Glucose	50 mM NaOAc pH6 2 mM DTT 100 mM NaCl 0.05% PEG4000 500 mM Glucose	50 mM NaOAc pH6 2 mM DTT 0.05% PEG4000 500 mM Glucose
D	50 mM NaOAc pH4 2 mM DTT 200 mM NaCl 0.05% PEG4000	50 mM NaOAc pH4 2 mM DTT 800 mM Arg-HCl	50 mM NaOAc pH5 2 mM DTT 200 mM NaCl 0.05% PEG4000	50 mM NaOAc pH5 2 mM DTT 800 mM Arg-HCl	50 mM NaOAc pH6 2 mM DTT 200 mM NaCl 0.05% PEG4000	50 mM NaOAc pH6 2 mM DTT 800 mM Arg-HCl

Table 10 (Continuted)

Well No.	7	8	9	10	11	12
A	50 mM Tris pH7 2 mM DTT 100 mM NaCl 20% Glycerol 500 mM Glucose	50 mM Tris pH7 2 mM DTT 100 mM KCl 0.05% PEG4000 1 mM EDTA	50 mM Tris pH8 2 mM DTT 100 mM NaCl 20% Glycerol 500 mM Glucose	50 mM Tris pH8 2 mM DTT 100 mM KCl 0.05% PEG4000 1 mM EDTA	50 mM Tris pH8.2 2 mM DTT 20 mM NaCl 20mM KCl	50 mM Tris pH8.2 2 mM DTT 100 mM Gd-HCl 440 mM Arg-HCl 20 mM NaCl 20mM KCl
B	50 mM Tris pH7 2 mM DTT 100 mM NaCl 0.05% PEG4000 800 mM Arg-HCl	50 mM Tris pH7 2 mM DTT 0.05% PEG4000 800 mM Arg-HCl	50 mM Tris pH8 2 mM DTT 100 mM NaCl 0.05% PEG4000 800 mM Arg-HCl	50 mM Tris pH8 2 mM DTT 0.05% PEG4000 800 mM Arg-HCl	50 mM Tris pH8.2 2 mM DTT 20 mM NaCl 400 mM Arg-HCl 20mM KCl	50 mM NaOAc pH4 2 mM DTT
C	50 mM Tris pH7 2 mM DTT 100 mM NaCl 0.05% PEG4000 500 mM Glucose	50 mM Tris pH7 2 mM DTT 0.05% PEG4000 500 mM Glucose	50 mM Tris pH8 2 mM DTT 100 mM NaCl 0.05% PEG4000 500 mM Glucose	50 mM Tris pH8 2 mM DTT 0.05% PEG4000 500 mM Glucose	50 mM Tris pH8.2 2 mM DTT 800 mM Arg-HCl 20 mM NaCl 20mM KCl	50 mM NaOAc pH5 2 mM DTT
D	50 mM Tris pH7 2 mM DTT 200 mM NaCl 0.05% PEG4000	50 mM Tris pH7 2 mM DTT 800 mM Arg-HCl	50 mM Tris pH8 2 mM DTT 200 mM NaCl 0.05% PEG4000	50 mM Tris pH8 2 mM DTT 800 mM Arg-HCl	50 mM Tris pH8.2 2 mM DTT 50 mM Gd-HCl 20 mM NaCl 20mM KCl	50 mM NaOAc pH6 2 mM DTT

Table 10 (Continuted)

Well No.	1	2	3	4	5	6
E	50 mM NaOAc pH4 2 mM DTT 200 mM NaCl 0.05% PEG4000 800 mM Arg-HCl	50 mM NaOAc pH4 2 mM DTT 200 mM NaCl 500 mM Glucose	50 mM NaOAc pH5 2 mM DTT 200 mM NaCl 0.05% PEG4000 800 mM Arg-HCl	50 mM NaOAc pH5 2 mM DTT 200 mM NaCl 500 mM Glucose	50 mM NaOAc pH6 2 mM DTT 200 mM NaCl 0.05% PEG4000 800 mM Arg-HCl	50 mM NaOAc pH6 2 mM DTT 200 mM NaCl 500 mM Glucose
F	50 mM NaOAc pH4 2 mM DTT 200 mM NaCl 0.05% PEG4000 1 mM EDTA	50 mM NaOAc pH4 2 mM DTT 100 mM KCl 800 mM Arg-HCl	50 mM NaOAc pH5 2 mM DTT 200 mM NaCl 0.05% PEG4000 1 mM EDTA	50 mM NaOAc pH5 2 mM DTT 100 mM KCl 800 mM Arg-HCl	50 mM NaOAc pH6 2 mM DTT 200 mM NaCl 0.05% PEG4000 1 mM EDTA	50 mM NaOAc pH6 2 mM DTT 100 mM KCl 800 mM Arg-HCl
G	50 mM NaOAc pH4 2 mM DTT 100 mM KCl 20% Glycerol 500 mM Glucose	50 mM NaOAc pH4 2 mM DTT 100 mM KCl 20% Glycerol	50 mM NaOAc pH5 2 mM DTT 100 mM KCl 20% Glycerol 500 mM Glucose	50 mM NaOAc pH5 2 mM DTT 100 mM KCl 20% Glycerol	50 mM NaOAc pH6 2 mM DTT 100 mM KCl 20% Glycerol 500 mM Glucose	50 mM NaOAc pH6 2 mM DTT 100 mM KCl 20% Glycerol
H	50 mM NaOAc pH4 2 mM DTT 100 mM KCl 0.05% PEG4000 800 mM Arg-HCl	50 mM NaOAc pH4 2 mM DTT 0.05% PEG4000	50 mM NaOAc pH5 2 mM DTT 100 mM KCl 0.05% PEG4000 800 mM Arg-HCl	50 mM NaOAc pH5 2 mM DTT 0.05% PEG4000	50 mM NaOAc pH6 2 mM DTT 100 mM KCl 0.05% PEG4000 800 mM Arg-HCl	50 mM NaOAc pH6 2 mM DTT 0.05% PEG4000

Table 10 (Continued)

Well No.	7	8	9	10	11	12
E	50 mM Tris pH7 2 mM DTT 200 mM NaCl 0.05% PEG4000 800 mM Arg-HCl	50 mM Tris pH7 2 mM DTT 200 mM NaCl 500 mM Glucose	50 mM pH8 2 mM DTT 200 mM NaCl 0.05% PEG4000 800 mM Arg-HCl	50 mM Tris pH8 2 mM DTT 200 mM NaCl 500 mM Glucose	50 mM Tris pH8.2 2 mM DTT 50 mM Gd-HCl 20 mM NaCl 20mM KCl 400 mM Arg-HCl	50 mM Tris pH7 2 mM DTT
F	50 mM Tris pH7 2 mM DTT 200 mM NaCl 0.05% PEG4000 1 mM EDTA	50 mM Tris pH7 2 mM DTT 100 mM KCl 800 mM Arg-HCl	50 mM Tris pH8 2 mM DTT 200 mM NaCl 0.05% PEG4000 1 mM EDTA	50 mM Tris pH8 2 mM DTT 100 mM KCl 800 mM Arg-HCl	50 mM Tris pH8.2 2 mM DTT 50 mM Gd-HCl 20 mM NaCl 20mM KCl 400 mM Arg-HCl	50 mM Tris pH8 2 mM DTT
G	50 mM Tris pH7 2 mM DTT 100 mM KCl 20% Glycerol 500 mM Glucose	50 mM Tris pH7 2 mM DTT 100 mM KCl 20% Glycerol	50 mM Tris pH8 2 mM DTT 100 mM KCl 20% Glycerol 500 mM Glucose	50 mM Tris pH8 2 mM DTT 100 mM KCl 20% Glycerol	50 mM Tris pH8.2 2 mM DTT 20 mM NaCl 20mM KCl	H_2O
H	50 mM pH7 2 mM DTT 100 mM KCl 0.05% PEG4000 800 mM Arg-HCl	50 mM pH7 2 mM DTT 0.05% PEG4000	50 mM pH8 2 mM DTT 100 mM KCl 0.05% PEG4000 800 mM Arg-HCl	50 mM pH8 2 mM DTT 0.05% PEG4000	50 mM pH8.2 2 mM DTT 100 mM Gd-HCl 400 mM Arg-HCl 20 mM NaCl 20mM KCl	H_2O

5. Tyrosine kinase activity assay

5.1 Antibody beacon tyrosine kinase assay

Tyrosine kinases play an important role in a variety of cellular pathways and processes, as well as pathologies such as cancer. The antibody beacon tyrosine kinase assay kit (A-35725) provides a simple and robust assay for measuring the activity of tyrosine kinases and their inhibitors and modulators. The assay is based on a detection complex comprised of small-molecule tracer ligand that exhibits quenched fluorescence when bound to anti-phosphotyrosine antibodies. In the presence of phosphortyrosine containing peptides, the ligand is rapidly displaced and there is an increase in fluorescence (Figure 17).

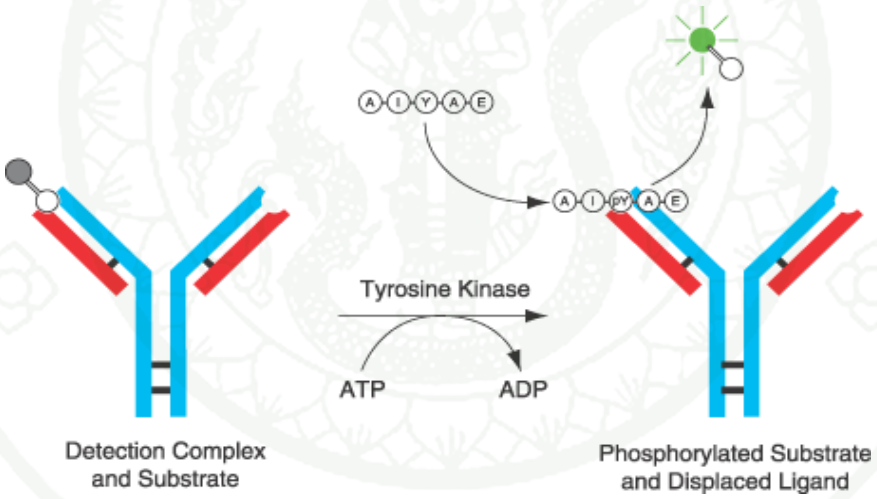

Figure 17 Antibody beacon tyrosine kinase assay reaction scheme.

Source: Anderson (1996)

Each component of the detection complex has been optimized for minimal background fluorescence, maximal displacement of the ligand in the presence of phosphotyrosine-containing peptides and a large increase in fluorescence upon displacement. The approximately 4-fold fluorescence enhancement of the ligand upon

displacement by the phosphopeptide provides excellent signal-to-background discrimination (Figure 18).

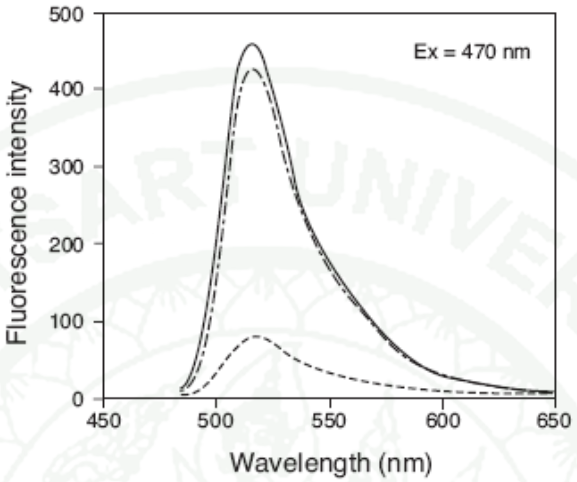

Figure 18 Fluorescence response of the antibody beacon detection complex in the presence of a phosphotyrosine-containing peptide. The fluorescence of Oregon Green 488 ligand (solid line), Antibody Beacon detection complex (dashed line) or the Antibody Beacon detection complex plus phosphorylated Abl substrate peptide (EAIpYAAPFAKKK; – – - – – dashed line) was measured in kinase assay buffer. In the presence of the phosphopeptide, the Oregon Green 488 ligand was displaced from the Antibody Beacon complex and exhibited a 4-fold enhancement over the fluorescence of the Antibody Beacon complex in buffer alone.

Source: Anderson (1996)

The excitation and emission spectra of the Oregon Green 488 dye closely match those of fluorescein thus making this assay readily compatible with any fluorescence multiwell plate reader. The antibody component provides detection specificity for phosphotyrosine peptides and minimal interference from coexisting assay components such as ATP (up to 1 mM) or reducing agents, such as dithiothreitol (up to 2 mM). The Antibody Beacon tyrosine kinase assay, unlike most

other commercially available tyrosine kinase activity assays, allows for the real-time monitoring of kinase activity. Real-time assays are possible due to the rapid dissociation of the detection complex and the capacity for the assay components to be simultaneously combined. The assay is also easily adapted for measuring the effectiveness of tyrosine kinase inhibitors (Figure 19). Additional features of the assay include its use of unlabeled peptide substrates, its low limit of detection (≤50 nM of phosphotyrosine-containing peptide) and its broad signal window, indicated by a *Z′* factor 2 of 0.9.

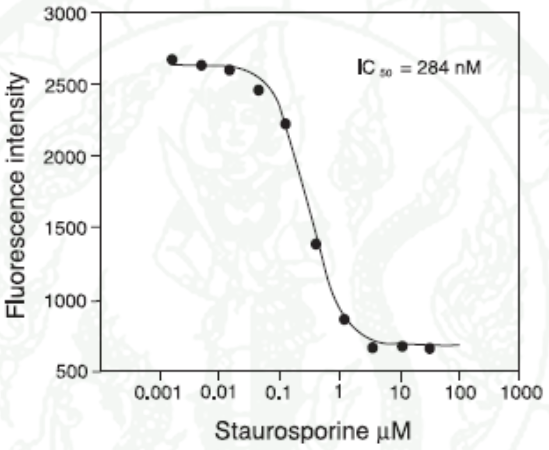

Figure 19 Inhibition of src kinase by staurosporine. Varying concentrations of staurosporine were incubated with src kinase (25 U/mL in reaction buffer) for 20 min at 37°C. The Antibody Beacon tyrosine kinase detection complex, kinase substrate (poly (Glu:Tyr), 4:1) and ATP were then added to each well, and the reactions were incubated at 37°C. After 1 hour, fluorescence was measured in a fluorescence microplate reader using excitation at 485 nm and emission at 535 nm.

Source: Anderson (1996)

The reaction mixture of 50 µl contained 150 nM Anti-phosphotyrosine antibody, 75 nM Oregon Green 488 ligand, 0.6 mg/ml poly(Glu:Tyr), various [ATP] = 0.025 – 0.8 mM**.** The reaction was started by adding EGFR, GST-TK or TK 25 µl

and 1X kinase buffer plus 2 mM DTT for adjust volume to 200 µl. The mixture solution was measured for 15 min at 492/517 nm. We used reference phosphotyrosine-containing peptide for standard curve (1 unit enzyme = µmol phosphotyrosine/min).

5.2 ATP/NADH couple assay

The assay is based on a reaction in which the regeneration of hydrolyzed ATP is coupled to the oxidation of NADH. Following each cycle of ATP hydrolysis, the regeneration system consisting of phosphoenolpyruvate (PEP) and pyruvate kinase (PK) converts one molecule of PEP to pyruvate when the ADP is converted back to the ATP (Figure 20). The pyruvate is subsequently converted to lactate by Lactate dehydrogenase (LDH) resulting in the oxidation of one NADH molecule.

The assay measures the rate of NADH absorbance decrease at 340 nm, which is proportional to the rate of steady-state ATP hydrolysis. The constant regeneration of ATP allows monitoring the TK activity for ATP hydrolysis rate over the entire course of the assay (Figure 21).

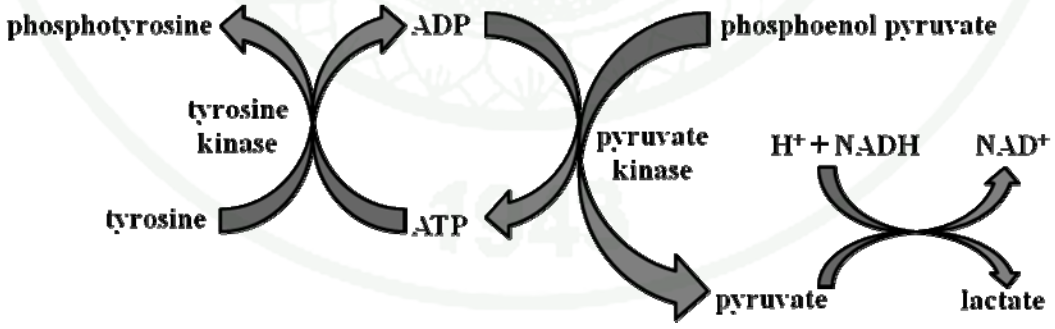

Figure 20 ATP/NADH couple assay reaction scheme.

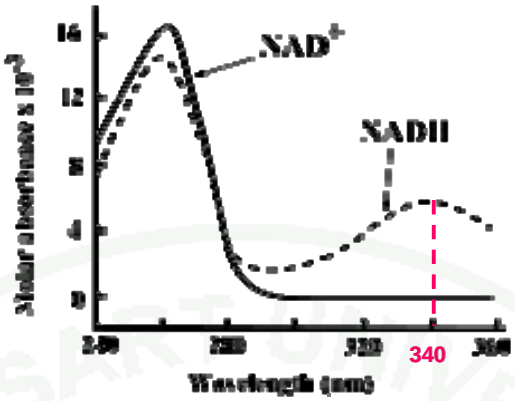

Figure 21 The ATP/NADH couple assay measures the rate of NADH absorbance decrease at 340 nm.

The reaction mixture of 50 µl contained 0.5 mg/ml BSA, 2 mM $MnCl_2$, 1 mM phospho(enol) pyruvic acid (PEP), 1 mM TCEP , 0.1 M MOPS pH 7.5, 0.6 mg/ml poly(Glu:Tyr), 1/50 (v/v) pyruvate kinase/lactic dehydrogenase , 0.5 mM NADH, various concentration of ATP (0.025 – 0.8 mM)**,** The reaction was started reaction by adding start reaction with EGFR, GST-TK or TK 5 µl. The mixture solution was pipetted to 96-well plate and was measured by using wavelength 340 nm, 15 min.

5.3 PURETIME assay

Fluorescence of PURETIME®17 is enhanced upon phosphorylation by the kinase enzyme, producing more intense emission and a longer fluorescence lifetime. The small fluorophore does not adversely affect the action of the kinase protein either binding ATP or phosphorylating the substrate. Fluorescence measurements can be made at any point during the kinase incubation, permitting time course experiments and direct determination of kinase reaction kinetics as well as end points. The reaction of PURETIME assay showed in figure 22

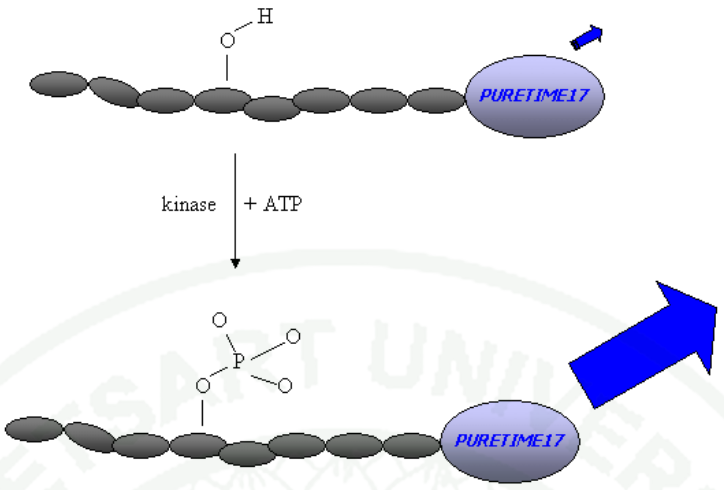

Figure 22 PURETIME assay assay reaction scheme.

Advantage of PURETIME assay is new TK assay activity, kinase and substrate additions only, No particles or antibodies and simple fluorescence intensity or fluorescence lifetime plate reading

The reaction mixture of 50 µl contained 500 nM PURETIME-17 EGF receptor tyrosine kinase substrate peptide: AEEEEYFELV-PT17 , 50 mM Tris pH 7.5, 10 mM $MgCl_2$, 1 mM EDTA, 2 mM DTT, 0.01% Tween 20 and 40 µM ATP. The reaction was started by adding EGFR, GST-TK or TK 25 µl and 1X kinase buffer plus 2 mM DTT for adjust volume to 200 µl. The mixture solution was measured for 15 min at 420/460 nm.

6. Plaque assay

To determine the titer of a baculoviral stock, prepare plate Sf9 cells in 6-well plates, prepared 10^{-1}, 10^{-3} and 10^{-5} dilutions of your baculoviral stock. Added the different dilutions of baculovirus to Sf9 cells and infected cells for 1 hour. Removed the virus and overlaid the cell monolayer with plaquing medium. Stained with stain solution (1% agarose and 1mg/ml crystal violet in Sf-900 II medium. Incubated the cells for 7-10 days and counted the number of plaques in each dilution. Used the

following formula to calculate how much viral stock to add to obtain a specific multiplicity of infection (MOI): Inoculum required (ml) = MOI (pfu/cell) x number of cells / titer of viral stock (pfu/ml) and titer (pfu/ml) = number of plaques x dilution factor x (1/ml of inoculum/well).

7. Determined qualitative mono- and disaccharide analysis

7.1 Preparation of the reagent

- Orcine-reagent (80 mg of orcine monohydrate in 5 ml H_2O and 37.5 ml of 60% sulfuric acid)
- 1 mg/ml glucose was a positive control.

7.2 Measurement of sugar content in sample

Added 450 µl orcine-reagent to 50 µl sample. Incubated the reaction for 45 min at 80 °C in water bath. Added 550 µl H_2O to the tube. Mixed carefully and measured the absorbance at 425 nm in spectrophotometer.

8. Inhibiting Activity Assay

100 g dry weight of all Thai herbs (Table 11) was grinded with mortar and was extracted by checking in 500 ml of 95% ethanol for 2 days at room temperature. The supernatant was filtered with 10 mm Whatman filter paper and ethanol was removed by rotary evaporation. The crude extractions were frozen in -20 °C for the inhibiting activity assay.

Table 11 List of Thai herbs for 24 species

List of Thai herbs	Common Name (in Thai)	Scientific Name
1	สะเดา	*Azadirachta indica*
2	ทองพันชั่ง	*Rhinacanthus nasutus*
3	ราชดัด	*Brucea amarissima*
4	อบเชยญวน	*Cinnamomum loureiroi*
5	เบญกานี	*Quercus infectoria*
6	อ้อยแดง	*Saccharum officinarum*
7	จันทน์เทศ	*Myristica fragrans*
8	ต้อยติ่ง	*Ruellia tuberosa*
9	ขมิ้นชัน	*Curcuma longa*
10	เทียนกิ่ง	*Lawsonia inermis*
11	โกฐกะกลิ้ง	*Strychnos nux-vomica*
12	ว่านชักมดลูก	*Curcuma xanthorrhiza*
13	สมอพิเภก	*Terminalia belirica*
14	สมอทะเล	*Sapium indicum*
15	สมอไทย	*Terminalia chebula*
16	กำแพงเจ็ดชั้น	*Salacia chinensis*
17	ดอกคำแสด	*Mallotus philippensis*
18	ไพล	*Zingiber montanum*
19	เปลือกนนทรี	*Peltophorum pterocarpum*
20	มะกอก	*Spondias pinnata*
21	แกแล	*Maclura cochinchinensis*
22	สีเสียดเปลือก	*Acacia catechu*
23	สีเสียดยางก้อน	*Acacia catechu*
24	ฝาง	*Caesalpinia sappan*

The reaction mixture of 50 µl contained 150 nM anti-phosphotyrosine antibody, 75 nM Oregon Green 488 ligand, 0.6 mg/ml poly(Glu:Tyr), 0.05 mM ATP and 0.025 mg/µl Thai herb extract or 0.01-10 µM gefitinib for K_i study. The reaction was started by adding EGFR or TK 20 µl and 1X kinase buffer plus 2 mM DTT for adjust volume to 200 µl. The mixture solution was measured for 15 min at 492/517 nm. We used 0.025 mg/ml gefitinib for a reference inhibitor. % inhibition for each extract is expressed as the % relative to % inhibition for gefitinib in our assay condition.

RESULTS AND DISCUSSION

1. Bacterial cells expression system

1.1 Cloning and expression of recombinant TK in bacterial cells

We constructed individual plasmids to express TK in 2 forms (fusion and non-fusion proteins) in bacterial cells. The recombinant plasmids with TK genes were called pGEX-GST-TK and pET-TK**.** The PCR products of TK gene showed the expected DNA fragments of approximately 837 bp (Figure 23). After digestion and purification of the PCR products, the DNA fragments were ligated into plasmid pGEX-4T-1 and pET-15b. The constructed plasmids, pGEX-GST-TK and pET-TK were amplified by PCR. The PCR products of GST-TK and TK genes showed the expected DNA fragments of approximately 1,499 bp and 837 bp, respectively (Figure 24). Then each plasmid was individually transformed into the *E.coli* strain BL21 (DE3). The protein expression of plasmids which were under the control of the *tac*/T7 promoter was induced by 1 mM IPTG. Upon induction at 37°C and 16°C, significant amounts of target proteins appear as major bands with molar masses of 55 kDa and 29 kDa for GST-TK and TK, respectively (Figure 25 and Figure 26).

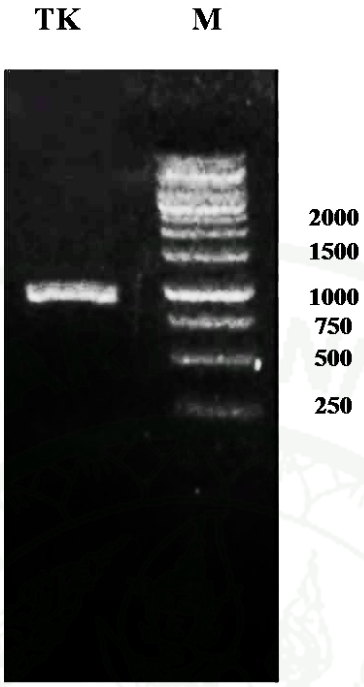

Figure 23 The PCR products of TK genes showed the expected DNA fragments of 837 bp.

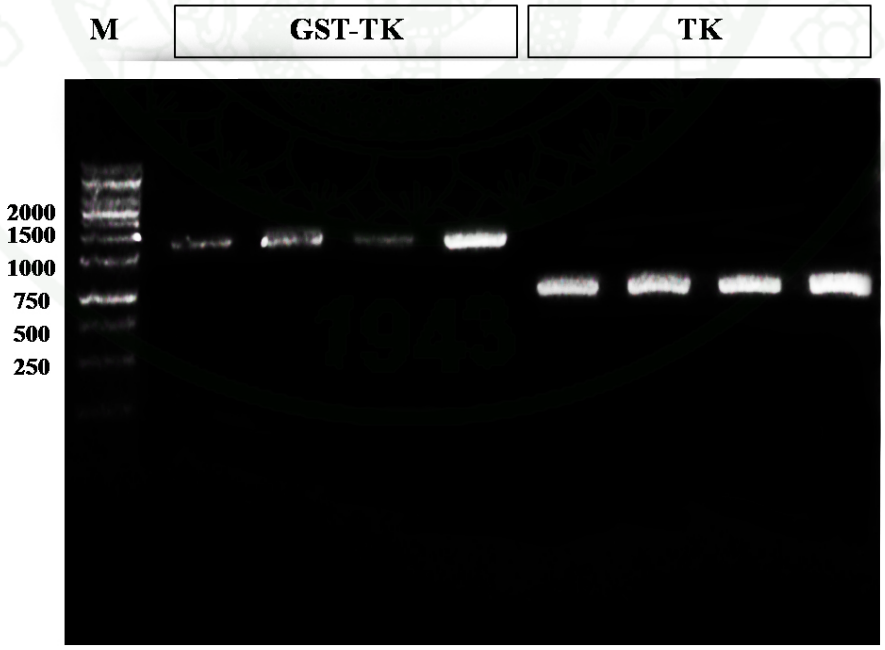

Figure 24 The PCR products of GST-TK and TK gene showed the expected DNA fragments of 1,499 bp and 837 bp, respectively.

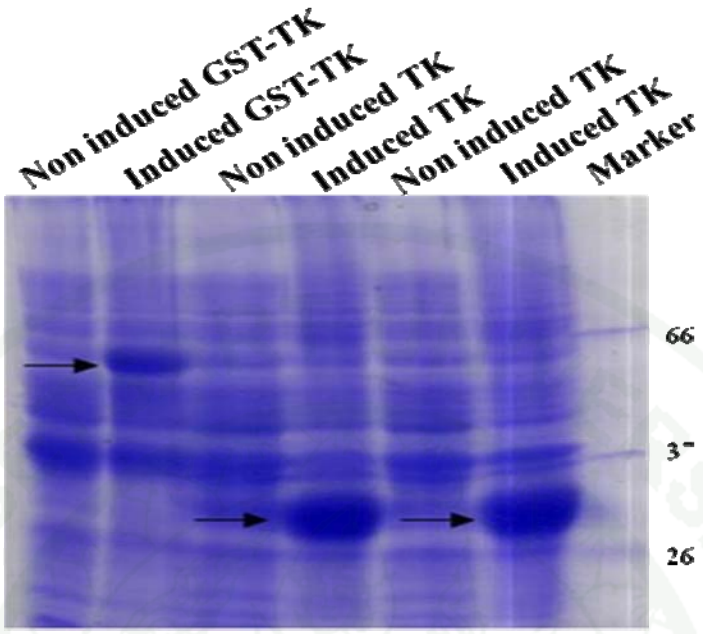

Figure 25 The individual expression of GST-TK and TK proteins in *E.coli* strain BL21 (DE3) cells at 37°C.

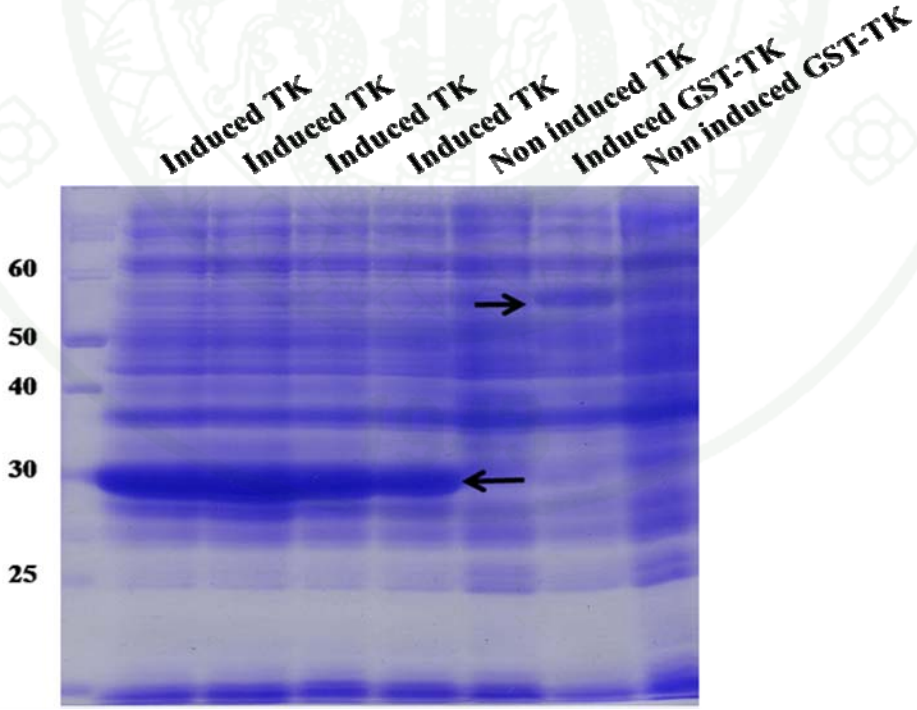

Figure 26 The individual expression of GST-TK and TK proteins in *E.coli* strain BL21 (DE3) cells at 16°C.

In bacterial cells expression system, both GST-TK and TK could express at 37°C and 16°C. The collected cells that expressed at 37°C were lysed by lysis buffer. The lysed cells were centrifuged at 12000xg, 15 min, 4°C for separating supernatant and pellet and detected by using 12% SDS-PAGE. The result showed that most GST-TK and TK protein were in pellet or inclusion body form (Figure 27). Therefore the recombinant TK could not expressed in soluble form at 37°C. Then, the collected cells that expressed at 16°C were lysed by lysis buffer A. The lysed cells were centrifuged at 12000xg, 15 min, 4°C and proteins in both supernatant and pellets were detected by using 12% SDS-PAGE. The result showed that TK protein was in pellet or in an inclusion body form (Figure 28) but GST-TK was in soluble form, therefore we used glutathione-sepharose column and Ni-agarose column for purify GST-TK protein.

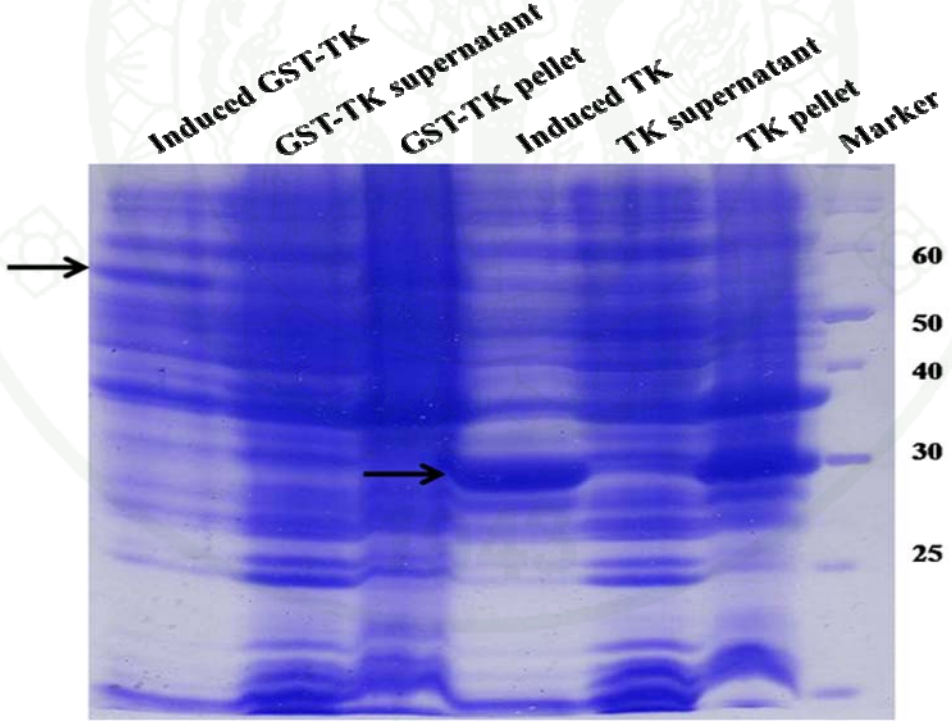

Figure 27 GST-TK and TK proteins that expressed in *E.coli* cells at 37°C.

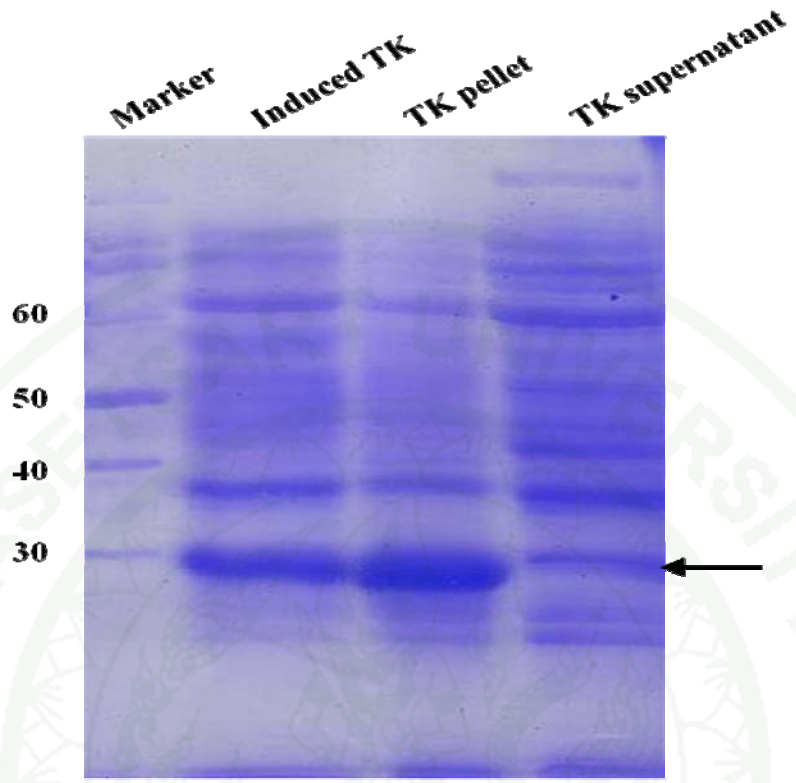

Figure 28 TK protein that expressed in *E.coli* cells at 16°C.

1.2 Purification of recombinant TK in bacterial cells

1.2.1 Glutathione-sepharose column

The collected cells that expressed GST-TK in *E.coli* cells at 16°C were lysed by lysis buffer A. Then, the lysed cells were centrifuged at 12000xg, 15 min, 4°C. The GST-TK supernatant was purified by GST-column. The results showed that in the eluted fraction appeared as two major bands at 55 KDa and 30 KDa, approximately (Figure 29). Therefore, GST-TK protein could partial purify by glutathione-sepharose column.

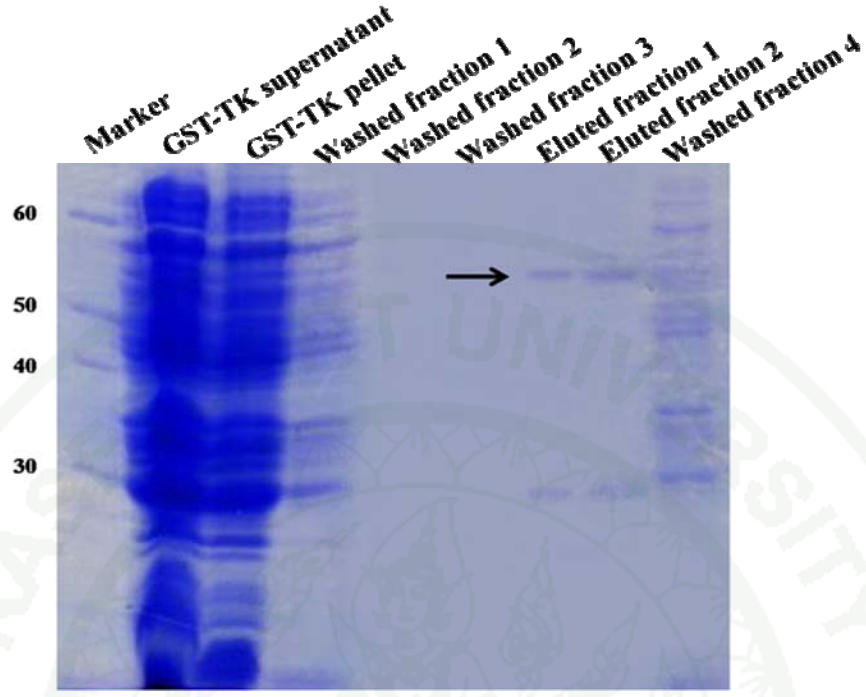

Figure 29 Purification of GST-TK protein that expressed in *E.coli* cells at 16°C by GST-column.

The concentration of GST-TK protein was determined with Lowry assay. From I L culture the concentration of GST-TK in supernatant and after purification were 20.6 mg/ml and 0.77 mg/ml, respectively. In conclusion the bacterial expression of recombinant TK, GST-TK protein, in low temperature could express protein in low yield (Table 12).

1.2.2 Ni-agarose column

Since the construction of pGEX-TK also had thehis-tag at the C-terminal, we also tried to purify by Ni-agarose bead to test whether we can get a higher yield than pervious method. The collected cells that expressed GST-TK in *E.coli* cells at 16°C were lysed by lysis buffer B. Then, the lysed cells were centrifuged at 12000xg, 15 min, 4°C. The supernatant of TK and GST-TK were purified by Ni-NTA column. The results showed that the GST-TK protein bands were

found in the washed fraction and no protein detection in the eluted fraction (Figure 30). Therefore, GST-TK protein could not purify by Ni-agarose column this may due to folding of His-tag at C-terminal of GST-TK protein was not exposing to the water for binding to Ni-agarose column.

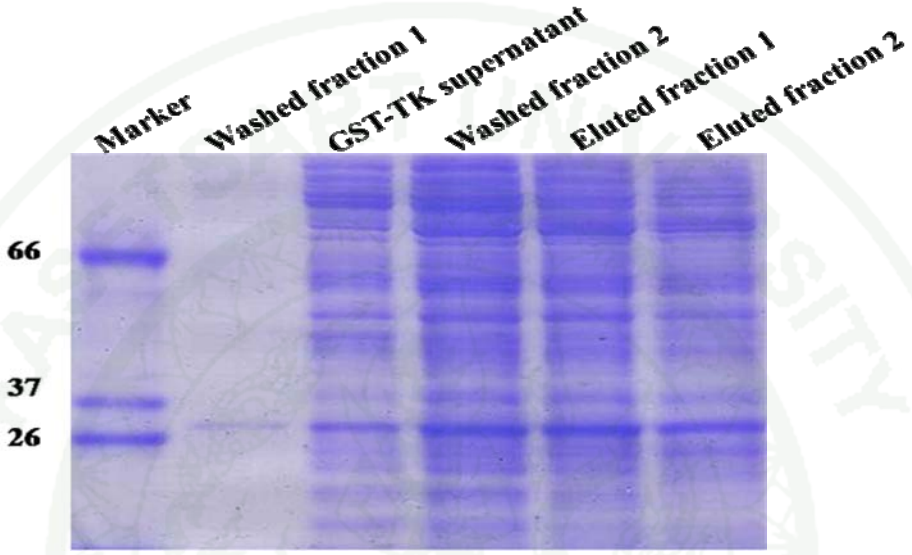

Figure 30 Purification of GST-TK protein that expressed in *E.coli* cells at 16°C by Ni-column.

1.3 Refolding of recombinant TK in bacterial cells

The GST-TK and TK pellets of *E.coli* cells that expressed at 37°C (as inclusion body form) were dissolved in the buffer D. Then, the solution was sonicated by sonicator at power 1000 watt, 20 kHz for 15 min, 4 times and centrifuged at 10,000xg, 15 min. The pellet was collected and then dissolved in denaturing buffer. The TK protein in denatured solution was detected by 12 % SDS-PAGE (Figure 31). The result showed that after re-sonication, the GST-TK and TK were majority protein in the denatured solution. These result indicated that the repeated sonication method could separate the other proteins that could also soluble from GST-TK and TK pellets.

In the small scale refolding, we measured turbidity of the solution at 540 nm and compared the absorbance at 540 nm of before and after incubation with the

refolding buffer. We found that there were two conditions showing the lower absorbance after incubation. Therefore the result indicated that the solution was less turbidity than the starting condition, hence, the protein can be folded. One of a refolding buffer I contains 50 mM Tris-HCl pH 7.0, 800 mM arginine hydrochioride, 2 mM DTT, while another refolding buffer II contains 50 mM Tris-HCl pH 8.0, 800 mM arginine hydrochioride, 2 mM DTT and 0.05% PEG 4000, which the refolding buffer I and II were similar to the patented condition: EP1538201 (1 M Tris HCl pH 7.0, 500 mM arginine, 10 mM DTT). These result indicated that PEG 4000 and arginine hydrochioride contribute to refold protein may due to PEG 4000 has an effect on osmotic stress and arginine might work through a unique mechanism to increase the solubility of aggregation prone proteins through interaction with them and nevertheless could not facilitate the refolding (Arakawa and Tsumoto, 2003). However, Reddy *et al.* (2005) demonstrated that arginine promoted the solubility of unfolded species by binding to them and thus accelerated oxidative refolding of reduced-denatured lysozyme albeit it did not influence the thermodynamic stability of protein. Tsumoto *et al.* (2004) summarized all the effects of arginine on proteins and suggested that interactions between the guanidine group of arginine and tryptophan side chains may be responsible for suppression of protein aggregation. But the detailed pathway of arginine assisted protein refolding remains somewhat unclear.

For the large scale, Refolding buffer I and II were used for refolding both GST-TK and TK proteins in dialysis method and drop-wise method. Then protein was concentrated using freeze-dry. The refolded GST-TK and TK were measured their activities by using both ABTK assay and ATP/NADH couple assay. The result showed that the refolded GST-TK and TK had no activity (data not show).

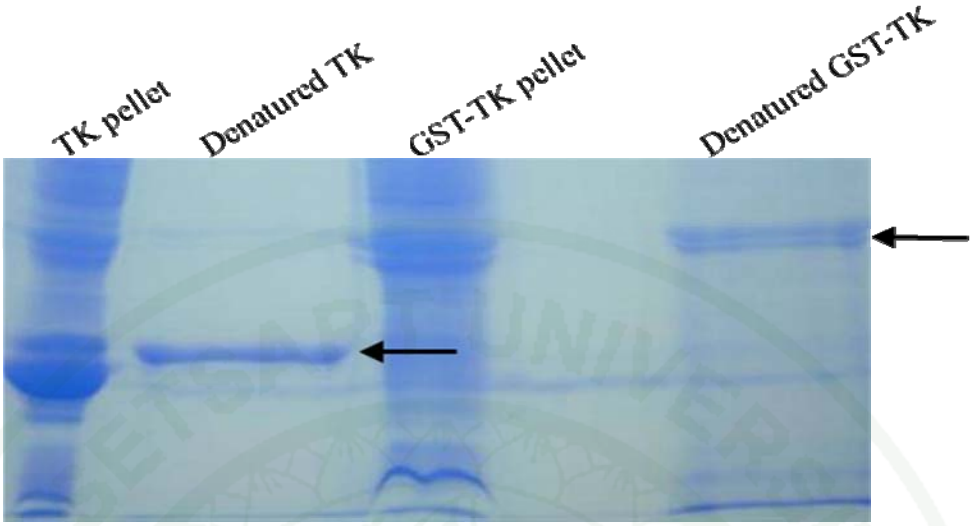

Figure 31 Repeated sonication of GST-TK and TK pellets ready to use for refolding

1.4 Activity assay of recombinant TK in bacterial cells

The expression of GST-TK and TK in *E.coli* cells at 16°C could express protein in soluble form. These supernatants were measured activities by using ABTK assay and ATP/NADH couple assay. The result showed that only GST-TK supernatant had activity and it could measure activity only with the ABTK assay method. From this assay, K_m of ATP equal to 2.10 ± 3.16 mM and V_{max} equal to 0.175 ± 2.07 nM/min (Figure 32). However, for the ATP/NADH couple assay that we measured the usage of ATP by measuring the decrease of OD. 340 caused lower amount of NADH, we could not see the decreasing of intensity at all. The reason that the activity of GST-TK supernatant could not be measured with ATP/NADH couple assay may due to ability of GST that can convert NAD back to NADH. Therefore, it made our measurement unreliable. Although, GST-TK supernatant that expressed at 16°C had activity but the K_m was very high and V_{max} was very low when compared with the full-length human EGFR (Table 12). This may due to bacterial expression system does not have post-translational modification like in humans. Using ABTK assay, GST-TK supernatant that was purified by glutathione-sepharose column observed to have no activity. This assay may be due to low protein concentration.

Previous study indicated that the high concentration of TK in millimolar range can mimic the dimeric receptor and causes the activation of TK (Zhang et al., 2006).

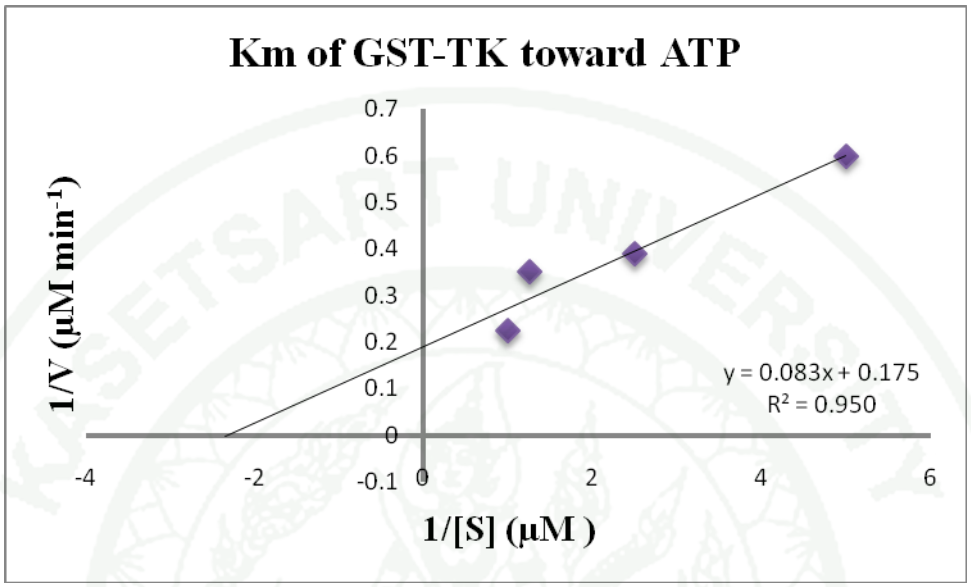

Figure 32 K_m and V_{max} of GST-TK toward ATP that expressed at 16°C in *E.coli* cells by using antibody beacon tyrosine kinase assay.

Table 12 Comparison activity assays of full-length EGFR and GST-TK that expressed in bacterial cells at 16 °C.

Protein	Protein concentration	Yield (mg)	Antibody Beacon tyrosine kinase assay	
			K_m of ATP (µM)	V_{max} (nM/min)
Full-length human EGFR	39,465 U/mg protein	-	112.23 ± 1.58	36.885 ± 0.11
GST-TK supernatant	0.206 mg/ml	20.6	2,100 ± 3.16	0.175 ± 2.07
Purified GST-TK	0.77 mg/ml	7.7	N.A.	N.A.

* N.A. = No activity

According to the expression of recombinant TK in bacterial cells system, both 37°C and 16°C could not expressed efficiency of TK enzyme activity may due to

bacterial cells are a prokaryotic cell, they have no post-translational modification (such as glycosylation, methylation and acetylation) and folding helper proteins, which may involve in the corrected folding of active TK. Therefore, we used insect cells expression system to express recombinant active TK because the insect cells are eukaryote cell and have post-translational modification and folding helper proteins like in humans.

2. Insect cells expression system

2.1 Cloning and expression of recombinant TK plasmid in insect cells

The GST-TK and TK genes in pGEX-GST-TK were amplified by a polymerase chain reaction (PCR) using primers TK/*BssH*II_F and TK/*XhoI*_R for constructing plasmid expressing TK protein with His-tag at C-terminus, then using primers GST/*BssH*II_F and TK/*XhoI*_R for generating a plasmid expressing GST-TK fusion protein with GST at N-terminus and His-tag at C-terminus. The PCR products, GST-TK and TK genes were purified by GeneJET Plasmid Miniprep kit and cut with *BssH*II and *Xho*I for ligation into pFastBac-1expression vector**.** The construction of plasmids pFastBac-GST-TK and pFastBac-TK were individually transformed into the *E.coli* strain DH10Bac^{TM} to create bacmids. The bacmids contain M13 Forward and M13 Reverse priming sites flanking the mini-*att*Tn7 site within the *lacZα*-complementation region to facilitate PCR analysis, so the size of PCR product of bacmids is the size of target gene plus ~2300 bp. The approximately size of PCR products of GST-TK gene is 1,499 bp plus 2,300 bp of *lacZα* gene, which is equal to 3.8 Kb and PCR of TK gene is 837 bp plus 2,300 bp of *lacZα* gene, which is equal to 3.1 Kb. The recombinant bacmids were checked by PCR products using M13 primers which were 3.8 Kb and 3.1 Kb for GST-TK and TK, respectively (Figure 33) implying that GST-TK gene were insert to baculovirus gene. For insect cells transfection, the recombinant bacmids were transfected into Sf9 cell line using Cellfectin Reagent. The transfected cells were incubated at 26 °C for 72 h until granular was observed (Figure 34), then cell were lysed (Figure 35). The appearance of granular in transfected cells indicated that the protein expression of baculovirus

particles and recombinant TK protein were expressed in the cells. The lysed cells indicated that the baculovirus particles lysed cells into medium. For amplification P1 viral baculovirus, we collected medium and repeated transfection in 6-well plate.

In the large scale expression, Sf9 cells were sub-cultured into 5 TC-flask size 75 cm^2 and were incubated at 26°C for 72 h or until monolayer cells appear. Then, amplifying baculovirus was added to each flask, incubated at 26°C until granular and cell lysis was observed. The transfected cells were harvested by centrifugation at 500xg for 15 min and collected cells to purify TK. The expressed protein was detected by using 12% SDS-PAGE. The expression of plasmids containing the TK-ORFs was under the control of the polyhedrin promoter (P_{PH}). Upon expression of bacmid GST-TK and bacmid TK, significant amounts of new proteins appear as major bands with molar masses of 55 kDa and 50 kDa, respectively (Figure 36).

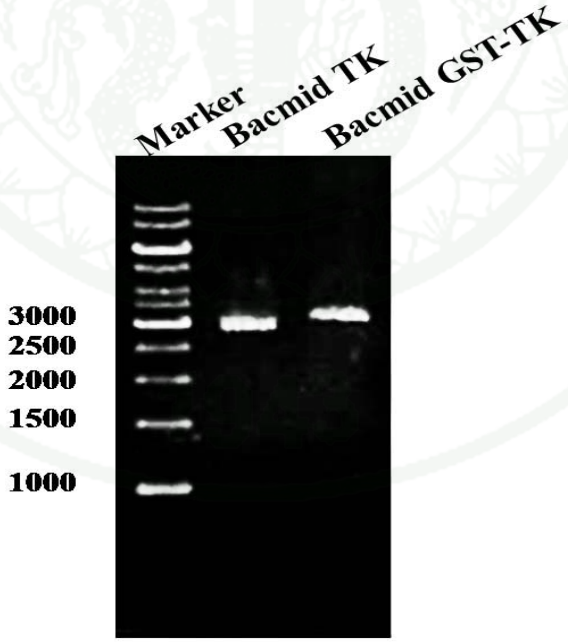

Figure 33 The PCR products of bacmid GST-TK and bacmid TK gene showed the expected DNA fragments of 3.8 Kb and 3.1 Kb, respectively.

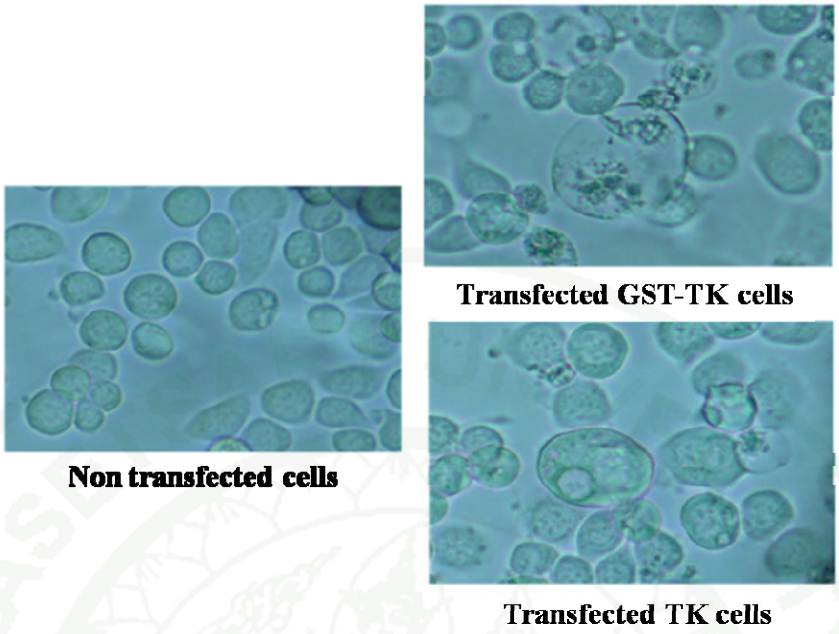

Figure 34 Transfected GST-TK and TK cells. After two days, the cells had granular appearance and increased cell diameter when compared with non-transfected cells.

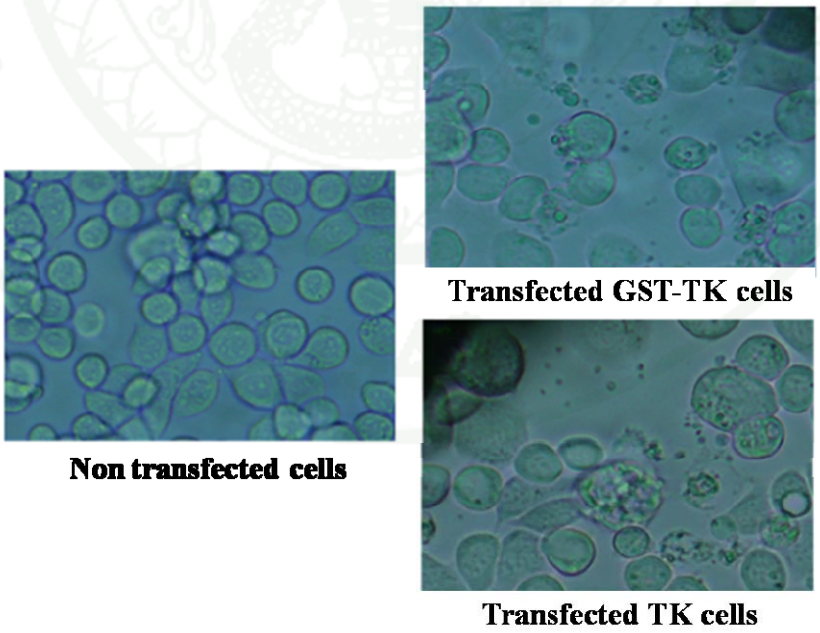

Figure 35 Transfected GST-TK and TK cells. After three days, the cells appeared lysed by baculovirus particles.

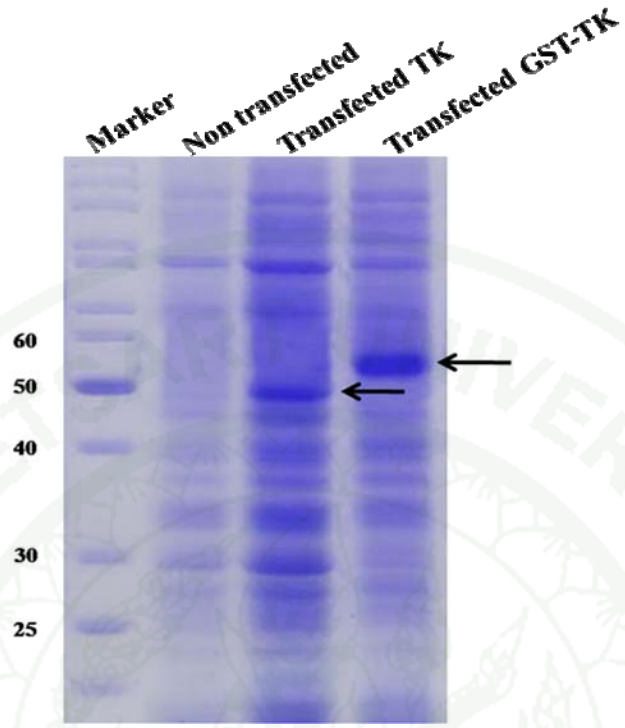

Figure 36 The expression of GST-TK and TK proteins in insect cells. The expected TK and GST-TK protein sizes of approximately 50 KDa and 55 KDa, respectively.

2.2 Plaque assay

The plaque assay is originally a virological assay developed to count and measure infectivity of bacteriophages (Anderson *et al.*, 1996). The basis of the technique is to measure the ability of a single infectious virus to form a "plaque" on a confluent monolayer culture of cells. A plaque is formed as a result of infection of one cell by a single virus particle followed by the replication of that virus. The newly replicated virus particles will then infect and kill surrounding cells. The culture will then be stained with a dye, which stains only viable cells but not the dead cells. Hence, the dead cells in the plaque will appear unstained against the colored background. Use the following formula to calculate how much viral stock to add to obtain a specific multiplicity of infection (MOI): Inoculum required (ml) = MOI (pfu/cell) x number of cells / titer of viral stock (pfu/ml) and titer (pfu/ml) = number of plaques x dilution

factor x (1/ml of inoculum/well). The optimal MOI has important to expressed protein in insect cell. The optimal MOI of Sf9 cells is 1.0 pfu/cell. Thus, we could adjust volume of inoculum required (ml) at optimal MOI for efficiency transfection.

In this plaque assay of baculoviral stock of GST-TK and TK found that all dilutions had clear zone spots. At 10^{-5} fold of GST-TK viral dilutions had 33 and 30 spots (Figure 37A). At 10^{-5} fold of TK viral dilutions had 24 and 19 spots (Figure 37B). The MOI of GST-TK was 0.7875 pfu/cell and MOI of TK was 0.5375 pfu/cell.

A

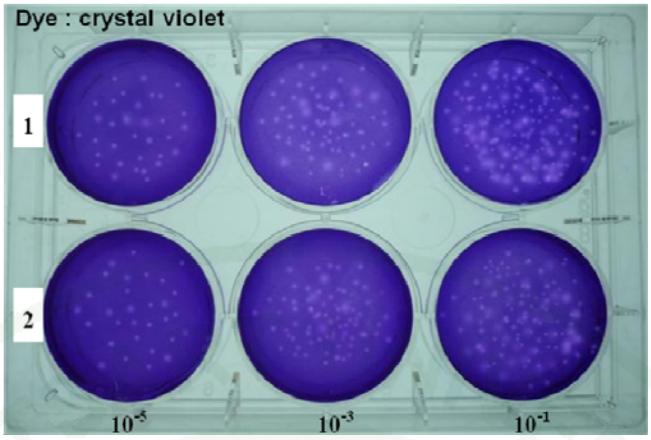

$$\text{titer (pfu/ml)} = \text{number of plaques} \times \text{dilution factor} \times \frac{1}{\text{ml of inoculum/well}}$$

$$\text{titer (pfu/ml)} = \frac{33+30}{2} \times 10^5 \times \frac{1}{1} = 3.15 \times 10^6$$

$$\text{Inoculum required (ml)} = \left(\frac{\text{MOI (pfu/cell)} \times \text{number of cells}}{\text{titer of viral stock (pfu/ml)}}\right)$$

$$\text{MOI (pfu/cell)} = \frac{0.5\ (\text{ml}) \times 3.15 \times 10^6\ (\text{pfu/ml})}{2 \times 10^6\ (\text{cell})} = 0.7875$$

B

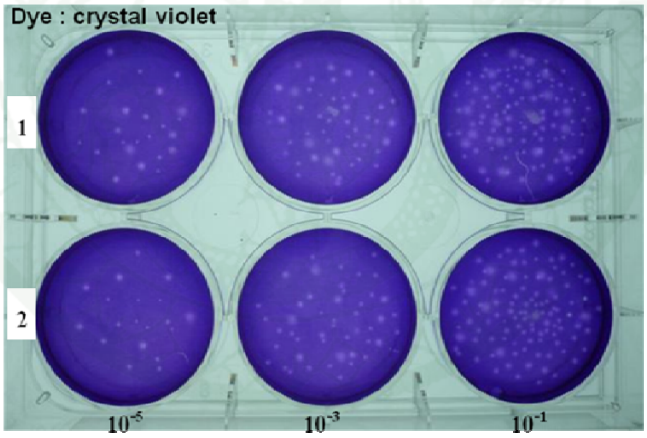

$$\text{titer (pfu/ml)} = \text{number of plaques} \times \text{dilution factor} \times \frac{1}{\text{ml of inoculum/well}}$$

$$\text{titer (pfu/ml)} = \frac{24+19}{2} \times 10^5 \times \frac{1}{1} = 2.15 \times 10^6$$

$$\text{Inoculum required (ml)} = \left(\frac{\text{MOI (pfu/cell)} \times \text{number of cells}}{\text{titer of viral stock (pfu/ml)}}\right)$$

$$\text{MOI (pfu/cell)} = \frac{0.5\ (\text{ml}) \times 2.15 \times 10^6\ (\text{pfu/ml})}{2 \times 10^6\ (\text{cell})} = 0.5375$$

Figure 37 Plaque assay of recombinant TK. GST-TK baculoviral stock at 10^{-1}, 10^{-3} and 10^{-5} dilutions (A). TK baculoviral stock at 10^{-1}, 10^{-3} and 10^{-5} dilutions (B).

2.3 Purification of recombinant TK in insect cells by poly(Glu:Tyr) column

The transfected cells were lysed by lysis buffer C. Then, the lysed cells were centrifuged at 12000xg, 15 min and 4°C. The supernatant of TK and GST-TK were purified by poly (Glu:Tyr) column because this column is a Poly(Glu:Tyr) substrate immobilized beads. Therefore, if recombinant TK from insect cells bind to poly (Glu:Tyr) column, it can imply that TK has the corrected folding and is active. Thus purification of recombinant TK by the poly (Glu:Tyr) column is better than glutathione-sepharose column and Ni-agarose column.

The results of SDS-PAGE showed that molecular weight of TK and GST-TK was 50 kDa and 55 kDa, respectively (Figure 38A and 38B). In expression of GST-TK and TK in bacterial cells found that molecular weight of GST-TK was 55 kDa and the molecular weight of TK was 29 kDa (Koland *et al.,* 1990). When we compared the molecular weight of recombinant TK in two hosts, we found that molecular weight of TK increased from 29 kDa in bacterial cells to 50 kDa in insect cells (Figure 39), but molecular weights of GST-TK in both cells were not different. These results implied that non-fusion TK protein that expressed in insect cells may had post-translational modification especially glycosylation. Therefore, we determined qualitative mono- and disaccharide analysis by orcine reagent (Staudacher, 2008) by using glucose as a positive control. The results showed that there is a sugar content in TK but not in GST-TK implying that TK was expressed in insect cells had glycosylation but GST-TK had no glycosylation.

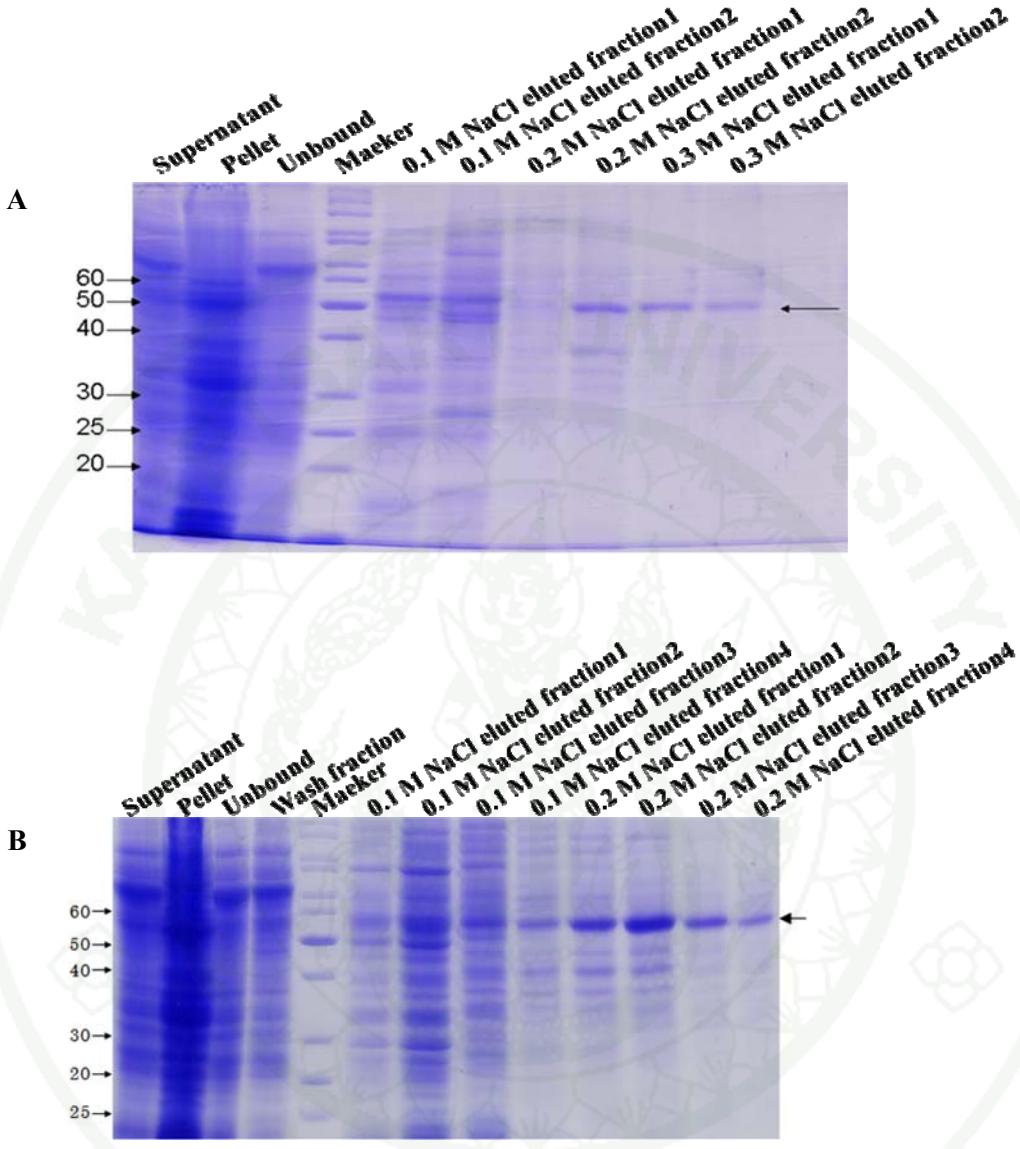

Figure 38 SDS-PAGE of purified TK and GST-TK, molecular weight of TK is 50 kDa (A) and molecular weight of GST-TK is 55 kDa (B).

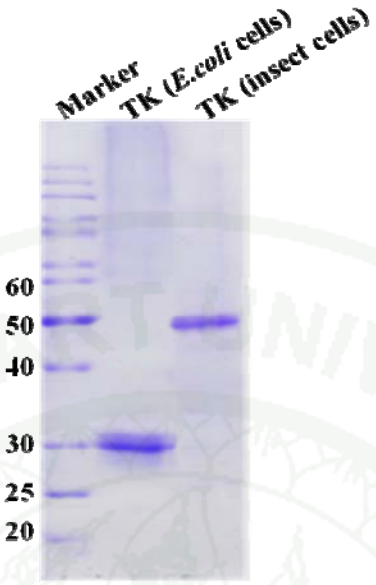

Figure 39 SDS-PAGE of purified TK in bacterial cells and insect cells.

Protein concentration of TK and GST-TK were measured by Lowry assay. The protein concentration of purified TK and GST-TK were 6.74 mg protein/15 ml culture medium and 6.06 mg protein/15 ml culture medium, respectively. In previous study, the yield of recombinant TK expression in bacterial cells was 1-10 mg/1 L culture and has no activity, therefore the expression of active TK in insect cells system has a higher yield expression than bacterial cells. The ABTK assay showed that the specific activity of crude TK and GST-TK were 0.0064 U/mg protein and 0.0019 U/mg protein, respectively, and specific activities of purified TK and GST-TK were 0.0026 U/mg protein and 0.0021 U/mg protein, respectively. Percent yields of purified TK and GST-TK were 4.54% and 10.22%. Purification folds of purified TK and GST-TK were 0.41 fold and 1.06 fold (Table 13). The purified TK had purification fold less than 1.0. This result may due to the low concentration of TK which cannot mimic dimeric form in full-length receptor since there is a report that only the high concentration of TK in millimolar range can be active (Zhang et al., 2006). It may also due to the purified TK was unstable in solution cause the activity become lower. In summary, the active TK can express in the insect cells does not without GST fusion protein but it has a high degree of glycosylation and it was less

stable. On another hand, the expression of TK as the GST fusion protein which was reported before by Yun *et al.*, 2007 showed the advantage than without GST fusion protein. The GST-TK had no glycosylation and it was more stable than nonfusion TK. Therefore the expression of recombinant TK in fusion protein form (GST-TK) could be useful for further studies.

Table 13 Purification procedure of TK and GST-TK

TK Procedure	[protein] (mg/ml)	Protein (mg)	Activity (U/ml)	Total activity (U)	Specific activity (U/mg protein)	Yield (%)	Purification (fold)
Crude	4.10	61.50	0.026	0.39	0.0064	100	1
Poly(Glu:Tyr)	3.37	6.74	0.009	0.02	0.0026	4.54	0.41
GST-TK Procedure	[protein] (mg/ml)	Protein (mg)	Activity (U/ml)	Total activity (U)	Specific activity (U/mg protein)	Yield (%)	Purification (fold)
Crude	4.18	62.7	0.008	0.12	0.0019	100	1
Poly(Glu:Tyr)	3.03	6.06	0.006	0.01	0.0021	10.22	1.06

2.4 Activity assay of recombinant TK in insect cells

In insect cell expression system, GST-TK and TK had activity by ABTK assay. The results showed that the K_m of GST-TK toward ATP was equal to 255.50 ± 2.14 μM and V_{max} was equal to 3.132 ± 1.09 nM/min (Figure 40A). The K_m of TK toward ATP was equal to 370.24 ± 2.01 μM and $V_{max}$was equal to 4.564 ± 1.56 nM/min (Figure 40B). The K_m and V_{max} of full-length EGFR and recombinant TK that expressed in insect cells were concluded in Table 14. From Table 14, The K_m of full-length EGFR and recombinant TK toward ATP were similar when we compared with previous reports, the K_m of TK toward ATP that expressed in insect cells was about 10-50 μM. The K_m values in several papers were different depended on method of each activity assay such as using radioactive method (γ-^{32}P) and ATP/NADH couple assay (Table 15). When we compared the K_m value on Table 14 and Table 15, we found that the K_m value in ours assay differ from the papers less than 10 folds.

Thus, the insect cells expression system is a suitable host for expressed recombinant TK and implying that recombinant TK that expressed in insect cells system had enough efficiency for inhibiting assay or structural study in future.

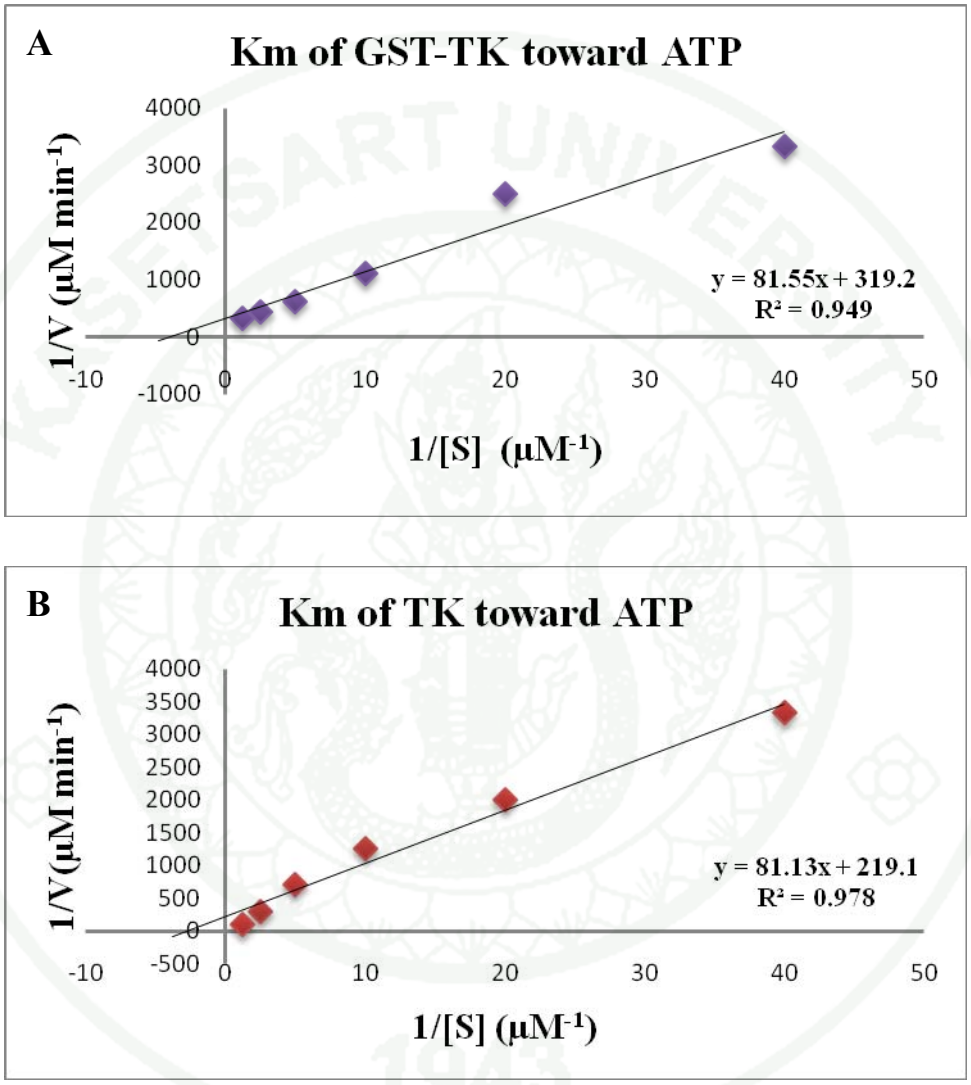

Figure 40 K_m and V_{max} of GST-TK (A) and TK (B) toward ATP that expressed in insect cells by Antibody Beacon tyrosine kinase assay.

Table 14 Comparison activity assay of full-length EGFR and recombinant TK

Protein	Protein concentration	Antibody Beacon tyrosine kinase assay	
		K_m of ATP (μM)	V_{max} (nM/min)
Full-length human EGFR	39,465 U/mg protein	112.23 ± 1.58	36.885 ± 0.11
GST-TK from SF9	4.18 mg/ml	255.50 ± 2.14	3.132 ± 1.09
TK from SF9	4.10 mg/ml	370.24 ± 2.01	4.564 ± 1.56

Table 15 Previous studies of K_m of TK toward ATP

Method	K_m of TK toward ATP (μM)	Reference
Radoactive method (γ-^{32}P)	61 ± 5	Ge *et al.*, 2002
	9 ± 0.9	Gilmer *et al.*, 2008
	26.0	Posner *et al.*, 1992
	23.0	Ciardiello and Tortora, 2001
	31 ± 4	Fan *et al.*, 2004
	17	Brignola *et al.*, 2002
ATP/NADH couple assay	5.2 ± 0.2	Yun *et al.*, 2007
	6.9 ± 0.9	Yun *et al.*, 2008

This should be noted that the V_{max} of both recombinant TK and GST-TK were less than the full-length EGFR. This may due the full-length EGFR that has mechanism to switch from inactive to active form that facilitates the enzyme reaction. Furthermore, the K_m value implied the affinity of enzyme to the substrate was found to be higher in both recombinant TK and GST-TK comparing to the full-length EGFR. These may due to the glycosylation and GST fusion steric hindrance in the recombinant TK and GST-TK, respectively causing the lower affinity to substrate of recombinant proteins.

3. Developing activity assay of tyrosine kinase

For calibrating our methods, we used a full-length EGFR as a control and used three assay methods for comparing efficiency, ABTK assay, ATP/NADH couple assay and PURETIME assay. At first, the full-length EGFR was measured by ABTK assay and ATP/NADH couple assay. The results showed that the ABTK assay had a K_m of ATP equal to 112.23 ± 1.58 μM and V_{max} equal to 36.885 ± 0.11 nM/min (Figure 41A), and the ATP/NADH couple assay had a K_m of ATP equal to 103.23 ± 2.97 μM and V_{max} was 0.148 ± 3.37 nM/min (Figure 41B), however the raw data with the ATP/NADH couple assay was less accuracy (R^2 = 0.5797) (Table 16), which may due to had several enzymes involving the assay reactions and kinase may be not a rate limiting step of the reactions. Thus, the K_m and V_{max} in this reaction were not really K_m and V_{max} of full-length EGFR. Therefore the ATP/NADH couple assay was not effective in kinetic activity assay.

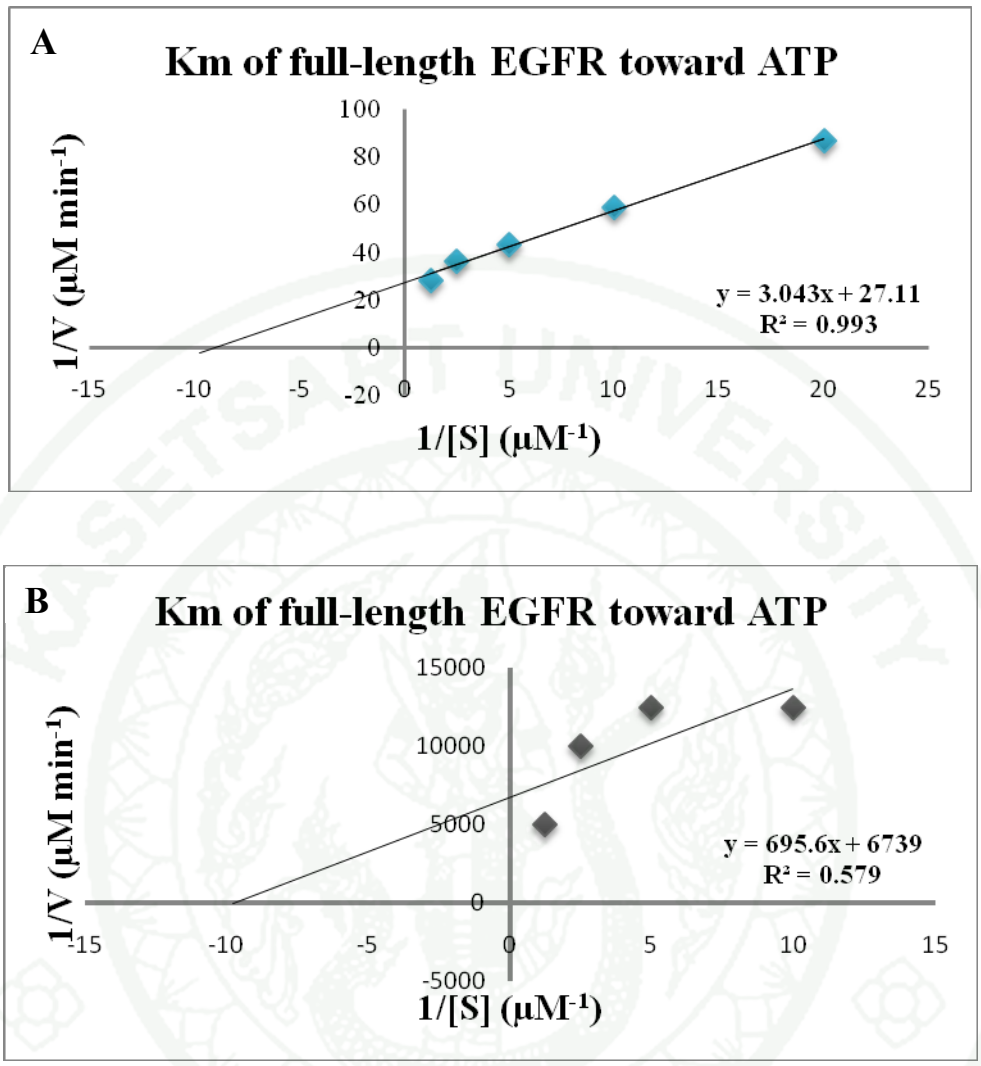

Figure 41 K_m and V_{max} of full-length EGFR toward ATP by Antibody Beacon tyrosine kinase assay (A) and ATP/NADH coupled assay (B).

Table 16 Comparison activity assay of the full-length EGFR by ABTK assay and ATP/NADH couple assay

Methods	K_m of ATP (µM)	V_{max} (nM/min)	R^2
Antibody Beacon tyrosine kinase assay	112.23 ± 1.58	36.885 ± 0.11	0.993
ATP/NADH coupled assay	103.23 ± 2.97	0.148 ± 3.37	0.5797

From the comparison activity of full-length EGFR by ABTK assay and ATP/NADH couple assay, we found that K_m of ATP measured by ABTK assay was lower than ATP/NADH couple assay, also V_{max} and R^2 from ABTK assay was better than ATP/NADH couple assay. Nevertheless, The ABTK assay kit measuring is expensive because this assay uses antibody against phosphotyrosine and fluorescent dye for emission. Therefore, we interested in development of new activity assay that is cheaper. This technique is PURETIME assay, the fluorophore couples with peptide substrate and emits fluorescence when peptide substrate is phosphorylated.

In PURETIME assay, we used the full-length EGFR to optimize conditions in the reaction by using the fluorescence spectroscopy. The results showed that the PURETIME assay could not measure activity of the full-length EGFR (Figure 42). So we compared the full-length EGFR activity in PURETIME assay method and ABTK assay method. The results showed that the full-length EGFR had activity in ABTK assay method but no activity in PURETIME assay method (Figure 43). Therefore we sent the control solution (only peptide substrate) and reaction mixture of full-length EGFR to determined molecular mass by mass spectroscopy at BIO-TEC for checking the phosphorylation in peptide substrate (PURETIME-17 EGF receptor tyrosine kinase substrate peptide). The results showed that the molecular masses were not different in control and full-length EGFR reaction mixture, so the peptide substrate that used in PURETIME assay method did not phosphorylation (Figure 44) may due to the peptide substrate that was synthesized and couple with fluorophore by AssayMetrics company had an effect on phosphorylation. The bulky fluorophore that was coupled with peptide substrate may block phosphorylation of tyrosine kinase**.** Therefore, in this study, we used ABTK assay for measured inhibition of recombinant TK by gefitinib (anticancer drug) and Thai herbs extractions. However, in continued study, if we use peptide coupled fluorophore assay method, we should try to change the fluorophore for efficiency developing of activity assay.

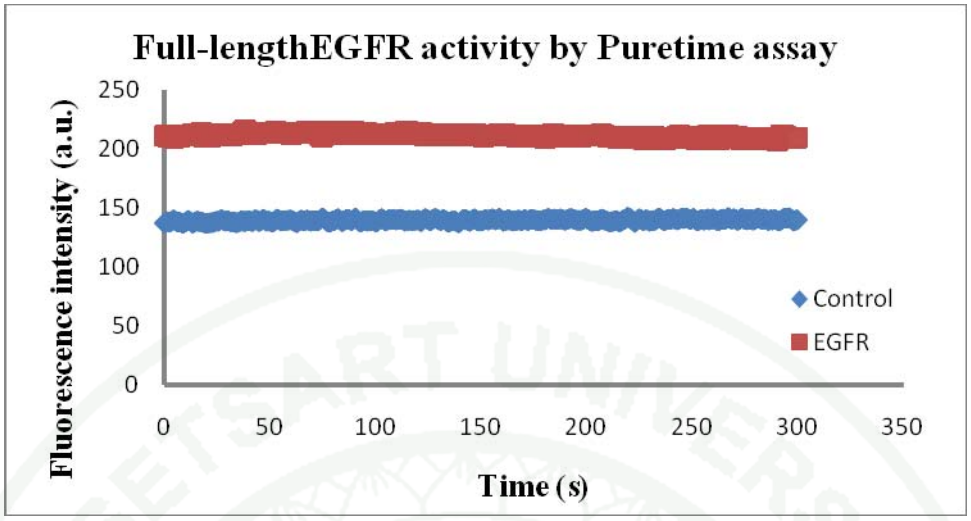

Figure 42 Realtime full-length EGFR activity in PURETIME assay method compare with control.

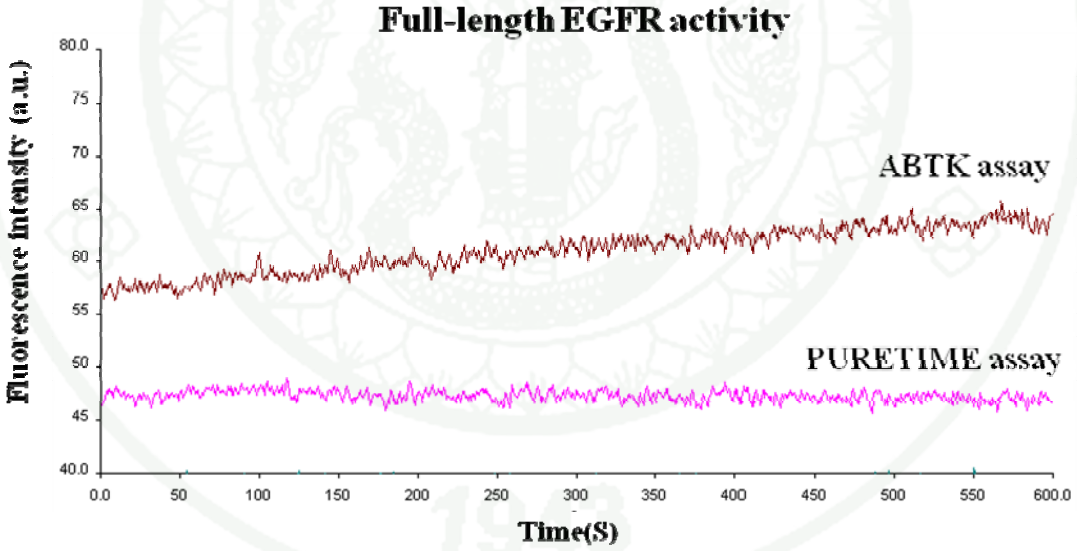

Figure 43 Comparative full-length EGFR activity in PURETIME assay method and ABTK assay method.

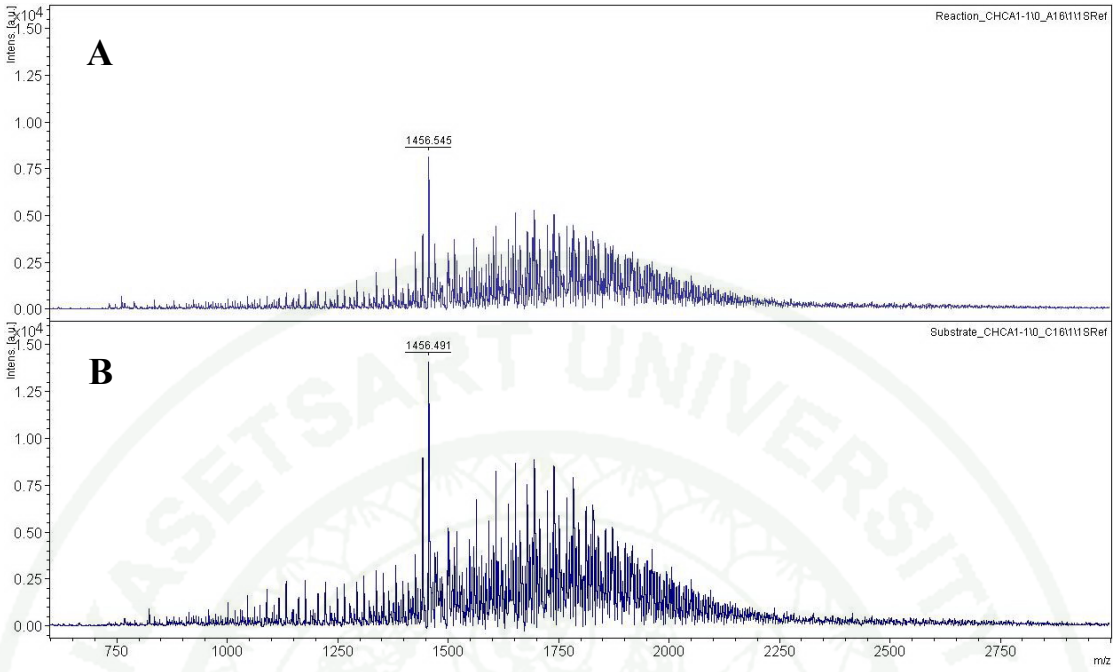

Figure 44 Mass spectrophotometer of the reaction mixture (A) and peptide substrate (PURETIME-17 EGF receptor tyrosine kinase substrate peptide) (B)

4. Inhibiting activity assay

In inhibiting activity assay, we used active TK from insect cells and gefitinib for measure kinetic inhibition (K_i) by ABTK assay compare with full-length EGFR. The result showed that K_i of full-length EGFR equal to 13.07 ± 0.47μM, K_i of GST-TK equal to 0.355 ± 0.15 μM and K_i of TK equal to 6.734 ± 0.22 μM (Figure 45 and Table 17). In previous study, the kinetic inhibitions of gefitinib toward EGFR were measured in K_i and IC_{50}. The K_i and IC_{50} were different depend on the methods of activity assay (Table 18). The K_i of gefitinib toward full-length EGFR and recombinant TK in this study had lower than previous study maybe cause the differentiation of expression hosts and inhibiting activity assay methods. From these results demonstrated that gefitinib could inhibit recombinant TK better than full-length EGFR, because the gefitinib was non-competitive inhibitor (Sequist *et al.*, 2008).

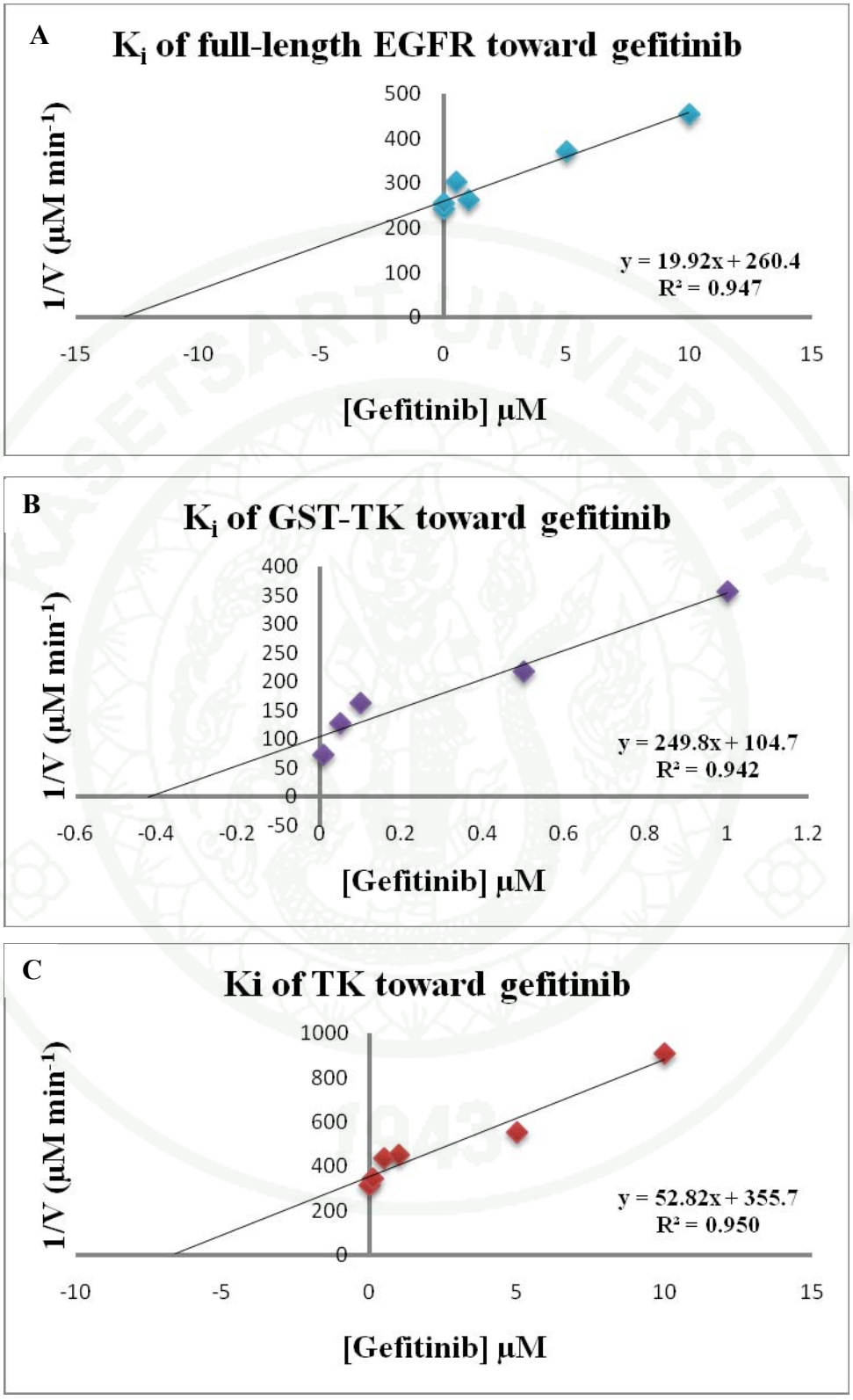

Figure 45 K_i of full-length EGFR (A), GST-TK (B) and TK (C) toward gefitinib.

Table 17 Comparison of inhibiting activity assays of gefitinib toward the full-length EGFR and recombinant TK

Protein	Protein concentration	K_i of gefitinib (μM)
Full-length human EGFR	39,465 U/mg protein	13.07 ± 0.47
GST-TK from SF9	4.18 mg/ml	0.355 ± 0.15
TK from SF9	4.10 mg/ml	6.734 ± 0.22

Table 18 Previous study of inhibiting activity assay of gefitinib

Method	K_i of gefitinib (nM)	Reference
Radoactive method (γ-^{32}P)	0.19 ± 0.11	Gilmer *et al.*, 2008
	3.0 ± 0.2	Wood *et al.,* 2004
	24	Wakeling *et al.*, 2002
	23	Kris *et al.*, 2000
	20	Jimeno and Hidalgo, 2005
Substrate coated plate	24.71 ± 0.06	Varkondi *et al.,* 2008

Herbs have been considered valuable sources for anticancer drug discovery. Herbal medicine, recorded in many countries, e.g., Chinese pharmacopoeia, has been prescribed for many diseases over centuries and began to be attractive by increasing scientific attention (Vickers, 2002). Based on recent scientific research on herbs, herbal therapies have been considered alternative treatments for malignancies (Risberg *et al.*, 1998). Several studies have demonstrated that extracts from several herbal medicines or mixtures have an anticancer potential and could inhibit cancer cell proliferation *in vitro* or *in vivo* (Harvey, 2008).

In inhibiting study of Thai herbs, we choose 24 species of Thai herbs from Chemiebase (Thai herbs database) and journal of Thai herbs medicine that were treated as quick medicines but also lack molecular study in enzyme kinetic and

structure of the lead compounds. Therefore, we interested in inhibiting study of local Thai herbs to continually study structure of the lead compounds for development of anti cancer drugs in future.

Furthermore, we used 24 species of Thai herbs and active TK from insect cell expression for screening TK inhibitor by using ABTK assay comparing with gefitinib (known anticancer drug). To determine concentration of ethanol which able to inhibit TK activity, different concentration of ethanol were used in inhibiting assay. The results showed that more than 10% ethanol can inhibit TK activity (data not show). Therefore we used 0.025 mg/ml Thai herbs to get the final concentration of ethanol lower than 10 %. The result showed that crude extraction of *Sapium indicum* and *Maclura cochinchinensis* had 75 % inhibition, crude extraction of *Terminalia chebula* had 50 % inhibition and crude extraction of *Cinnamomum loureiroi* and *Ruellia tuberose* had 25 % inhibition when compared with gefitinib (Figure 46).

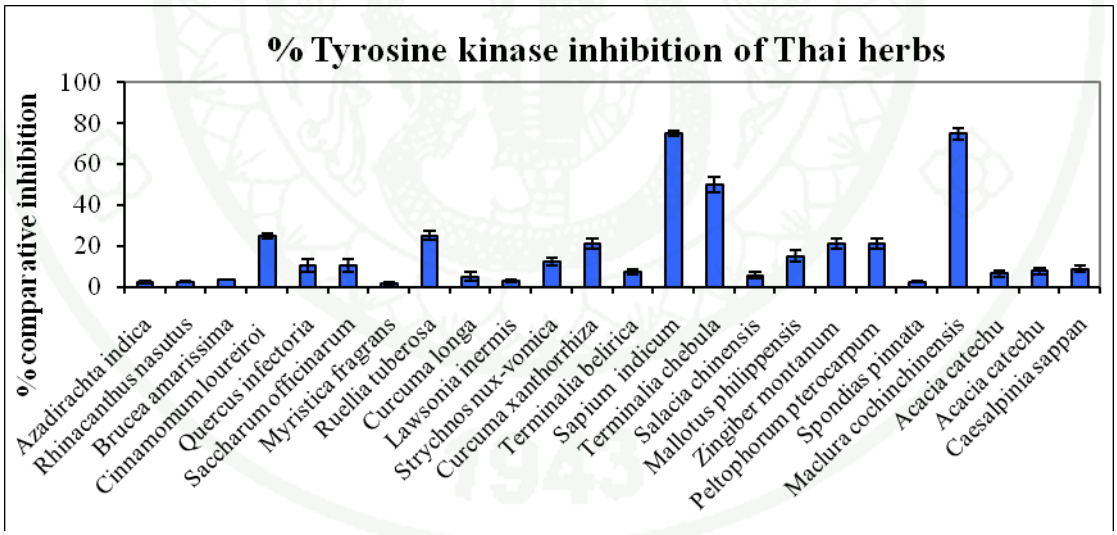

Figure 46 Percent of tyrosine kinase inhibitions of 24 crude extracted Thai herbs comparing with gefitinib.

When we reviewed the inhibition study of *Sapium indicum*, *Maclura cochinchinensis* and *Terminalia chebula,* we found that there are no repoet of three herbs in anticancer activity. Oil fruits of *Sapium indicum* was studied that

compounds were isolated from the fruit oil of *Sapium indicum* were tested for production of erythematic in vivo and induction of human and rabbit platelet aggregation *in vitro* (Taylor *et al.,* 1982; Edwards *et al.,* 1983). Moreover *Sapium indicum* exhibited antimycobacterial activity with minimum inhibitory concentrations (Chumkaew *et al.,* 2003). Oil fruits of *Terminalia belirica* was studied that reportedly possess anti-infective and anti-inflammatory properties. There were no side effects observed during the course of the study and the eye drop was well tolerated by the patients. The herbal eye drop Ophthacare has a useful role in a variety of infective, inflammatory and degenerative ophthalmic disorders (Biswas *et al.,* 2001). *Maclura cochinchinensis* was studied that extraction of leaves had the powerful anti-herpes simplex virus (HSV) activity (Bunyapraphatsara *et al.,* 2000; Yoosook *et al.,* 2000) and extraction of root had inhibitors of the Na^+/H^+ exchange system of arterial smooth muscle cells (Kobayashi *et al.,* 1997). Therefore, in ours study is the first time of discovery lead species from these Thai herbs by using molecular techniques and kinetic study that can inhibit EGFR and cause develop anticancer drug in future.

CONCLUSION

In this study, we cloned and expressed recombinant TK in bacterial cells and insect cells in fusion and non-fusion forms. We purified recombinant TK from bacterial cells by glutathione-sepharose column and Ni-agarose column and purified recombinant TK from insect cells by Poly (Glu:Tyr) column. The concentration of recombinant TK in each purification steps was determined by Lowry method. The activity assay of recombinants TK was measured by ABTK assay, ATP/NADH couple assay and PURETIME assay.

From bacterial cells expression system, size of TK gene and GST-TK gene were 837 bp and 1,499 bp, respectively and size of TK protein and GST-TK protein were 29 KDa and 55 KDa, respectively. We purified recombinant TK from bacterial cells by glutathione-sepharose column and Ni-agarose column. The TK protein had no activity and but only supernatant of GST-TK that expressed at 16°C had activity but were not efficiency enough for kinetic assay due to lower V_{max} and higher K_m value. The concentration of GST-TK protein was determined with Lowry assay. From 1 l culture the concentration of GST-TK in supernatant and after purification were 20.6 mg/ml and 0.77 mg/ml, respectively. In conclusion, the bacterial expression of recombinant TK, GST-TK protein, in low temperature could express protein in low yield.

From insect cells expression system, we purified recombinant TK by Poly (Glu:Tyr) column and size of TK protein and GST-TK protein were 50 KDa and 55 KDa, respectively. The molecular weight of TK protein increased from 29 kDa (bacterial cells) to 50 kDa (insect cells) but molecular weight of GST-TK was not different in bacterial and insect cells. We determined qualitative mono- and disaccharide analysis by orcine reagent using glucose as a positive control. The results showed that there is a sugar content in TK but not in GST-TK implying that TK was expressed in insect cells and undergone glycosylation but GST-TK had no glycosylation. Protein concentration of TK and GST-TK were measured by Lowry assay. The protein concentration of purified TK and GST-TK were 6.74 mg

protein/15 ml culture medium and 6.06 mg protein/15 ml culture medium, respectively. The expression of active TK in insect cells system is higher yield expression than in the bacterial cells. The K_m and V_{max} of recombinant TK were nearly theirs full-length EGFR and previous reports. Thus, the insect cells expression system is suitable host for expressed recombinant TK and implying that recombinant TK expressed in insect cells system had enough efficiency for inhibiting assay or structural study in the future.

From developing activity assay of TK, we ordered the full-length EGFR as a control and used three methods for comparing efficiency; ABTK assay, ATP/NADH couple assay and PURETIME assay. The ABTK assay had sensitivity and specificity more than other methods. For the ATP/NADH couple assay, it had several enzymes involving the assay reactions and kinase may be not a rate limiting step of the reactions. Thus, the K_m and V_{max} in this reaction were not really K_m and V_{max} of TK. Therefore the ATP/NADH couple assay was not effective in kinetic activity assay. In the PURETIME assay, PURETIME assay could not measure activity of full-length EGFR and the PURETIME substrate could not be phosphorylated. This may due to the bulky size of fluorophore that was coupled with substrate peptide.

From inhibiting activity assay, we used supernatant TK and ABTK assays measured kinetic inhibition of gefitinib compared with 24 species of Thai herbs. We found that that crude extraction of *Sapium indicum* and *Maclura cochinchinensis* had 75 % inhibition, crude extraction of *Terminalia chebula* had 50 % inhibition and crude extraction of *Cinnamomum loureiroi* and *Ruellia tuberose* had 25 % inhibition when compared with gefitinib. Therefore, this is the first time of discovery lead species from these Thai herbs by using molecular techniques and kinetic study that can inhibit EGFR and may lead to development of anticancer drug in future.

LITURATURE CITED

Adams, T. E., V. C. Epa, T. P. Garrett and C. W. Ward. 2000. Structure and function of the type 1 insulin-like growth factor receptor. **Cell Mol. Life Sci.** 57: 1050-1093.

Alessi, D. R. and P. Cohen. 1998. Mechanism of activation and function of protein kinase B. **Curr. Opin. Genet. Dev.** 8: 55-62.

Alimandi, M., A. Romano and M. C. Curia. 1995. Cooperative signaling of ErbB3 and ErbB2 in neoplastic transformation and human mammary carcinomas. **Oncogene.** 10: 1813-1821.

Alroy, I. and Y. Yarden. 1997. The ErbB signaling network in embryogenesis and oncogenesis: signal diversification through combinatorial ligand-receptor interactions. **FEBS Lett.** 410: 83-86.

Anderson, D., R. Harris, D. Polayes, V. Ciccarone, R. Donahue, G. Gerard and J. Jessee. 1996. Rapid Generation of Recombinant Baculoviruses and Expression of Foreign Genes Using the Bac-To-Bac® Baculovirus Expression System. **Focus.** 17: 53-58.

Arakawa, T. and K. Tsumoto. 2003. The effects of arginine on refolding of aggregated proteins: not facilitate refolding, but suppress aggregation. **Biochem. Biophys. Res. Commun.** 304: 148-152.

Baker, D. D. 2007. The value of natural products to future pharmaceutical discovery. **Nat. Prod. Rep.** 24: 1225-1244.

Ballif, B. A. and B. J. Blenis. 2001. Molecular mechanisms mediating mammalian mitogenactivated protein kinase (MAPK) kinase (MEK)-MAPK cell survival signals. **Cell Growth Differ.** 12: 397-408.

Barker, A. J., K. H. Gibson, W. Grundy, A. A. Godfrey, J. J. Barlow, M. P. Healy, J. R. Woodburn, S. E. Ashton, B. J. Curry, L. Scarlett, L. Henthorn and L. Richards. 2001. Studies leading to the identification of ZD1839 (IRESSA): an orally active, selective epidermal growth factor receptor tyrosine kinase inhibitor targeted to the treatment of cancer. **Bioorg. Med. Chem. Lett**. 11: 1911-1914.

Barak, L., S. Ferguson, J. Zhang and M. Caron. 1997. A beta-arrestin/GFP biosensor for detecting GPCR activation. **J. Biol. Chem.** 272: 27497-27500.

Bar-Sagi, D. and A. Hall. 2000. Ras and Rho GTPases: a family reunion. **Cell.** 103: 227-238.

Baselga, J. and J. Cortes. 2005. Epidermal growth factor receptor pathway inhibitors. **Cancer Chemother. Biol. Response Modif.** 22: 205-223.

Bassing, C. H., J. M. Yingling and D. J. Howe. 1994. A transforming growth factor beta type I receptor that signals to activate gene expression. **Science.** 263: 87-89.

Berezov, A., J. Chen, Q. Liu, H. T. Zhang, M. I. Greene and R. Murali. 2002. Disabling receptor ensembles with rationally designed interface peptidomimetics. **J. Biol. Chem.** 277: 28330-28339.

Beveridge, M., Y. W. Park, J. Hermes, A. Marenghi, G. Brophy and A. Santos. 2000. Detection of p56lck kinase activity using scintillation proximity assay in 384-well format and imaging proximity assay in 384- and 1536-well format. **J. Biomol. Screen.** 5: 205-212.

Bigner, S. H., P. A. Humphrey and A. J. Wong. 1990. Characterization of the epidermal growth factor receptor in human glioma cell lines and xenografts. **Cancer Res.** 50: 8017-8022.

Bischoff, K. M., L. Shi and P. J. Kennelly. 1998. The detection of enzyme activity following sodium dodecyl sulfate-polyacrylamide gel. **Anal. Biochem.** 260: 1-17.

Biswas, N. R., S. K. Gupta, G. K. Das, N. Kumar, P. K. Mongre, D. Haldar and S. Beri. 2001. Evaluation of Ophthacare eye drops--a herbal formulation in the management of various ophthalmic disorders. **Phytother. Res.** 15: 618-620.

Bjorge, J. D., T. O. Chan and M. Antczak. 1990. Activated type I phosphatidylinositol kinase is associated with the epidermal growth factor (EGF) receptor following EGF stimulation. **Proc. Natl. Acad. Sci. USA.** 87: 3816-3820.

Bouchard, L., L. Lamarre and P. J. Tremblay. 1989. Stochastic appearance of mammary tumors in transgenic mice carrying the MMTV/c-neu oncogene. **Cell.** 57: 931-936.

Boute, N., K. Pernet and T. Issad. 2001. Monitoring the activation state of the insulin receptor using bioluminescence resonance energy transfer. **Mol. Pharmacol.** 60: 640-645.

Boulanger, M. J. and K. C. Garcia. 2004. Shared cytokine signaling receptors: structural insights from the Gp130 system. **Adv. Protein Chem.** 68: 107-146

Bouyain, S., P. A. Longo, S. Li, K. M. Ferguson and D. J. Leahy. 2005. The extracellular region dimerization of ErbB4 adopts a tethered conformation in the absence of ligand. **Proc. Natl. Acad. Sci. USA**. 102: 15024-15029.

Braunwalder, A. F., D. R. Yarwood, M. A. Sills and K. E. Lipson. 1996. Measurement of the protein tyrosine kinase activity of c-src using time-resolved fluorometry of europium chelates. **Anal. Biochem.** 238: 159-164.

Brignola, P. S., K. Lackey, S. H. Kadwell, C. Hoffman, E. Horne, H. L. Carter, J. D. stuart, K. Blackburn, M. B. Moyer, K. J. Alligood, W. B. Knight and E. R. Wood. 2002. Comparison of the biochemical and kinetic properties of the type 1 receptor tyrosine kinase intracellular domains. **J. Biol. Chem.** 277: 1576-1585.

Brown, R. J., J. J. Adams, R. A. Pelekanos, Y. Wan, W. J. McKinstry and K. Palethorpe. 2005. Model for growth hormone receptor activation based on subunit rotation within a receptor dimer. **Nat. Struct. Mol. Biol.** 12: 814-821.

Bunyapraphatsara, N., S. Dechsree, C. Yoosook, A. Herunsalee and Y. Panpisutchai. 2000. Anti-herpes simplex virus component isolated from Maclura cochinchinensis. **Phytomedicine.** 6: 421-424.

Burgess, A. W., H. S. Cho, C. Eigenbrot, K. M. Ferguson and T. P. Garrett. 2003. An open-and-shut case? Recent insights into the activation of EGF/ErbB receptors. **Mol. Cell.** 12: 541-552.

Butler, M. S. 2008. Natural products to drugs: natural product-derived compounds in clinical trials. **Nat. Prod. Rep.** 25: 475-516.

Cadena, D. L., C. L. Chan and G. N. Gill. 1994. The intracellular tyrosine kinase domain of the epidermal growth factor receptor undergoes a conformational change upon autophosphorylation. **J. Biol. Chem.** 269: 260-265.

Cai, Y. C., Z. Jiang and F. Vittimberga. 1999. Expression of transforming growth factor-alpha and epidermal growth factor receptor in gastrointestinal stromal tumours. **Virchows Arch.** 435: 112-115.

Cardone, M. H., N. Roy and H. R. Stennicke. 1998. Regulation of cell death protease caspase-9 by phosphorylation. **Science.** 282: 1318-1321.

Carpenter, C. D., H. A. Ingraham, C. Cochet, G. M. Walton and C. S. Lazar. 1991. Structural analysis of the transmembrane domain of the epidermal growth factor receptor. **J. Biol. Chem.** 266: 5750-5755.

Carraway, K. L., S. P. Soltoff and S. A. Prigent. 1994. ErbB3 is involved in activation of phosphatidylinositol 3-kinase by epidermal growth factor. **Mol. Cell Biol.** 14: 3550-3558.

Carter, P., L. Presta and C. M. Gorman. 1992. Humanization of an anti-p185HER2 antibody for human cancer therapy. **Proc. Natl. Acad. Sci. USA.** 89: 4285-4289.

Chan, S. K., W. J. Gullick and M. E. HILL. 2006. Mutations of the epidermal growth factor receptor in non-small cell lung cancer – search and destroy. **Eur. J. Cancer.** 42: 17-23.

Charlish, P. 2008. **Traditional remedies: latter day medicines.** Scrip World Pharmaceutical News**,** PJB Publications. 3351: 31-34.

Charter, N. W., L. Kauffman, R. Singh and R. M. Eglen. 2006. A generic, homogenous method for measuring kinase and inhibitor activity via adenosine 5'-diphosphate accumulation. **J. Biomol. Screen.** 11: 390-399.

Chen, W. S., C. S. Lazar and M. Poenie. 1987. Requirement for intrinsic protein tyrosine kinase in the immediate and late actions of the EGF receptor. **Nature.** 328: 820-823.

Chin, Y. W. 2006. Drug discovery from natural sources. **AAPS J.** 8: E239-E253.

Cho, H. S. and D. J. Leahy. 2002. Structure of the extracellular region of HER3 reveals an interdomain tether. **Science.** 297: 1330-1333.

Cho, H. S., K. Mason, K. X. Ramyar, A. M. Stanley and S. B. Gabelli. 2003. Structure of the extracellular region of HER2 alone and in complex with the Herceptin Fab. **Nature.** 421: 756-760.

Choi, S. H., J. M. Mendrola and M. A. Lemmon. 2007. EGF-independent activation of cell-surface EGF receptors harboring mutations found in gefitinib-sensitive lung cancer. **Oncogene.** 26: 1567-1576.

Chu, C. T., K. D. Everiss and C. J. Wikstrand. 1987. Receptor dimerization is not a factor in the signalling activity of a transforming variant epidermal growth factor receptor (EGFRvIII). **Biochem J.** 324: 855-861.

Chumkaew P., C. Karalai, C. Ponglimanont and K. Chantrapromma. 2003. Antimycobacterial activity of phorbol esters from the fruits of *Sapium indicum*. **J. Nat. Prod.** 66: 540-543.

Ciardiello, F. and G. Tortora. 2001. A novel approach in the treatment of cancer: targeting the epidermal growth factor receptor. **Clin. Cancer Res**. 7: 2958-2970.

Ciardiello, F. and G. Tortora. 2008. EGFR Antagonists in Cancer Treatment. **N. Engl. J. Med.** 358: 1160-1174

Citri, A., K. B. Skaria and Y. Yarden. 2003. The deaf and the dumb: the biology of ErbB-2 and ErbB-3. **Exp. Cell Res.** 284: 54-65.

Cook, N., A. Harris, A. Hopkins and K. Hughes. 2002. Scintillation proximity assay (SPA) technology to study biomolecular interactions. **Curr. Protoc. Protein Sci.** Chapter 19: Unit 19.8.

Corthals, G.L., R. Aebersold and D.R. Goodlett. 2005. Identification of phosphorylation sites using microimmobilized metal affinity chromatography. **Methods Enzymol.** 405: 66-81.

Couturier, C. and R. Jockers. 2003. Activation of the leptin receptor by a ligand induced conformational change of constitutive receptor dimers. **J. Biol. Chem.** 278: 26604-26611.

Cross, D. A., D. R. Alessi and P. Cohen. 1995. Inhibition of glycogen synthase kinase-3 by insulin mediated by protein kinase B. **Nature.** 378: 785-789.

Czech, M. P. 2000. PIP2 and PIP3: complex roles at the cell surface. **Cell.** 100: 603-606.

Damjanovich, S., L. Bene, J. Matko, A. Alileche, C. Goldman, S. Sharrow. 1997. Preassembly of interleukin 2 (IL-2) receptor subunits on resting Kit 225 K6 T cells and their modulation by IL-2, IL-7, and IL-15: a fluorescence resonance energy transfer study. **Proc. Natl. Acad. Sci. USA**. 94: 13134-13139.

Datta, S. R., A. Brunet and M. E. Greenberg. 1999. Cellular survival: a play in three Akts. **Genes Dev.** 13: 2905-2927.

Davis, R. J. 2000. Signal transduction by the JNK group of MAP kinases. **Cell.** 103: 239-252.

Dawson, J. P., M. B. Berger, C. C. Lin, J. Schlessinger, M. A. Lemmon and K. M. Ferguson. 2005. Epidermal growth factor receptor dimerization and activation require ligand-induced conformational changes in the dimer interface. **Mol. Cell. Biol.** 25: 7734-7742.

D'Errico, A., C. Barozzi and M. Fiorentino. 2000. Role and new perspectives of transforming growth factor-alpha (TGF-alpha) in adenocarcinoma of the gastrooesophageal junction. **Br. J. Cancer.** 82: 865-870.

Di Fiore, P. P., J. H. Pierce, T. P. Fleming. 1987. Overexpression of the human EGF receptor confers an EGF-dependent transformed phenotype to NIH 3T3 cells. **Cell.** 51: 1063-1070.

Diks, S. H., K. Kok, T. O'Toole, D. W. Hommes, P. van Dijken and J. Joore. 2004. Kinome profiling for studying lipopolysaccharide signal transduction in human peripheral blood mononuclear cells. **J. Biol. Chem.** 279: 49206-49213.

Downward, J. 1998. Mechanisms and consequences of activation of protein kinase B/Akt. **Curr. Opin. Cell. Biol.** 10: 262-267.

_____, Y. Yarden and E. Mayes. 1984. Close similarity of epidermal growth factor receptor and v-erb-B oncogene protein sequences. **Nature.** 307: 521-527.

Drebin, J. A., V. C. Link and D. F. Stern. 1985. Down-modulation of an oncogene protein product and reversion of the transformed phenotype by monoclonal antibodies. **Cell.** 41: 697-706.

Edwards, M. C., S. E. Taylor, E. M. Williamson and F. J. Evans. 1983. New phorbol and deoxyphorbol esters: isolation and relative potencies in inducing platelet aggregation and erythema of skin. **Acta Pharmacol. Tox.** 53: 177-187.

Eglen, R. M. 2002. Enzyme fragment complementation: a flexible high throughput screening assay technology. **Assay Drug Dev. Technol.** 1: 97-108.

_____ and T. Reisine. 2009. The Current Status of Drug Discovery Againt the Human Kinome. **Assay Drug Dev. Technol.** 7: 22-43.

Eglen, R. M. and R. Singh. 2003. β-Galactosidase enzyme fragment complementation (EFC) as a novel technology for high throughput screening. **Comb. Chem. High T. Scr.** 6: 381-387.

Ekstrand, A. J., N. Sugawa and C. D. James. 1992. Amplified and rearranged epidermal growth factor receptor genes in human glioblastomas reveal deletions of sequences encoding portions of the N- and/or C-terminal tails. **Proc. Natl. Acad. Sci. USA**. 89: 4309-4313.

Elleman, T. C., T. Domagala, N. M. McKern, M. Nerrie and B. Lonnqvist. 2001. Identification of a determinant of epidermal growth factor receptor ligand-binding specificity using a truncated, high-affinity form of the ectodomain. **Biochemistry**. 40: 8930-8939.

Falls, D. L. 2003. Neuregulins: functions, forms, and signaling strategies. **Exp. Cell Res.** 284: 14-30.

Fan, Y. X., L.Wong, B. D. Tushar and G. R. Johnson. 2004. Ligand regulates epidermal growth factor receptor kinase specificity. **J. Biol. Chem.** 279: 38143-38150.

Feldkamp, M. M., P. Lala and N. Lau. 1999. Expression of activated epidermal growth factor receptors, Ras-guanosine triphosphate, and mitogen-activated protein kinase in human glioblastoma multiforme specimens. **Neurosurgery.** 45: 1442-1453.

Ferguson, K. M. 2004. Active and inactive conformations of the epidermal growth factor receptor. **Biochem. Soc. Trans.** 32: 742-745.

_____. 2008. Structure-Based View of Epidermal Growth Factor Receptor Regulation. **Annu. Rev. Biophys.** 37:353-373.

Ferguson, K. M., M. B. Berger, J. M. Mendrola, H. S. Cho, D. J. Leahy and M. A. Lemmon. 2003. EGF activates its receptor by removing interactions that autoinhibit ectodomain dimerization. **Mol. Cell.** 11: 507-517.

Franklin, M. C., K. D. Carey, F. F. Vajdos, D. J. Leahy, A. M. deffos and M.X. Sliwkowski. 2004. Insights into ErbB signaling from the structure of the ErbB2-pertuzumab complex. **Cancer Cell.** 5: 317-328.

Friesel, R. E. and T. Maciag. 1995. Molecular mechanisms of angiogenesis: fibroblast growth factor signal transduction. **Faseb J.** 9: 919-25.

Fujioka, A., K. Terai, R. Itoh, K. Aoki, T. Nakamura and S. Kuroda. 2006. Dynamics of the Ras/ERK MAPK cascade as monitored by fluorescent probes. **J. Biol. Chem.** 281: 8917-8926.

Fung, P., K. Peng, P. Kobel, H. Dotimas, L. Kauffman and K. Olson. 2006. A homogeneous cell-based assay to measure nuclear translocation using betagalactosidase enzyme fragment complementation. **Assay Drug Dev. Technol.** 4:263-272.

Gallegos, L., M. Kunkel and A. Newton. 2006. Targeting protein kinase C activity reporter to discrete intracellular regions reveals spatiotemporal differences in agonist-dependent signaling. **J. Biol. Chem.** 281: 30947-30956.

Ganesan, A. 2008. The impact of natural products upon modern drug discovery. **Curr. Opin. Chem. Biol.** 12: 306-317.

Garrett, T. P., N. M. McKern, M. Lou, T. C. Elleman and T. E. Adams. 2002. Crystal structure of a truncated epidermal growth factor receptor extracellular domain bound to transforming growth factor alpha. **Cell.** 110: 763-773.

Garrington, T. P. and G. L. Johnson. 1999. Organization and regulation of mitogen-activated protein kinase signaling pathways. **Curr. Opin. Cell Biol.** 11: 211-218.

Ge, G., J. Wu, Y. Wang and Q. Shi. 2002. Activation mechanism of solubilized epidermal growth factor receptor tyrosine kinase. **Biochem. Biophys. Res. Commun.** 290: 914-920.

Geyer, C. E., J. Forster, D. Lindquist, S. Chan, C. G. Romieu, T. Pienkowski, A. Jagiello-Gruszfeld, J. Crown, A. Chan, B. Kaufman, D. Skarlos, M. Campone, N. Davidson, M. Berger, C. Oliva, S. D. Rubin, S. Stein and D. Cameron. 2006. Lapatinib plus capecitabine for HER2-positive advanced breast cancer. **N. Engl. J. Med.** 355: 2733-2743.

Gilmer, T. M., L. Cable, K. Alligood, D. Rusnak, G. Spehar, K. T. Gallagher, E. Woldu, H. L. Carter and A. T. Truesdale. 2008. Impact of common epidermal growth factor receptor and HER2 variants on receptor activity and inhibition by lapatinib. **Cancer Res.** 68: 571-579.

Gingras, A. C., S. G. Kennedy and M. A. O'Leary. 1998. 4E-BP1, a repressor of mRNA translation, is phosphorylated and inactivated by the Akt(PKB) signaling pathway. **Genes Dev.** 12: 502-513.

Goldstein, B. J. 1992. Protein-tyrosine phosphatases and the regulation of insulin action. **J. Cell Biochem.** 48: 33-42.

Goldstein, N. I., M. Prewett and K. Zuklys. 1995. Biological efficacy of a chimeric antibody to the epidermal growth factor receptor in a human tumor xenograft model. **Clin. Cancer Res.** 1:1311-1318.

Gomez, H. L., D. C. Doval, M. A. Chavez, P. C. Ang, Z. Aziz, S. X. Franco, L. W. Chow, M. C. Arbushites, M. A. Casey, M. S. Berger, S. H. Stein and G. W. Sledge. 2008. Efficacy and safety of lapatinib as first-line therapy for ErbB2-amplified locally advanced or metastatic breast cancer. **J. Clin. Oncol**. 26: 2999-3005.

Gotoh, N., A. Tojo, M. Hino, Y. Yazaki and M. Shibuya. 1992. A highly conserved tyrosine residue at codon 845 within the kinase domain is not required for the transforming activity of human epidermal growth factor receptor. **Biochem. Biophys. Res. Commun.** 186: 768-774.

Guenat, S., N. Rouleau, C. Bielmann, J. Bedard, F. Maurer, N. Allaman-Pillet. 2006. Homogeneous and nonradioactive high-throughput screening platform for the characterization of kinase inhibitors in cell lysates. **J. Biomol. Screen.** 11: 1015-1026.

Guy, C. T., M. A. Webster and M. Schaller. 1992. Expression of the neu protooncogene in the mammary epithelium of transgenic mice induces metastatic disease. **Proc. Natl. Acad. Sci. USA**. 89: 10578-10582.

Grünwald, V. and M. Hidalgo. 2002. The Epidermal Growth Factor Receptor: A New Target for Anticancer Therapy. **Curr. Probl. Cancer.** 26: 109-164.

Halter, S. A., P. Dempsey and Y. Matsui. 1992. Distinctive patterns of hyperplasia in transgenic mice with mouse mammary tumor virus transforming growth factoralpha. Characterization of mammary gland and skin proliferations. **Am. J. Pathol.** 140: 1131-1146.

Han, S., V. Zhou, S. Pan, Y. Liu, M. Hornsby and D. McMullan. 2005. Identification of coumarin derivatives as a novel class of allosteric MEK1 inhibitors. **Bioorg. Med. Chem. Lett.** 15: 5467-5473.

Hardie, D. G. 1999. **Protein Phosphorylation: A Practical Approach.** Oxford University Press, New York.

Harris, R. C., E. Chung and R. J. Coffey. 2003. EGF receptor ligands. **Exp. Cell Res.** 284: 2-13.

Harvey, A. L. 2001. **Natural Product Pharmaceuticals: A Diverse Approach to Drug Discovery, Scrip Reports.** PJB Publications.

Harvey, A. L. 2008. Natural products in drug discovery. **Drug Discov. today.** 13: 894-901.

Holbro, T. and N. E. Hynes. 2004. ErbB receptors: directing key signaling networks throughout life. **Annu. Rev. Pharmacol. Toxicol**. 44: 195-217.

Hsieh, E. T., F. A. Shepherd and M. S. Tsao. 2000. Co-expression of epidermal growth factor receptor and transforming growth factor-alpha is independent of ras mutations in lung adenocarcinoma. **Lung Cancer.** 29: 151-157.

Hubbard, S. R. 2004. Juxtamembrane autoinhibition in receptor tyrosine kinases. **Nat. Rev. Mol. Cell Biol.** 5: 464-471.

_____, and J. H. Till. 2000. Protein tyrosine kinase structure and function. **Annu. Rev. Biochem.** 69: 373-398.

Humphrey, P. A., L. M. Gangarosa and A. J. Wong. 1991. Deletion-mutant epidermal growth factor receptor in human gliomas: effects of type II mutation on receptor function. **Biochem. Biophys. Res. Commun.** 178: 1413-1420.

Humphrey, P. A., A. J. Wong and B. Vogelstein. 1990. Anti-synthetic peptide antibody reacting at the fusion junction of deletion-mutant epidermal growth factor receptors in human glioblastoma. **Proc. Natl. Acad. Sci. USA**. 87: 4207-4211.

Hundsrucker, C., G. Krause, M. Beyermann, A. Prinz, B. Zimmermann and O. Diekmann. 2006. High-affinity AKAP7delta-protein kinase A interaction yields novel protein kinase A-anchoring disruptor peptides. **Biochem J.** 396: 297-306.

Hunter, T. 2000. Signaling—2000 and beyond. **Cell.** 100: 113-127.

Huse, M. and J. Kuriyan. 2002. The conformational plasticity of protein kinases. **Cell.** 109: 275-282.

Ishida, A., I. Kameshita, N. Sueyoshi, T. Takanobu, T. Taniguchi and Y. Shigeri. 2007. Recent advances in technologies for analyzing protein kinases. **J. Pharmacol. Sci.** 103: 5-11.

Issing, W. J., C. Liebich and T. P. Wustrow. 1996. Coexpression of epidermal growth factor receptor and TGF-alpha and survival in upper aerodigestive tract cancer. **Anticancer Res.** 16: 283-238.

Jeffrey, P. D., A. A. Russo, K. Polyak, E. Gibbs and J. Hurwitz. 1995. Mechanism of CDK activation revealed by the structure of a cyclinA-CDK2 complex. **Nature.** 376: 313-320.

Jia, Y., C. M. Quinn, S. Kwak and R. V. Talanian. 2008. Current in vitro kinase assays; the quest for a universal format. **Curr. Drug Discov. Technol**. 5: 59-69.

Jiang, Y., J. L. Chan and C. S. Zong. 1996. Effect of tyrosine mutations on the kinase activity and transforming potential of an oncogenic human insulin-like growth factor I receptor**. J. Biol. Chem.** 271: 160-7.

Jimeno, A. and M. Hidalgo. 2005. Blockade of epidermal growth factor receptor (EGFR) activity. **Crit. Rev. Oncol. Hemat.** 53: 179-192.

Johnson, L. N. 2009. Protein kinase inhibitors: contributions from structure to clinical compounds. **Biophysics.** 42: 1-40.

Kashles, O., D. Szapary, F. Bellot, A. Ullrich, J. Schlessinger and A. Schmidt. 1988. Ligandinduced stimulation of epidermal growth factor receptor mutants with altered transmembrane regions. **Proc. Natl. Acad. Sci. USA**. 85: 9567-9571.

Klapper, L. N., M. H. Kirschbaum and M. Sela. 2000. Biochemical and clinical implications of the ErbB/HER signaling network of growth factor receptors. **Adv. Cancer Res.** 77: 25-79.

Klumpp, M., A. Boettcher, D. Becker, G. Meder, J. Blank and L. Leder. 2006. Readout technologies for highly miniaturized kinase assays applicable to high-throughput screening in a 1536-well format. **J. Biomol. Screen.** 11: 617–633.

Kobayashi, M., T. Mahmud, N. Yoshioka, H. Shibuya and I. Kitagawa. 1997. Indonesian medicinal plants. XXI. Inhibitors of Na+/H+ exchanger from the bark of Erythrina variegata and the roots of Maclura cochinchinensis. **Chem. Pharm. Bull**. 45: 1615-1619.

Kobayashi, S., T. J. Boggon, T. Dayaram, P. A. Janne, O. Kocher, M. Meyerson, B. E. Johnson, M. J. Eck, D. G. Tenen, and B. Halmos. 2005. EGFR Mutation and Resistance of Non–Small-Cell Lung Cancer to Gefitinib. **N. Engl. J. Med.** 352: 786-792.

Koland, J. G., K. M. O'Brien and R. A. Cerione. 1990. Expression of epidermal growth factor recrptor sequences as E.coli fusion proteins: application in the study of tyrosine kinase function. **Biochem. Biophys. Res. Commun.** 166: 90-100.

Koresawa, M. and T. Okabe. 2004. High-throughput screening with quantitation of ATP consumption: a universal non-radioisotope, homogeneous assay for protein kinase. **Assay Drug Dev. Technol.** 2: 153-160.

Kris, M. G., R. Herbst, D. Rischin, , P. LoRusso, , J. Baselga, , L. Hammond, A. Feyereislova, O. Ochs and S. Averbuch. 2000. Objective regressions in non-small cell lung cancer patients treated in Phase I trials of oral ZD1839 ('Iressa'), a selective tyrosine kinase inhibitor that blocks the epidermal growth factor receptor (EGFR). **Lung Cancer**. 29: 72.

Kumar, A., E. T. Petri, B. Halmos and T. J. Boggon. 2008. Structure and clinical relevance of the epidermal growth factor receptor in human cancer. **J. Clin. Oncol**. 26: 1742-1751.

Lam, K. S. 2007. New aspects of natural products in drug discovery. **Trends Microbiol.** 15: 279-289.

Laurent-Puig, P. and J. Taieb. 2008. Lessons from Tarceva in pancreatic cancer: where are we now and how should future trials be designed in pancreatic cancer? **Curr. Opin. Oncol**. 20: 454-458.

Leahy, D.J. 2004. Structure and function of the epidermal growth factor (EGF/ErbB) family of receptors. **Adv. Protein Chem.** 68: 1-27.

Lee, J. C., I. Vivanco, R. Beroukhim, J. H. Huang and W. L. Feng. 2006. Epidermalgrowth factor receptor activation in glioblastoma through novel missense mutations in the extracellular domain. **PLOS Med.** 3: 485.

Lee, N. Y. and J. G. Koland. 2005. Conformational changes accompany phosphorylation of the epidermal growth factor receptor C-terminal domain. **Protein Sci.** 14: 2793-2803.

_____, _____ and T. L. Hazlett. 2006. Structure and dynamics of the epidermal growth factor receptor C-terminal phosphorylation domain. **Protein Sci.** 15: 1142-1152.

Li, S., K. R. Schmitz, P. D. Jeffrey, J. J. Wiltzius, P. Kussie and K. M. Ferguson. 2005. Structural basis for inhibition of the epidermal growth factor receptor by cetuximab. **Cancer Cell.** 7: 301-311.

Linggia, B. and G. Carpenter. 2006. ErbB receptors: new insights on mechanisms and biology. **Trends Cell Biol.** 16: 649-656.

Liu, H., X. Chen, P. J. Focia and X. He. 2007. Structural basis for stem cell factor-KIT signaling and activation of class III receptor tyrosine kinases. **EMBO J.** 26: 891–901

Lynch, T. J., D. W. Bell, R. Sordella, S. Gurubhagavatula, R. A. Okimoto, B. W. Brannigan, P. L. Harris, S. M. Haserlat, J. G. Supko, F. G. Haluska, D. N. Louis, D. C. Christiani, J. Settleman and D. A. Haber. 2004. Activating mutations in the epidermal growth factor receptor underlying responsiveness of non-small-cell lung cancer to gefitinib. **N. Engl. J. Med**. 350: 2129-2139.

Margolis, B., J. P. Borg and S. Straight. 1999. The function of PTB domain proteins. **Kidney Int.** 56: 1230-1237.

Mathis, G. 1999. HTRF® technology. **J. Biomol. Screen**. 4: 309-314.

Matsui, Y., S. A. Halter and J. T. Holt. 1990. Development of mammary hyperplasia and neoplasia in MMTV-TGF alpha transgenic mice. **Cell.** 61:1147-1155.

Mayo, L. D. and D. B. Donner. 2001. A phosphatidylinositol 3-kinase/Akt pathway promotes translocation of Mdm2 from the cytoplasm to the nucleus. **Proc. Natl. Acad. Sci. USA**. 98: 11598-11603.

McChesney, J. D. 2007. Plant natural products: back to the future or into extinction? **Phytochemistry** 68: 2015-2022.

McLaughlin, S., S. O. Smith, M. J. Hayman and D. Murray. 2005. An electrostatic engine model for autoinhibition and activation of the epidermal growth factor receptor (EGFR/ErbB) family. **J. Gen. Physiol.** 126: 41-53.

McMenamin, M. E., P. Soung, S. Perera. 1999. Loss of PTEN expression in paraffin-embedded primary prostate cancer correlates with high Gleason score and advanced stage. **Cancer Res.** 59: 4291-4296.

Mendelsohn, J. and J. Baselga. 2000. The EGF receptor family as targets for cancer therapy. **Oncogene.** 19: 6550–6565.

Mendrola, J. M., M. B. Berger, M. C. King and M. A. Lemmon. 2002. The single transmembrane domains of ErbB receptors self-associate in cell membranes. **J. Biol. Chem.** 277: 4704-4712.

Menzo, S., M. Clementi and E. Alfani. 1993. Trans-activation of epidermal growth factor receptor gene by the hepatitis B virus X-gene product. **Virology.** 196: 878-882.

Miettinen, P. J., J. E. Berger and J. Meneses. 1995. Epithelial immaturity and multiorgan failure in mice lacking epidermal growth factor receptor. **Nature.** 376: 337-341.

Milano, G., J. P. Spano and B. Leyland-Jones. 2008. EGFR-targeting drugs in combination with cytotoxic agents: from bench to bedside, a contrasted reality. **Brit. J. Cancer**. 99: 1–5.

Miller, W. E., G. Mosialos and E. Kieff. 1987. Epstein-Barr virus LMP1 induction of the epidermal growth factor receptor is mediated through a TRAF signaling pathway distinct from NF-kappaB activation. **J. Virol.** 71: 586-594.

Moll, D., A. Prinz, F. Gesellchen, S. Drewianka, B. Zimmermann and F. W. Herberg. 2006. Biomolecular interaction analysis in functional proteomics. **J. Neural. Transm.** 113: 1015-1032.

Morgan, A. G., T. J. McCauley, M. L. Stanaitis, M. Mathrubutham and S. Z. Millis. 2004. Development and validation of a fluorescence technology for both primary and secondary screening of kinases that facilitates compound selectivity and site-specific inhibitor determination. **Assay Drug Dev. Technol.** 2: 171-181.

Moscatello, D. K., M. Holgado-Madruga, A. K. Godwin. 1995. Frequent expression of a mutant epidermal growth factor receptor in multiple human tumors. **Cancer Res.** 55: 5536-5539.

_____, _____ and D. R. Emlet. 1998. Constitutive activation of phosphatidylinositol 3-kinase by a naturally occurring mutant epidermal growth factor receptor. **J. Biol. Chem.** 273: 200-206.

Moscatello, D. K., R. B. Montgomery and P. Sundareshan. 1996. Transformational and altered signal transduction by a naturally occurring mutant EGF receptor. **Oncogene.** 13: 85-96.

Moser, K. and F. M. White. 2006. Phosphoproteomic analysis of rat liver by high capacity IMAC and LC-MS/MS. **J. Proteome. Res.** 5: 98-104.

Moyer, J. D., E. G. Barbacci, K. K. Iwata, L. Arnold, B. Boman, A. Cunningham, C. Diorio, J. Doty, M. J. Morin, M. P. Moyer, M. Neveu, V. A. Pollack, L. R. Pustilnik, M. M. Reynolds, D. Sloan, A. Theleman and P. Miller. 1997. Induction of apoptosis and cell cycle arrest by CP-358,774, an inhibitor of epidermal growth factor receptor tyrosine kinase. **Cancer Res.** 57: 4838-4848.

Muller, W. J., C. L. Arteaga and S. K. Muthuswamy. 1996. Synergistic interaction of the Neu proto-oncogene product and transforming growth factor alpha in the mammary epithelium of transgenic mice. **Mol. Cell Biol.** 16: 5726-5736.

Newman, D. J. and G. M. Cragg. 2007. Natural products as sources of new drugs over the last 25 years. **J. Nat. Prod.** 70: 461-477.

Ogiso, H., R. Ishitani, O. Nureki, S. Fukai and M. Yamanaka. 2002. Crystal structure of the complex of human epidermal growth factor and receptor extracellular domains. **Cell.** 110: 775-787.

Okano, J., I. Gaslightwala and M. J. Birnbaum. 2000. Akt/protein kinase B isoforms are differentially regulated by epidermal growth factor stimulation. **J. Biol. Chem.** 275: 30934-30942.

Olapade-Olaopa, E. O., D. K. Moscatello, E. H. MacKay. 2000. Evidence for the differential expression of a variant EGF receptor protein in human prostate cancer. **Br. J. Cancer.** 82: 186-194.

Olayioye, M. A., R. M. Neve and H. A. Lane. 2000. The ErbB signaling network: receptor heterodimerization in development and cancer. **EMBO J.** 19: 3159-3167.

Olive, D. M. 2004. Quantitative methods for the analysis of protein phosphorylation in drug development. **Expert Rev. Proteomic.** 1: 327-341.

Paez, J. G., P. A. Janne, J. C. Lee, S. Tracy, H. Greulich, S. Gabriel, P. Herman, F. J. Kaye, N. Lindeman, T. J. Boggon, K. Naoki, H. Sasaki, Y. Fujii, M. J. Eck, W. R. Sellers, B. E. Johnson and M. Meyerson. 2004. EGFR mutations in lung cancer: correlation with clinical response to gefitinib therapy. **Science.** 304: 1497-1500.

Palo, K., L. Brand, C. Eggeling, S. Jager, P. Kask and K. Gall. 2002. Fluorescence intensity and lifetime distribution analysis: toward higher accuracy in fluorescence fluctuation spectroscopy. **Biophys. J.** 83: 605-618.

Pao, W., V. Miller, M. Zakowski, J. Doherty, K. Politi, I. Sarkaria, B. Singh, R. Heelan, V. Rusch, L. Fulton, E. Mardis, D. Kupfer, R. Wilson, M. Kris and H. Varmus. 2004. EGF receptor gene mutations are common in lung cancers from 'never smokers' and are associated with sensitivity of tumors to gefitinib and erlotinib. **Proc. Natl. Acad. Sci. USA**. 101: 13306-13311.

Pawson, T. 1995. Protein modules and signalling networks. **Nature.** 373: 573-580.

Posner, I., M. England and A. Levitzki. 1992. Kinetic model of the epidermal growth factor receptor tyrosine kinase and a possible mechanism of its activation by EGF. **J. Biol. Chem.** 267: 20638-20647.

Prenzel, N., O. M. Fischer and S. Streit. 2001. The epidermal growth factor receptor family as a central element for cellular signal transduction and diversification. **Endocr. Relat. Cancer.** 8: 11-31.

Prinz, A., M. Diskar and F. W. Herberg. 2006. Application of bioluminescence resonance energy transfer (BRET) for biomolecular interaction studies. **Chembiochem.** 7: 1007-1012.

Rameh, L. E. and L. C. Cantley. 1999. The role of phosphoinositide 3-kinase lipid products in cell function. **J. Biol. Chem.** 274: 8347-8350.

Raught, B., A. C. Gingras and N. Sonenberg. 2001. The target of rapamycin (TOR) proteins. **Proc. Natl. Acad. Sci. USA.** 98: 7037-7044.

Reddy, K. R., H. Lilie, R. Rudolph and C. Lange. 2005. L-arginine increases the solubility of unfolded species of hen egg white lysozyme. **Protein Sci.** 14: 929-935.

Remy, I. and S. Michnick. 1999. Clonal selection and in vivo quantitation of protein interactions with protein-fragment complementation assays. **Proc. Natl. Acad. Sci. USA.** 96: 5394-5399.

Riese, D. J., R. M. Gallo and J. Settleman. 2007. Mutational activation of ErbB family receptor tyrosine kinases: insights into mechanisms of signal transduction and tumorigenesis. **Bioessays.** 29: 558-565.

Risberg, T., E. Lund, E. Wist, S. Kaasa, T. Wilsgards. 1998. Cancer patients use nonproven therapy: 5-year follow-up study. **J. Clin. Oncol.** 16: 1-2.

Rishton, G. M. 2008. Natural products as a robust source of new drugs and drug leads: past successes and present day issues. **Am. J. Cardiol.** 101: 43D-49D.

Rodems, S. M., B. D. Hamman, C. Lin, J. Zhao, S. Shah and D. Heidary. 2002. A FRET based assay platform for ultra-high density drug screening of protein kinases and phosphatases. **Assay Drug Dev. Technol.** 1: 9-19.

Romashkova, J. A. and S. S. Makarov. 1999. NF-kappaB is a target of AKT in anti-apoptotic PDGF signalling. **Nature.** 401: 86-90.

Roskoski, R. 2004. The ErbB/HER receptor protein-tyrosine kinases and cancer. **Biochem. Biophys. Res. Commun.** 319: 1-11.

Rowinsky, E. K. 2004. The erbB family: targets for therapeutic development against cancer and therapeutic strategies using monoclonal antibodies and tyrosine kinase inhibitors. **Annu. Rev. Med.** 55: 433-457.

Rusch, V., J. Mendelsohn and E. Dmitrovsky. 1996. The epidermal growth factor receptor and its ligands as therapeutic targets in human tumors. **Cytokine Growth Factor Rev.** 7:133-141.

Rusnak, D. W., K. Affleck, S. G. Cockerill, C. Stubberfield, R. Harris, M. Page, K. J. Smith, S. B. Guntrip, M. C. Carter, R. J. Shaw, A. Jowett, J. Stables, P. Topley, E. R. Wood, P. S. Brignola, S. H. Kadwell, B. R. Reep, R. J. Mullin, K. J. Alligood, B. R. Keith, R. M., Crosby, D. M., Murray, W. B. Knight, T. M. Gilmer and K. Lackey. 2001. The characterization of novel, dual ErbB-2/EGFR, tyrosine kinase inhibitors: potential therapy for cancer. **Cancer Res**. 61: 7196-7203.

Sachsenmaier, C. and C. Schachtele. 2002. Integrated technology platform protein kinases for drug development in oncology. **Biotechniques.** 101-106.

Salomon, D. S., R. Brandt and F. Ciardiello. 1995. Epidermal growth factor-related peptides and their receptors in human malignancies. **Crit. Rev. Oncol. Hematol.** 19: 183-232.

Schlessinger, J. 2000. Cell signaling by receptor tyrosine kinases. **Cell.** 103: 211-225.

Schlessinger, J. 2002. Ligand-induced, receptor-mediated dimerization and activation of EGF receptor. **Cell.** 110:669-672.

_____ and D. Bar-Sagi. 1997. Activation of Ras and other signaling pathways by receptor tyrosine kinases. **Cold Spring Harb Symp.** 59: 173-179.

Schröter, T., D. Minond, A. Weiser, C. Dao, J. Habel and T. Spicer. 2008. Comparison of miniaturized time-resolved fluorescence resonance energy transfer and enzyme-coupled luciferase high-throughput screening assays to discover inhibitors of Rho-kinase II (ROCK-II). **J. Biomol. Screen.** 13: 17-28.

Schulze, W.X., L. Deng and M. Mann. 2005. Phosphotyrosine interactome of the ErbB-receptor kinase family. **Mol. Syst. Biol.** 1: 5-13.

Schwechheimer, K., S. Huang and W. K. Cavenee. 1995. EGFR gene amplification-rearrangement in human glioblastomas. **Int. J. Cancer.** 62: 145-148.

Seethala, R. and R. Menzel. 1997. A homogeneous, fluorescence polarization assay for src-family tyrosine kinases. **Anal. Biochem.** 253: 210-218.

Seethala, R. and R. Menzel. 1998. A fluorescence polarization competition immunoassay for tyrosine kinases. **Anal. Biochem.** 255: 257-262.

Sequist, L. V. and T. J. Lynch. 2008. EGFR tyrosine kinase inhibitors in lung cancer: an evolving story. **Annu. Rev. Med**. 59: 429-442.

_____, R. G. Martins, D. Spigel, S. M. Grunberg, A. Spira, P. A. Janne, V. A. Joshi, D. Mccollum, T. L. Evans, A. Muzikansky, G. L. Kuhlmann, M. Han, J. S. Goldberg, J. Settleman, A. J. Iafrate, J. A. Engelman, D. A. Haber, B. E. Johnson and T. J. Lynch. 2008. First-line gefitinib in patients with advanced non-small-cell lung cancer harboring somatic EGFR mutations. **J. Clin. Oncol**. 26: 2442-2449.

Seth, D., K. Shaw and J. Jazayeri. 1999. Complex post-transcriptional regulation of EGF-receptor expression by EGF and TGF-alpha in human prostate cancer cells. **Br. J. Cancer.** 80: 657-669.

Shigematsu, H. and A. F. Gazdar. 2006. Somatic mutations of epidermal growth factor receptor signaling pathway in lung cancers. **Int. J. Cancer**. 118: 257-262.

Sibilia, M. and E. F. Wagner. 1995. Strain-dependent epithelial defects in mice lacking the EGF receptor. **Science.** 269: 234-8.

Singh, P., B. J. Harden, B. J. Lillywhite and P. M. Broad. 2004. Identification of kinase inhibitors by an ATP depletion method. **Assay Drug Dev. Technol.** 2: 161-169.

Singh, S. B. and J. F. Barrett. 2006. Empirical antibacterial drug discovery–foundation in natural products. **Biochem. Pharmacol.** 71: 1006-1015.

Sneader, W. 1996. **Drug Prototypes and Their Exploitation**. Wiley, UK.

Sonenberg, N. and A. C. Gingras. 1998. The mRNA 5' cap-binding protein eIF4E and control of cell growth. **Curr. Opin. Cell Biol.** 10: 268-275.

Sportsman, J. R., E. A. Gaudet and A. Boge. 2004. Immobilized metal ion affinity-based fluorescence polarization (IMAP): advances in kinase screening. **Assay Drug Dev. Technol.** 2: 205-214.

Stamos, J., M. X. Sliwkowski and C. Eigenbrot. 2002. Structure of the epidermal growth factor receptor kinase domain alone and in complex with a 4-anilinoquinazoline inhibitor. **J. Biol. Chem.** 277: 46265-4672.

Staudacher, E. 2008. **Program for Workshop on "Glycomics: Biochemistry and Analysis of Glycans**. 110-111.

Stefan, E., S. Aquin, N. Berger, C. Landry, B. Nyfeler and M. Bouvier. 2007. Quantification of dynamic protein complexes using *Renilla* luciferase fragment complementation applied to protein kinase A activities in vivo. **Proc. Natl. Acad. Sci. USA.** 104: 16916-16921.

Straight, S. W., P. M. Hinkle and R. J. Jewers. 1993. The E5 oncoprotein of human papillomavirus type 16 transforms fibroblasts and effects the downregulation of the epidermal growth factor receptor in keratinocytes. **J. Virol.** 67: 4521-4532.

Sugawa, N., J. A. Ekstrand, D. C. James and P. V. Collins. 1990. Identical splicing of aberrant epidermal growth factor receptor transcripts from amplified rearranged genes in human glioblastomas. **Proc. Natl. Acad. Sci. USA.** 87: 8602-8606.

Tang, C. K., X. Q. Gong and D. K. Moscatello. 2000. Epidermal growth factor receptor vIII enhances tumorigenicity in human breast cancer. **Cancer Res.** 60:3081-7.

Taylor, S. E., M. A. Gafur, A. K. Choudhury and Evans, F. J. 1982. Sapatoxins, aliphatic ester tigliane diterpenes from Sapium indicum. **Phytochemistry.** 21: 405-407.

Thatcher, N., A. Chang, P. Parikh, J. R. Pereira, T. Ciuleanu, J. V. Pawel, S. Thongprasert, E. H. Tan, K. Pemberton, V. Archer and K. Carroll. 2005. Gefitinib plus best supportive care in previously treated patients with refractory advanced non-small-cell lung cancer: results from a randomised, placebocontrolled, multicentre study (Iressa Survival Evaluation in Lung Cancer). **Lancet.** 366: 1527-1537.

Threadgill, D. W., A. A. Dlugosz and L. A. Hansen. 1995. Targeted disruption of mouse EGF receptor: effect of genetic background on mutant phenotype. **Science.** 269: 230-234.

Tsumoto, K., M. Umetsu, I. Kumagai, D. Ejima, J.S. Philo and T. Arakawa. 2004. Role of arginine in protein refolding, solubilization, and purification. **Biotechnol. Prog.** 20: 1301-1308.

Ullrich, A. and J. Schlessinger. 1990. Signal transduction by receptors with tyrosine kinase activity. **Cell.** 61: 203-212.

Vainshtein, I., S. Silveria, P. Kaul, R. Rouhani, R. M. Eglen and J. Wang. 2002. A highthroughput, nonisotopic, competitive binding assay for kinases using nonselective inhibitor probes (ED-NSIP™). **J. Biomol. Screen.** 7: 497-504.

van der Geer, P., T. Hunter and R. A. Lindberg. 1994. Receptor protein-tyrosine kinases and their signal transduction pathways. **Annu. Rev. Cell Biol.** 10: 251-337.

Varkondi, E., F. Pinter, K. Robert, R. Schwab, N. Breza, L. Orfi, G. Keri and I. Petak. 2008. Biochemical assay-based selectivity profiling of clinically relevant kinase inhibitors on mutant forms of EGF receptor. **J. Recept. Sig. Transd.** 28: 295-306.

Vickers, A. 2002. Botanical Medicines for the Treatment of Cancer: Rationale, Overview of Current Data, and Methodological Considerations for Phase I and II Trials. **Cancer Invest.** 20: 1069-1079.

Vincentelli, R., S. Canaan, V. Campanacci, C. Valencia, D. Maurin, F. Frassinetti, L. S. Calvo, Y. Bourne, C. Cambillau and C. Bignon. 2004. High-thoughput automated refolding screening of inclusion bodies. **Protein Sci**. 13: 2782-2792.

Violin, J. D., J. Zhang, R. Y. Tsien and A. C. Newton. 2003. A genetically encoded fluorescent reporter reveals oscillatory phosphorylation by protein kinase C. **J. Cell Biol.** 161: 899-909.

Visser, J. A., R. Olaso and M. Verhoef-Post. 2001. The serine/threonine transmembrane receptor ALK2 mediates Mullerian inhibiting substance signaling. **Mol. Endocrinol.** 15: 936-945.

Wakeling, A. E. 2005. Inhibitors of growth factor signaling. **Endocr-Relat. Cancer.** 12: S183-S187.

_____, S. P. Guy, J. R. Woodburn, S. E. Ashton, B. J. Curry and A. J. Barker. 2002. ZD1839 (Iressa): an orally active inhibitor of epidermal growth factor signaling with potential for cancer therapy. **Cancer Res**. 62:5749-5754.

Walker, F., S. G. Orchard, R. N. Jorissen, N. E. Hall, H. H. Zhang. 2004. CR1/CR2 interactions modulate the functions of the cell surface epidermal growth factor receptor. **J. Biol. Chem.** 279: 22387–22398.

Walton, G. M., W. S. Chen, M. G. Rosenfeld and G. N. Gill. 1990. Analysis of deletions of the carboxyl terminus of the epidermal growth factor receptor reveals self-phosphorylation at tyrosine 992 and enhanced in vivo tyrosine phosphorylation of cell substrates. **J. Biol. Chem.** 265: 1750-1754.

Ward, C. W., M. C. Lawrence, V. A. Streltsov, T. E. Adams and N. M. McKern. 2007. The insulin and EGF receptor structures: new insights into ligand-induced receptor activation. **Trends Biochem. Sci.** 32: 129-137.

Warner, G., C. Illy, L. Pedro, P. Roby and R. Bosse. 2004. AlphaScreen kinase HTS platforms. **Curr. Med. Chem**. 11: 721-730.

Wehrman, T., X. He, W. Raab, A. Dukipatti, H. Blau and K. Garcia. 2007. Structural and mechanistic insights into nerve growth factor interactions with the TrkA and p75 receptors. **Neuron.** 53: 25-38.

Wesche, H., S. H. Xiao and S. W. Young. 2005. High throughput screening for protein kinase inhibitors. **Comb. Chem. High T. Scr.** 8: 181-195.

Whitney, J. A. 2004. Reference systems for kinase drug discovery; chemical genetic approaches to cell-based assays. **Assay Drug Dev. Technol.** 2: 417-430.

Wissner, A. and T. S. Mansour. 2008. The development of HKI-272 and related compounds for the treatment of cancer. **Arch. Pharm.** 341: 465-477.

Wood, E. R., A. T. Truesdale, O. B. McDonald, D. Yuan and A. Hassell. 2004. A unique structure for epidermal growth factor receptor bound to GW572016 (Lapatinib): relationships among protein conformation, inhibitor off-rate, and receptor activity in tumor cells. **Cancer Res.** 64: 6652-6659.

Yacoub, L., H. Goldman and R. D. Odze. 1987. Transforming growth factor-alpha, epidermal growth factor receptor, and MiB-1 expression in Barrett's-associated neoplasia: correlation with prognosis. **Mod. Pathol.** 10: 105-112.

Yang, X. D., X. C. Jia and J. R. Corvalan. 1999. Eradication of established tumors by a fully human monoclonal antibody to the epidermal growth factor receptor without concomitant chemotherapy. **Cancer Res.** 59: 1236-1243.

Yarden, Y. 2001. The EGFR family and its ligands in human cancer. Signalling mechanisms and therapeutic opportunities**. Eur. J. Cancer.** 37: 3-8.

_____ and M. X. Sliwkowski. 2001. Untangling the ErbB signalling network. **Nat. Rev. Mol. Cell Biol.** 2: 127-137.

Yoosook C., N. Bunyapraphatsara, Y. Boonyakiat and C. Kantasuk. 2000. Anti-herpes simplex virus activities of crude water extracts of Thai medicinal plants. **Phytomedicine.** 6: 411-419.

Yun, C. H., T. J. Boggon, Y. Li, M. S. Woo and H. Greulich. 2007. Structures of lung cancerderived EGFR mutants and inhibitor complexes: mechanism of activation and insights into differential inhibitor sensitivity. **Cancer Cell.** 11: 217-227.

_____, K. E. Mengwasser, A. V. Toms, M. S. Woo, H. Greulich, K. K. Wong, M. Meyerson and M. J. Eck. 2008. The T790M mutation in EGFR kinase causes drug resistance by increasing the affinity for ATP. **PNAS.** 105: 2070-2075.

Yuzawa, S., Y. Opatowsky, Z. Zhang, V. Mandiyan, I. Lax and J. Schlessinger. 2007. Structural basis for activation of the receptor tyrosine kinase KIT by stem cell factor. **Cell.** 130: 323-334.

Zhang, K., N. Liu, D. Wen, D. Chang, A. Thomason, S. K. Yoshinaga. 1996. Transformation of NIH 3T3 cells by HER3 or HER4 receptors requires the presence of HER1 or HER2. **J. Biol. Chem.** 271: 3884-3890.

Zhang, W. G., B. Shor and K. Yu. 2006. Identification and characterization of a constitutively T-loop phosphorylated and active recombinant S6K1: expression, purification, and enzymatic studies in a high capacity non-radioactive TR-FRET Lance assay. **Protein Expr. Purif.** 46: 414-420.

Zhang, X., J. Gureasko, K. Shen, P. A. Cole and J. Kuriyan. 2006. An allosteric mechanism for activation of the kinase domain of epidermal growth factor receptor. **Cell.** 125: 1137-1149.

Zimmermann, S. and K. Moelling. 1999. Phosphorylation and regulation of Raf by Akt (protein kinase B). **Science.** 286:1741-4.

APPENDIX

1. Bacteria media

LB broth / 1000 ml

Tryptone	10 g
Yest extract	5 g
NaCl	5 g

2. DNA extraction

- TE buffer (10mM Tris, 1mM EDTA) pH 8.0
- 0.67% Sucrose
- Lysozyme (70 mg/ml)
- 20% SDS
- Phenol: Chloroform (1:1)
- Chloroform: Isoamylalcohol (24:1)
- Isopopanol
- 70% Ethanol

3. Plasmid extraction

Alkaline lysis Solution I (Resuspension buffer) /100 ml

50 mM Glucose	2.5 ml
25 mM Tris-Hcl, pH 8	5 ml
10 mM EDTA	2 ml

Alkaline lysis Solution II (Lysis buffer) / 100 ml

0.2 NaOH	2 ml
1% (w/v SDS)	5 ml

Alkaline lysis Solution III / 100 ml

5M Potassium acetate	50 ml
0.2 M Glacial acetic acid	11.5 ml

4. Agarose electrophoresis

10X TBE stock solution 1000 ml	
Tris base	108 g
Boric acid	55 g
EDTA	5.84 g
DNA Loading dye	
0.25% bromophenol blue	
30% glycerol in TE (pH 8.0)	

5. Lowry reagent

Reagent 1: Mix one volume of reagent B (0.5% copper sulfate pentahydrate, 1% sodium or potassium tartrate) with 50 volumes of reagent A (2% sodium carbonate, 0.4% NaOH). Both reagents A and B are supposed to be stable for a long time but I have had a problem with precipitation in reagent B that seems to be remedied by adding a little NaOH.

Reagent 2: Dilute commercial Folin-Ciocalteu phenol reagent with an equal volume of water. Stable for a few days or weeks.

To quantify protein, mix 0.25 mL of protein with 2.5 mL of Lowry reagent 1. After 10 minutes, add 0.25 mL of Lowry reagent 2 and mix well immediately. After 30 minutes, measure the absorbance at 750 nm

6. Sodium dedocyl sulfate-polyacrylamide gel electrophoresis (SDS-PAGE)

30 % Acrylamide (30.8 % T, 2.6% C)/ 100 ml	
30% Acrylamide acrylamide	30 g
N,N'-methylenebisacrylamide (BIS)	0.8 g

10% Amonium persulfate / 1 ml

Amonium persulfate	100 mg

Separating sol 1.5 M tris pH 8.8 / 200 ml

Tris base	36.3 g

Stacking sol 0.5 M tris pH 6.8 / 100 ml

Tris base	6 g

Reagent	12% Separating Gel (ml)	5% Stacking Gel (ml)
30 % Bis-Acrylamide	2.0	0.33
Separating solution	1.3	-
Stacking solution	-	0.25
10% Amonium	0.05	0.02
persulfate	0.05	0.02
10% SDS	0.002	0.002
TEMED	1.6	1.4
Water	5.0	2.0

6x Protein loading dye

0.5M tris pH 6.8	7ml
Glycerol	3ml
SDS	1g
Bromophenol blue	1.2 mg

5x running buffer / 1000 ml

0.125 M Tris base	15.1 g
0.96 M Glycine	72.0 g
0.5%w/v SDS	5 g

5x Staining solution / 500ml

0.5%w/v Coomasie blue R250	2.5 g
40% Methanol	200 ml
10% Acetic acid	50 ml

Destain / 1000 ml

40 % Methanol or ethanol	400 ml
10 % Acetic acid	100 ml

7. Refolding of tyrosine kinase in 96-well plates

The screening of small scale refolding conditions was adapted from Vincentelli *et al.,* 2004. In each condition, we used GST-TK and TK protein 5 µl and measured turbidity of the solution at 540 nm, then incubated at 4 °C, 24 h and then measured the solution again. Compare the absorbance at 540 nm of pre-incubation and after incubation. Each condition was studied in three representatives. Table 3 when we compared pre-incubation and after incubation, condition number 8D and 10B were suitable for refolding of recombinant TK.

Appendix Table 1 Pre-incubation of GST-TK refolding in 96-well plate

	1	2	3	4	5	6	7	8	9	10	11	12
A	0.764	1.107	0.979	1.101	0.971	1.048	0.959	1.116	0.966	1.103	1.186	0.868
B	0.848	0.934	1.024	0.993	1.144	0.941	1.113	1.011	0.963	**1.061**	1.087	1.065
C	0.996	1.053	0.907	1.103	1.132	1.068	1.152	1.120	1.151	1.090	1.056	1.184
D	0.988	1.044	1.150	1.068	1.090	1.059	1.182	**1.144**	1.173	1.044	1.144	1.161
E	0.919	0.983	1.020	0.922	1.047	0.996	0.991	1.071	1.024	0.920	1.028	1.159
F	1.001	0.928	1.105	1.007	1.147	0.944	1.163	0.961	1.158	0.956	0.946	1.182
G	0.876	1.067	0.983	1.036	0.995	1.006	1.004	1.092	1.020	1.083	1.137	1.043
H	0.942	0.830	1.047	1.141	0.973	1.154	1.016	1.181	1.039	1.198	1.022	0.000

Appendix Table 2 After Incubation of GST-TK refolding in 96-well plate

	1	2	3	4	5	6	7	8	9	10	11	12
A	0.733	0.962	0.958	1.002	0.971	0.967	0.946	1.011	0.966	1.035	1.109	0.882
B	0.794	0.877	0.987	0.956	1.133	0.918	1.042	0.988	0.977	**0.781**	1.078	1.023
C	0.891	0.875	0.864	1.020	1.064	1.010	1.122	1.043	1.054	0.995	1.073	1.055
D	0.846	0.920	1.036	0.840	0.977	1.075	1.077	**0.821**	1.035	1.019	1.039	1.004
E	0.853	0.888	0.957	0.874	1.042	0.920	0.979	1.014	1.023	0.815	1.008	1.078
F	0.809	0.841	1.009	1.001	1.017	0.922	1.008	0.946	1.018	0.968	0.950	1.058
G	0.843	0.931	0.977	0.980	0.974	0.926	0.989	1.016	1.022	0.990	1.100	0.897
H	0.840	0.722	0.964	1.025	0.958	1.061	0.993	1.078	1.023	1.123	1.021	0.000

Appendix Table 3 Pre-incubation minus after Incubation of GST-TK refolding in 96-well plate

	1	2	3	4	5	6	7	8	9	10	11	12
A	0.031	0.145	0.021	0.099	0.000	0.081	0.013	0.105	0.000	0.068	0.077	0.014
B	0.054	0.057	0.037	0.037	0.011	0.023	0.071	0.023	0.014	**0.280**	0.009	0.042
C	0.105	0.178	0.043	0.083	0.068	0.058	0.030	0.077	0.097	0.095	0.016	0.129
D	0.142	0.124	0.114	0.228	0.113	0.016	0.105	**0.323**	0.138	0.025	0.105	0.157
E	0.066	0.095	0.063	0.048	0.005	0.076	0.012	0.057	0.001	0.105	0.020	0.081
F	0.192	0.087	0.096	0.006	0.130	0.022	0.155	0.015	0.140	0.012	0.004	0.124
G	0.033	0.136	0.006	0.056	0.021	0.080	0.015	0.076	0.002	0.093	0.037	0.146
H	0.102	0.108	0.083	0.116	0.015	0.093	0.023	0.103	0.016	0.075	0.001	0.000

Appendix Table 4 Pre-incubation of TK refolding in 96-well plate

	1	2	3	4	5	6	7	8	9	10	11	12
A	0.082	0.170	0.190	0.201	0.155	0.161	0.144	0.145	0.144	0.242	0.226	0.077
B	0.116	0.139	0.135	0.125	0.084	0.090	0.115	0.074	0.138	**0.167**	0.168	0.239
C	0.159	0.164	0.189	0.201	0.163	0.130	0.205	0.201	0.244	0.279	0.145	0.230
D	0.140	0.147	0.181	0.147	0.204	0.092	0.205	**0.145**	0.276	0.180	0.178	0.235
E	0.148	0.191	0.145	0.216	0.112	0.189	0.118	0.218	0.105	0.261	0.136	0.243
F	0.119	0.157	0.170	0.159	0.225	0.127	0.221	0.099	0.292	0.159	0.080	0.212
G	0.120	0.143	0.182	0.225	0.156	0.212	0.156	0.207	0.194	0.248	0.153	0.243
H	0.147	0.154	0.109	0.204	0.118	0.246	0.113	0.212	0.090	0.250	0.079	0.000

Appendix Table 5 After incubation of TK refolding in 96-well plate

	1	**2**	**3**	**4**	**5**	**6**	**7**	**8**	**9**	**10**	**11**	**12**
A	0.080	0.173	0.155	0.178	0.158	0.145	0.151	0.171	0.180	0.216	0.210	0.104
B	0.099	0.148	0.154	0.134	0.094	0.090	0.097	0.081	0.120	**0.122**	0.140	0.194
C	0.138	0.189	0.171	0.184	0.174	0.156	0.212	0.204	0.251	0.254	0.121	0.184
D	0.114	0.178	0.152	0.168	0.203	0.093	0.213	**0.104**	0.272	0.144	0.192	0.191
E	0.135	0.166	0.152	0.199	0.110	0.182	0.090	0.213	0.112	0.249	0.113	0.179
F	0.085	0.131	0.157	0.189	0.205	0.103	0.208	0.103	0.239	0.137	0.111	0.172
G	0.126	0.154	0.151	0.192	0.133	0.195	0.153	0.212	0.198	0.251	0.103	0.216
H	0.119	0.158	0.133	0.151	0.108	0.189	0.090	0.190	0.114	0.192	0.102	0.000

Appendix Table 6 Pre-incubation minus after Incubation of TK refolding in 96-well plate

	1	2	3	4	5	6	7	8	9	10	11	12
A	0.002	0.003	0.035	0.023	0.003	0.016	0.007	0.026	0.036	0.026	0.016	0.027
B	0.017	0.009	0.019	0.009	0.010	0.000	0.018	0.007	0.018	**0.045**	0.028	0.045
C	0.021	0.025	0.018	0.017	0.011	0.026	0.007	0.003	0.007	0.025	0.024	0.046
D	0.026	0.031	0.029	0.021	0.001	0.001	0.008	**0.041**	0.004	0.036	0.014	0.044
E	0.013	0.025	0.007	0.017	0.002	0.007	0.028	0.005	0.007	0.012	0.023	0.064
F	0.034	0.026	0.013	0.030	0.020	0.024	0.013	0.004	0.053	0.022	0.031	0.040
G	0.006	0.011	0.031	0.033	0.023	0.017	0.003	0.005	0.004	0.003	0.050	0.027
H	0.028	0.004	0.024	0.053	0.010	0.057	0.023	0.022	0.024	0.058	0.023	0.000

8. Purification of gefitinib from 250 mg Iressa® film-coated tablet

Description: IRESSA® (gefitinib tablets) contains 250 mg of gefitinib and is available as brown film-coated tablets for daily oral administration. Gefitinib is an anilinoquinazoline with the chemical name 4-Quinazolinamine, *N*-(3-chloro-4-fluorophenyl)-7-methoxy-6-[3-4-morpholin) propoxy]

It has the molecular formula $C_{22}H_{24}ClFN_4O_3$, a relative molecular mass of 446.9 and is a white-colored powder. Gefitinib is a free base. The molecule has pK_as of 5.4 and 7.2 and therefore ionizes progressively in solution as the pH falls. Gefitinib can be defined as sparingly soluble at pH 1, but is practically insoluble above pH 7, with the solubility dropping sharply between pH 4 and pH 6. In non-aqueous solvents, gefitinib is freely soluble in glacial acetic acid and dimethylsulphoxide, soluble in pyridine, sparingly soluble in tetrahydrofuran, and slightly soluble in methanol, ethanol (99.5%), ethyl acetate, propan-2-ol and acetonitrile. The inactive ingredients of IRESSA tablets are:

Tablet core: Lactose monohydrate, microcrystalline cellulose, croscarmellose sodium, povidone, sodium lauryl sulfate and magnesium stearate.

Coating: hypromellose, polyethylene glycol 300, titanium dioxide, red ferric oxide and yellow ferric oxide.

Procedure: A 250 mg gefitinib tablet was grinded in mortar and pestle. The powder was added into an elenmayer flask size 250 ml and added 10 ml of 100% ethanol. Then, the solution was warmed in a water bath at 40 °C for 10 min. The solution was filtered, the precipitant was collect to weigh (207 mg). The purity of the supernatant was determined by paper chromatography using 50 ml of 1:20 methanol/chloroform as a mobile phase solvent. The paper chromatogram was revealed by sprayed with vanilla in 95% ethanol or looked though a UV light at 254 nm. Then, the supernatant was evaporated by evaporator at 40 °C until dried. The white powder was collected to weigh (223 mg). Then, the white powder was dissolved in 100% ethanol in a water bath at 40 °C and keep in room temperature or 4 °C for crystallize. The white crystal was collected to weigh (162 mg) and keep at -20 °C for inhibiting study.

CURRICULUM VITAE

NAME : Ms. Sirigade Ruekit

BIRTH DATE : Nov 4, 1984

BIRTH PLACE : Bangkok, Thailand

EDUCATION :

YEAR	**INSTITUTE**	**DEGREE/DIPLOMA**
2006	Kasetsart Univ.	M.S. (Biochemistry)

SCHOLARSHIP/AWARDS: Thailand Research Fund and the Faculty of Science, Kasetsart University (TRF-MAG Window II: MRG-WII515S014), 2008